

# Coordination Chemistry of Bacterial Metal Transport and Sensing

Zhen Ma,<sup>†,‡,§</sup> Faith E. Jacobsen,<sup>†,§</sup> and David P. Giedroc<sup>\*,†</sup>

Department of Chemistry, Indiana University, Bloomington, Indiana 47401-7005 and Department of Biochemistry and Biophysics, Texas A&M University, College Station, Texas 77843-2128

Received February 27, 2009

## Contents

1. Introduction	4644	3.7.1. Structural Studies	4672
1.1. Metal Ion Homeostasis	4644	3.7.2. Metal Selectivity	4673
1.2. Introduction to Metal Transporters	4645	3.8. Other Metalloregulatory and Oxidative Stress-Sensing Proteins	4674
1.3. Introduction to Metal Sensor Proteins	4646	3.8.1. LysR Family Members ModE and OxyR	4674
1.4. Scope of This Review	4649	3.8.2. MarR Family Member AdcR	4675
2. Acquisition and Efflux of Transition Metal Ions in Bacteria	4649	3.8.3. TetR Family Member SczA	4675
2.1. Acquisition of Iron	4650	4. Perspectives	4676
2.2. Acquisition of Zinc and Manganese	4651	5. Acknowledgments	4676
2.3. Acquisition of Copper	4653	6. Note Added in Proof	4676
2.4. Acquisition of Cobalt and Nickel	4654	7. References	4677
2.5. Acquisition of Molybdenum and Tungsten	4655		
2.6. Efflux of Heavy Metal Ions	4655		
2.6.1. Metal Efflux by Cation Diffusion Facilitators	4655		
2.6.2. Metal Efflux by P-Type ATPases	4656		
2.6.3. Other Efflux Mechanisms	4658		
2.7. Metal Transporters: Summary	4659		
3. Prokaryotic Metal Sensor Proteins	4659		
3.1. ArsR/SmtB Family	4660		
3.1.1. Structural Studies	4660		
3.1.2. Metal Selectivity	4661		
3.1.3. Mechanism of Allosteric Regulation	4663		
3.1.4. Putative Nonmetal Ion-Sensing ArsR/SmtB Sensors	4663		
3.2. MerR Family	4664		
3.2.1. Metal Selectivity	4664		
3.2.2. Transcription Activation	4665		
3.2.3. Beyond the SoxR–SoxS Paradigm	4666		
3.3. CsoR/RcnR Family	4667		
3.3.1. CsoR-Like Cu(I) Sensors	4667		
3.3.2. RcnR-Like Co(II)/Ni(II) Sensors	4668		
3.3.3. Putative Nonmetal-Sensing CsoR/RcnR Regulators	4668		
3.4. CopY Family	4669		
3.5. Fur Family	4669		
3.5.1. Structural Studies	4669		
3.5.2. Iron Sensing without Fur	4670		
3.6. DtxR Family	4671		
3.6.1. DtxR-Like Fe(II)-Sensing Repressors	4671		
3.6.2. MntR-Like Mn(II)-Sensing Proteins	4671		
3.7. NikR	4672		

## 1. Introduction

The transition or d-block metal ions manganese, iron, cobalt, nickel, copper, zinc and to a more specialized degree molybdenum, tungsten, and vanadium have been shown to be important for biological systems. These metal ions are ubiquitously found in nature, nearly exclusively as constituents of proteins.<sup>1</sup> The unique properties of metal ions have been exploited by nature to perform a wide range of tasks. These include roles as structural components of biomolecules, signaling molecules, and catalytic cofactors in reversible oxidation–reduction and hydrolytic reactions and in structural rearrangements of organic molecules and electron-transfer chemistry.<sup>1</sup> Indeed, metal ions play critical roles in the cell that cannot be performed by any other entity and are therefore essential for all of life. However, an individual metal ion is capable of performing only one or a few of these functions but certainly not all; as a result, nature has evolved mechanisms to effectively distinguish one metal from another. The coordination chemistry of metal ion–protein complexes is fundamental to this biological discrimination and is largely the focus of this review.

### 1.1. Metal Ion Homeostasis

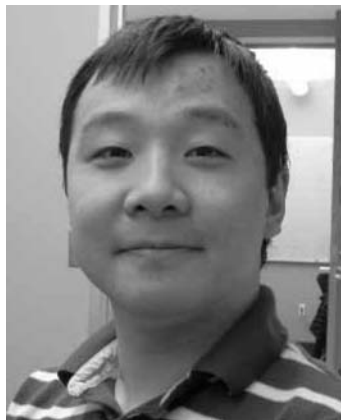
Extensive regulatory and protein-coding machinery is devoted to maintaining the “homeostasis” of biologically required metal ions and underscores the essentiality of this process for cell viability. Homeostasis is defined as the maintenance of an optimal bioavailable concentration, mediated by the balancing of metal uptake and intracellular trafficking with efflux/storage processes so that the needs of the cell for that metal ion are met, i.e., the “right” metal is inserted into the “right” macromolecule at the appropriate time.<sup>2,3</sup> Just as a scarcity of a particular metal ion induces a stress response that can lead to reprogramming of cellular metabolism to minimize the consequences of depletion of a particular metal ion, e.g., zinc in ribosome biogenesis<sup>4</sup> or

\* To whom correspondence should be addressed. E-mail: giedroc@indiana.edu.

<sup>†</sup> Indiana University.

<sup>‡</sup> Texas A&M University.

<sup>§</sup> These authors contributed equally to this work.



Zhen Ma was born in Shanghai, China, in 1981. He earned his B.S. degree in Biological Sciences from Fudan University in 2004. He became a graduate student at Texas A&M University in 2004 and started his thesis research with Professor David P. Giedroc. His thesis work was focused on the copper regulatory protein CsoR, aimed at understanding the molecular details of this new family of metalloregulatory proteins in bacteria. He defended his dissertation work in September 2009.



David Giedroc graduated from the Pennsylvania State University in 1980 with his B.S. degree in Biochemistry. After a brief stint in Joseph Villafranca's group at Penn State, he earned his Ph.D. degree in Biochemistry at Vanderbilt University in 1984, where he worked with David Puett on the calcium sensor calmodulin. From 1984 to 1988, he was an NIH postdoctoral fellow in the late Joseph E. Coleman's laboratory at Yale University, where he worked on zinc-finger DNA binding proteins. From 1988 to 2007, he was a member of the faculty in the Department of Biochemistry and Biophysics at Texas A&M University. He is now Professor of Chemistry at Indiana University, where he continues his studies of metalloregulatory proteins and viral RNA structure, folding, and function.



Faith E. Jacobsen graduated in 2002 from Point Loma Nazarene University in San Diego, CA, with her B.S. degree in Biology and Chemistry. In 2002 she started graduate school at the University of California, San Diego. She earned her M.S. degree in Chemistry in 2004 and her Ph.D. degree in Chemistry in 2007. Her Ph.D. thesis work, under the guidance of Professor Seth M. Cohen, consisted of examining novel zinc-specific chelators for incorporation into inhibitors of matrix metalloproteinases. In 2008 she started her NIH-funded postdoctoral research with Professor David P. Giedroc, studying zinc homeostasis in *Streptococcus pneumoniae*.

Cu vs Fe in photosynthesis by *Synechocystis*,<sup>5</sup> too much of the same metal ion can also be toxic to a cell or organism.

Metal homeostasis is governed by the formation of specific protein–metal coordination complexes used to effect uptake, efflux, intracellular trafficking within compartments, and storage (Figure 1). How metal ions move to and from their target destinations in the active site of a metalloenzyme or as a structural component of biomolecules also contributes to intracellular metal homeostasis (Figure 1). Metal transporters move metal ions or small molecule–metal chelates across otherwise impermeable barriers in a directional fashion, and most of these are integral membrane proteins embedded in the inner or plasma membrane (Figure 1). Specialized proteins designated metallochaperones traffic metals within a particular cellular compartment, e.g., the periplasm or the cytosol, and function to “hold” the metal in such a way that it can be readily transferred to an appropriate acceptor protein. This intermolecular transfer is known or projected to occur through transiently formed, specific protein–protein complexes that mediate coordinated

intermolecular metal–ligand exchange. Metallochaperones have been described for copper,<sup>6–9</sup> nickel,<sup>10</sup> and iron–sulfur protein biogenesis,<sup>11</sup> and recent work suggests that the periplasmic Zn(II) binding protein, YodA, has characteristics consistent with a role as a zinc chaperone in *E. coli* (Figure 1).<sup>12</sup> Salient features of these chaperones are discussed in more detail in the context of acquisition and efflux of individual metal ions (section 2). Finally, specialized transcriptional regulatory proteins, termed metalloregulatory or metal sensor proteins, control the expression of genes encoding these proteins that establish metal homeostasis in response to either metal deprivation or overload (section 3).

A hypothesis that emerges is that in order to effect the cellular homeostasis of a particular metal ion, each component of the homeostasis machinery (Figure 1) must be selective for that metal ion under the prevailing conditions to the exclusion of all others.<sup>13</sup> Furthermore, individual systems must be “tuned” such that the affinity or sensitivity of each component is well matched, either to coordinate gene expression by pairs of metal sensor proteins that coordinately shut off uptake and up-regulate efflux or detoxification systems or to facilitate vectorial transport from metal-donor to metal-acceptor target protein in a metal-trafficking pathway in the cell (Figure 1).<sup>14–16</sup>

## 1.2. Introduction to Metal Transporters

In bacterial systems, acquisition of essential metal ions from the extracellular milieu requires special consideration (Figure 1). All Gram-negative bacteria possess an outer membrane (OM), a periplasmic space, and an inner cytoplasmic or plasma membrane through which the metal must pass before entering the cytosol; Gram-positive bacteria, in contrast, lack a periplasm. Trimeric  $\beta$ -barrel proteins called porins embedded in the outer membrane allow for nonselective passive diffusion of metal ions across the OM (Figure 1). In order to meet cellular metal demands, however, the cytosol must effectively *concentrate* metal ions.<sup>14</sup> As a result, high-affinity active transport systems in the OM or embedded

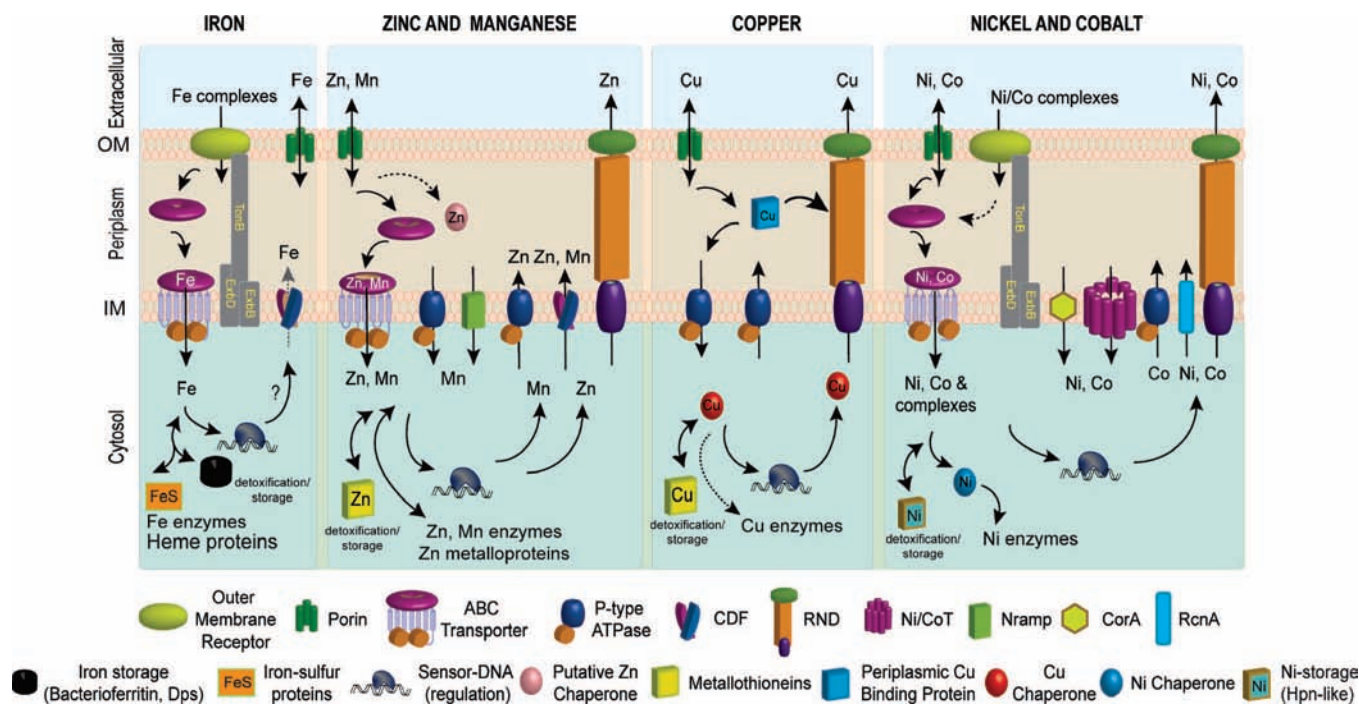


**Figure 1.** Schematic metal homeostasis models for iron, zinc and manganese, copper, and nickel and cobalt, shown specifically in Gram-negative bacteria. Homeostasis of molybdate and tungstate oxyanions are not shown, due primarily to a lack of knowledge of these systems, outside of uptake (section 2.5) and cytosolic sensing (section 3.8.1). This schematic is not representative for any one bacterium nor is it meant to be exhaustive but is instead simply designed to convey the potential fates of individual metal ions in distinct cellular compartments. Not all bacteria have all components of each homeostasis system indicated. The double-headed arrows are meant to illustrate that metals can move in and out of target protein destinations in response to proteome remodeling. Specific protein designations for individual homeostasis components are indicated in Figures 2 and 3. A putative chaperone shown for Zn(II) is YodA/ZinT,<sup>12</sup> while known metallochaperones for Cu(I) (Atx1<sup>221</sup> and CopZ<sup>407</sup>) and Ni(II) metalloenzymes (UreE<sup>10</sup>) or Ni-Fe hydrogenases (e.g., HypA<sup>10</sup>) are also shown. Iron metallochaperones for Fe-S cluster assembly are not shown for clarity.<sup>11</sup> Fe(II) efflux through YiiP<sup>175</sup> has not yet firmly established biochemically.<sup>176</sup> The cytosolic Cu(I) quota for a nonphotosynthetic bacterium may well be vanishingly small;<sup>7</sup> as a result, transfer from a Cu(I) chaperone is indicated by the dashed double-headed arrow.

in the plasma or inner membranes (PM or IM) function to transport and release metal ions into the cytosol. Inner membrane transport systems are driven either by the hydrolysis of ATP on the cytoplasmic side of the membrane, e.g., by ATP binding cassette (ABC) transporters and P-type ATPases, or by coupling to an energetically favorable transfer of protons or other ions across the bilayer, e.g., by Nramp proteins and cation diffusion facilitator (CDF) proteins. The presence of additional layers of extracellular lipopolysaccharide (LPS) or complex carbohydrate matrices, as well as a biofilm, is also likely to have a considerable impact on the rates and mechanisms of metal uptake and efflux.<sup>17</sup>

The expression of genes encoding plasma membrane-bound transporters that allow for the high-affinity uptake of specific metal ions or metal ion complexes into the cytosol may be constitutive or “on” under unstressed homeostatic conditions, i.e., most biologically required transition metal ions are limiting under these conditions. When the cytosolic concentration of a metal becomes too high, genes that encode for these transporters are repressed in an effort to decrease the cytosolic uptake of that metal ion. In addition to shutting “off” the import of metal ions into the cell, the effects of extremely high cytosolic concentrations of a particular metal ion also have to be mitigated. This can occur by sequestration of the metal ion by intracellular chelators, including low molecular weight Cys-rich metallothioneins<sup>18,19</sup> or ferritin-like bacterioferritins or Dps complexes<sup>20,21</sup> or via efflux of the metal from the cytosol (Figure 1).<sup>22</sup>

In this context, it is important to emphasize that cytosolic metal stress can derive not only from extracellular sources

but also from intracellular origins. Potential sources of intracellular metal stress include turnover of metalloenzymes and a shift from anaerobic to aerobic growth conditions or as a result of acute oxidative or nitrosative stress, the latter of which destroys Fe-S clusters, for example (Figure 1).<sup>21</sup> Indeed, a recent report reveals that the transcriptional response of *S. pneumoniae* to high extracellular Mn(II) vs intracellular Mn(II) accumulation due to deletion of a Mn(II) effluxer are distinguishable.<sup>23</sup> Although the mechanism by which this is achieved is not known, these findings suggest the possibility that cytosolic metal sensors may not “scan” the cytosol for metal toxicity (as schematized in Figure 1) but may instead be dedicated to sensing metal availability or flux through a specific transporter via protein-protein interactions. Alternatively, a sensor may not be capable of sensing such flux due to intracellular compartmentalization.<sup>24</sup> Two-component response-regulator systems that monitor “extracellular” or “periplasmic” (in the case of Gram-negative bacteria) metal stress may play a role in this process. These have been identified for copper, and this copper response is known to be distinct yet integrated with that required for sensing of cytosolic Cu(I).<sup>25</sup>

### 1.3. Introduction to Metal Sensor Proteins

All cells possess a battery of regulatory proteins that mediate homeostasis of transition metal ions by regulating the expression of genes that encode metal transporters, intracellular chelators, and/or other detoxification enzymes.<sup>22</sup> These proteins have been coined metal sensor<sup>22,26</sup> or metal-



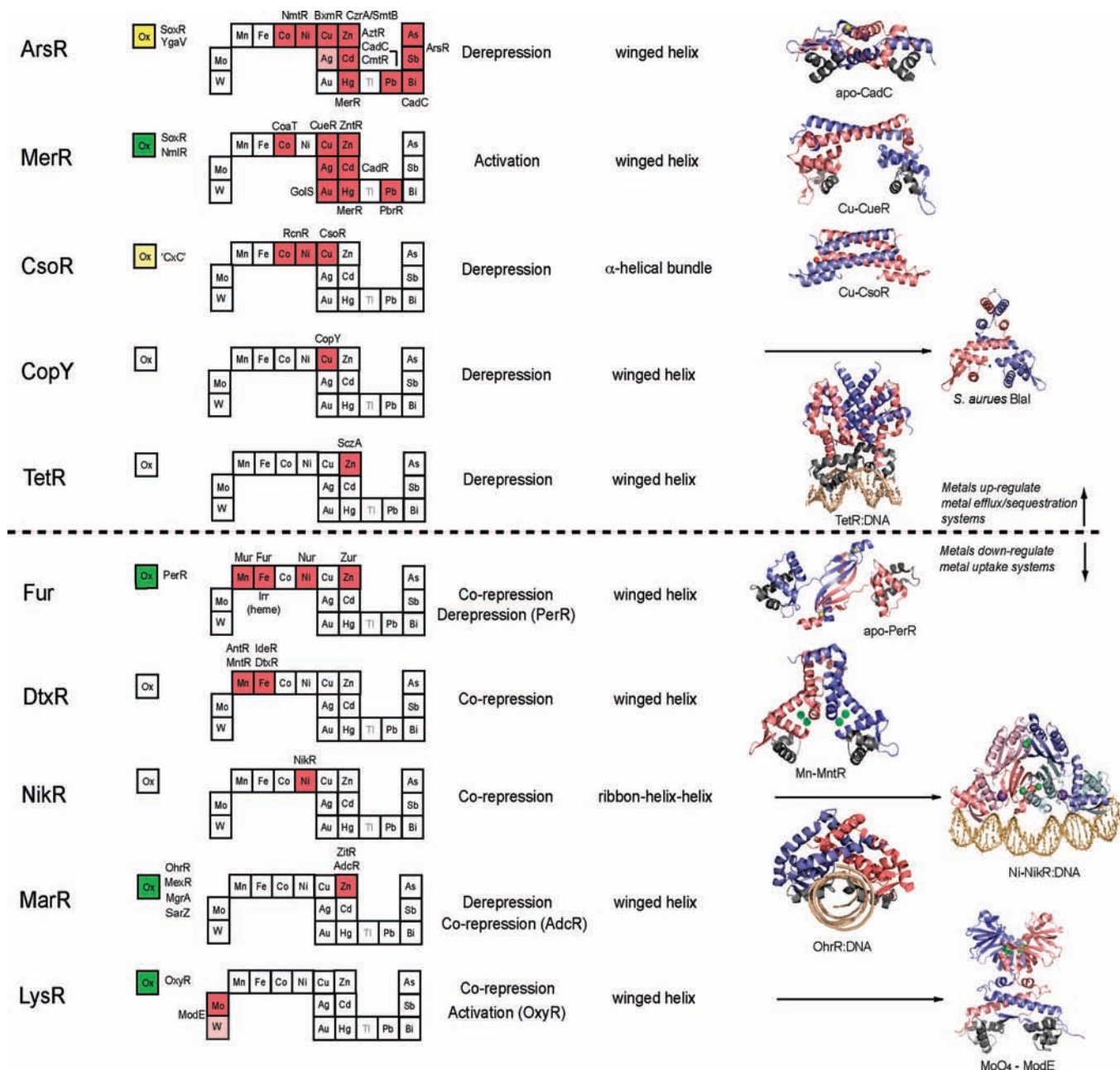


**Figure 2.** Structural families of metalloregulatory proteins. For each family, boxes for metals that are known to be sensed are shaded red on the abbreviated periodic table, while green boxes on the left denote family members that are known to sense cytosolic oxidative stress. Boxes identifying putative metal sensors and nonmetal-sensing oxidative stress regulators are shaded pink or yellow, respectively. The four-letter designations for individual proteins that perform the function listed in the nearby box are given (see text for details). The mechanism of regulation of gene expression is indicated as is the DNA binding domain that mediates operator–promoter DNA binding. Ribbon representations of selected representative members are shown on the right with individual protomers shaded red and blue in each case. Structures are from top to bottom: (1) apo *S. aureus* pI258 CadC with structural  $\alpha 5$ -Zn(II) ions shaded yellow (1U2W pdb code);<sup>255</sup> (2) *E. coli* Cu(I)–sensor CueR with regulatory Cu(I) ions in red (1Q05);<sup>34</sup> (3) *M. tuberculosis* Cu(I)–sensor CsoR with regulatory Cu(I) ions shaded red (2HH7);<sup>244</sup> (4) *S. aureus* BlaI as a model for *Enterococcus* CopY (1SD4);<sup>320</sup> (5) TetR-Tc-Mg DNA complex structure as model for *S. pneumoniae* SczA (3CDL);<sup>398</sup> (6) apo *B. subtilis* PerR with structural Zn(II) ions in yellow (2FE3);<sup>331</sup> (7) *B. subtilis* MntR with Mn<sub>A</sub>/Mn<sub>C</sub> binuclear cluster ions in green (2F5F);<sup>352</sup> (8) Ni(II)-bound *E. coli* NikR-nik operator DNA complex with high-affinity Ni(II) ions shown in green and regulatory K<sup>+</sup> ions in purple (2HZV);<sup>362</sup> (9) *B. subtilis* OhrR-DNA complex (1Z9C);<sup>390</sup> (10) molybdate sensor ModE with molybdate shaded green (1O71).<sup>387</sup> Adapted with permission from ref 22. Copyright 2007 Royal Society of Chemistry.

loregulatory<sup>27</sup> proteins. Each forms specific coordination complexes with metal ions that ultimately inhibit or activate operator DNA binding or directly enhances transcriptional activation. In this way, cells effectively control the expression of genes that mediate the homeostasis of metal ions.

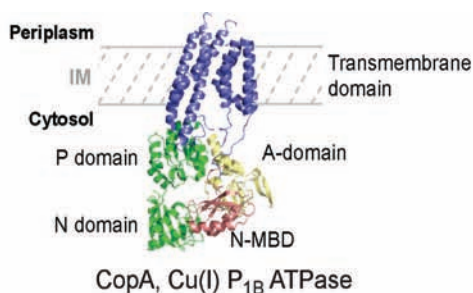
Metal sensor proteins can be functionally divided into two groups: those that control gene expression linked to metal-ion efflux and/or storage (Figure 2, top) and those that control

the expression of genes required for metal ion uptake (Figure 2, bottom). In general, metal sensor proteins that control metal uptake all bind metal ions as corepressors, exactly analogous to the well-studied bacterial Trp repressor that controls tryptophan biosynthetic genes in a Trp-dependent manner;<sup>28</sup> in other words, metal binding causes the repression of the genes that allow for metal ion uptake.<sup>22</sup> On the contrary, metal sensor proteins that regulate efflux and/or

## P-type ATPase

	Mn	Fe	Co	Ni	Cu	Zn		As
					Ag	Cd	CadA	Sb
Mo					Au	Hg	Tl	Pb
W								Bi

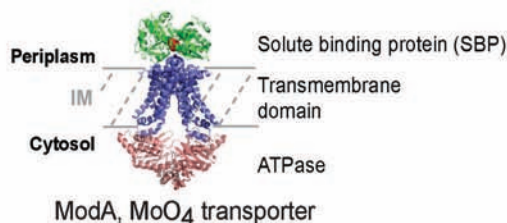
MntA, CoaT, CopA, CopB, CopA, AztA, ZiaA, ZntA, As, Mo, W, GoIT, Au, Hg, Tl, Pb, Bi



## ABC Transporter

	Mn	Fe	Co	Ni	Cu	Zn		As
					Ag	Cd		Sb
Mo					Au	Hg	Tl	Pb
W								Bi

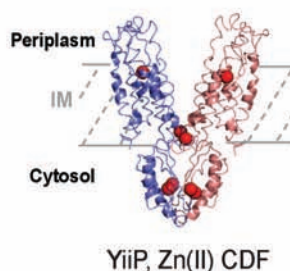
PsaA, FbpA, NikA, AdcA, MntC, BtuF, ZnuA, As, Mo, W, ModA, Au, Hg, Tl, Pb, Bi, ArsA



## Cation Diffusion Facilitator

	Mn	Fe	Co	Ni	Cu	Zn		As
					Ag	Cd		Sb
Mo					Au	Hg	Tl	Pb
W								Bi

MntE, YiiP, CzoD, YiiP, ZitB, As, Mo, W, Au, Hg, Tl, Pb, Bi



## Nramp

	Mn	Fe	Co	Ni	Cu	Zn		As
					Ag	Cd		Sb
Mo					Au	Hg	Tl	Pb
W								Bi

MntH, As, Mo, W, Au, Hg, Tl, Pb, Bi

No structures known

## RND

	Mn	Fe	Co	Ni	Cu	Zn		As
					Ag	Cd		Sb
Mo					Au	Hg	Tl	Pb
W								Bi

NocCBA, CnrCBA, CusCFBA, CzoCBA, As, Mo, W, SiICBA, Au, Hg, Tl, Pb, Bi

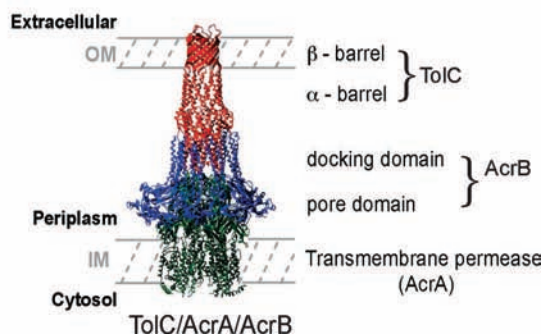


**Figure 3.** Structural families of metal transporters. Individual elements on the abbreviated periodic table are shaded red if they are specifically imported by a member of that particular family or blue if they are effluxed. Metal ions that are transported nonspecifically are shaded pink for uptake or light blue for efflux. The four-letter designations for individual proteins that perform the indicated function are given; this list is not meant to be comprehensive but rather shows representative members that have been structurally and/or functionally characterized (see text for details). Ribbon representations of crystallographic structures of one member of each family summarize salient structural features of each transporter. The structures shown are as follows: (1) *Archaeoglobus fulgidus* CopA monomer, a Cu(I)-selective P<sub>1B</sub>-type ATPase (2 VOY);<sup>71</sup> (2) *Archaeoglobus fulgidus* MoO<sub>4</sub><sup>-</sup>-ABC transporter with MoO<sub>4</sub><sup>-</sup> in red (2ONK);<sup>408</sup> (3) *E. coli* Zn(II) transporting CDF proteins YiiP with zinc atoms shaded red (2QFI);<sup>68</sup> (4) there are no reported structures for an Nramp transporter; (5) combined hypothetical structure of an RND complex. This panel adapted with permission from ref 409. Copyright 2004 Elsevier Limited.

intracellular storage function via a transcriptional derepression or an activation mechanism. In the vast majority of cases, metal binding causes the binding affinity of the sensor protein for its specific DNA operator sequence to decrease substantially and likely dissociate; this, in turn, exposes the promoter, the DNA binding site for RNA polymerase, permitting initiation of transcription. In much that same way, lactose and lactose analogs modulate the affinity of the lactose repressor, LacI, for operator DNA (section 3.1.3).<sup>29,30</sup>

Transcriptional activation by MerR regulators occurs via a DNA distortion or “underwinding” mechanism (section 3.2.2),<sup>22,31</sup> while other activators, e.g., OxyR (section 3.8.1), appear to undergo multimerization and make direct protein–protein contacts with RNA polymerase to enhance the initiation of transcription.<sup>32,33</sup>

Figure 2 summarizes the structural and functional properties of 10 families of structurally distinguishable regulatory proteins, each of which has at least one known or projected

member that senses metals directly. This summary is striking for a number of reasons. First, metal sensor proteins are evolutionarily related orthologs of other transcriptional regulatory proteins that control gene expression by binding small organic molecules, from lipophilic antimicrobial agents to intermediary metabolites to amino acids, rather than metal ions. In other words, there is nothing intrinsically unique about the global structures and mechanisms of action of metal sensor proteins relative to other ligand-regulated transcriptional switches, except in the evolution of “ligand” binding sites that optimize metal-specific coordination chemistry to effect the specificity of the biological response (section 3 below).<sup>13,26,34,35</sup>

Second, many metal sensor structural classes have known (green boxes, Figure 2) or predicted (yellow boxes, Figure 2) representatives that mediate resistance to oxidative and/or nitrosative stress. These proteins either exploit the reversible oxidation–reduction chemistry or intrinsic reactivity of cysteine thiols or use a direct metal-mediated sensing of reactive oxygen species, e.g., by the MerR family regulator SoxR (section 3.2.2) and the Fur family regulator PerR (section 3.5.1). While not metal sensors themselves, informative parallels between oxidative and metal stress-sensing systems will be discussed here. Third, some metal sensor families, notably the ArsR and MerR families, are very large and have members that sense a wide range of biologically required metal ions, heavy metal pollutants, and oxidative stress; in contrast, others do not. While this may be at least partly explained by our relatively advanced understanding of sensor proteins from these two structural classes,<sup>34,36–38</sup> other regulator folds may not be as malleable to evolutionary variation. For ArsR proteins in particular, allosteric *inhibition* of DNA binding by metal binding that leads to derepression of transcription may involve fewer evolutionary constraints relative to allosteric *activation* by MerR family proteins. This, in turn, might facilitate the evolution of multiple allosteric sites on a single-domain structural scaffold. In any case, detailed comparative studies of individual members from a single family provide significant insight into the evolution of metal specificity on a constant structural scaffold (sections 3.1.2, 3.2.1, and 3.3.2). Analogous studies of the origins of metal selectivity of the periplasmic binding proteins of ABC transporters and P-type ATPases provide many of the same insights and are also discussed below (section 2).

#### 1.4. Scope of This Review

This review will evaluate the degree to which bacterial metal transporters and metal sensor proteins are known to exploit specific coordination chemistries of metal–ligand complexes to “select” a cognate metal or metal complex in mediating the cellular metal homeostasis. An extensive discussion of bacterial metallochaperones is beyond the scope of this review, although reference is made here to those involved in bacterial copper homeostasis. The reader is directed to more comprehensive reviews on this subject<sup>9,15,39</sup> as well as those covering metallochaperones that function in metalloenzyme maturation.<sup>10,11</sup> Particular features of the coordination chemistry of metal transporters and sensor proteins discussed here are the metal–ligand geometry, nature and number of the coordinating atoms (coordination number,  $n$ ), and thermodynamic stability of these complexes. We begin by discussing the cellular uptake of each transition metal with emphasis on the degree to which coordination

chemistry dictates metal preference. A discussion of the various metal ion efflux mechanisms will follow, again highlighting the role that structural differences around the metal ion might play in metal discrimination. Finally, the structure and function of the metal sensor proteins will be examined in detail, focusing first on representative members of each family, followed by insights into ligand selectivity within individual families.

Our discussion of metalloregulatory proteins is limited to “one-component” metal-sensing systems in prokaryotes in which a single protein senses the metal *and* modulates the transcriptional profile directly in a reversible manner. As such, we will not discuss two-component, response regulator signal transduction systems, a few of which have been documented to detect metals, e.g., the Cu-sensing *cusRS*<sup>40</sup> and *cpxAR*<sup>41</sup> systems in *E. coli*, due largely to a lack of structural insight into these systems, nor do we discuss in any detail metal and heme-containing regulatory systems that specifically sense molecular oxygen or other diatomic gas molecules, CO and NO, that are not obviously evolutionarily related to the metal sensors discussed here. These include the 4Fe–4S cluster protein *E. coli* FNR (fumarate and nitrate reduction regulator), *E. coli* NorR, a nonheme mononuclear ferrous-ion-containing NO sensor,<sup>42,43</sup> and heme-based gas molecule-sensing systems, each of which has been recently reviewed elsewhere.<sup>44–48</sup> Finally, we attempt to highlight recent activity in the field, and the reader is referred to previous monographs that expand upon some aspects of what is covered here in greater detail.<sup>3,6,7,9,13,22,27,36</sup>

## 2. Acquisition and Efflux of Transition Metal Ions in Bacteria

ATP binding cassette transporters<sup>49,50</sup> and Nramp transporters<sup>51–53</sup> mediate the accumulation of specific metal ions in the cytosol of bacterial cells, while export (efflux) of these metal ions is largely carried out by cation diffusion facilitators (CDFs),<sup>54</sup> P-type ATPases,<sup>55–58</sup> and tripartite RND (resistance–nodulation–cell division) transporters.<sup>59</sup> In a couple of instances, P-type ATPases have been implicated in Cu(I)<sup>60–62</sup> or Mn(II)<sup>61</sup> uptake into the cytosol on the basis of whole cell experiments and in one case, *Lactobacillus plantarum* MntA, may be needed to satisfy a very large intracellular Mn(II) requirement; the mechanism and driving force of this transport remains unexplored.<sup>58</sup> Another major class of membrane permeases, the major facilitator superfamily (MFS) family of H<sup>+</sup> antiporters, the paradigm for which is *E. coli* lactose permease LacY,<sup>63</sup> while extensively characterized as effluxers of lipophilic drugs important for multidrug resistance,<sup>64</sup> have not yet been firmly linked to the metal efflux in bacteria, although this may well change.<sup>65–67</sup>

Individual members of each structural class of metal transporter are capable of transporting a variety of metals into and out of the cell, but some tend to be more selective for certain metals over others (Figure 3). For instance, Nramps have thus far only been identified as manganese and iron transporters, whereas ABC transporters have been identified and characterized for nearly every biologically required transition metal ion. High-resolution structures of representative members of a number of multisubunit ABC transporters,<sup>49</sup> a single CDF protein, the Zn(II) transporter *E. coli* YiiP,<sup>68</sup> and the Ca(II)-pumping P-type ATPase<sup>69,70</sup> have been solved, which when coupled with a lower resolution model of an archeal Cu(I)-translocating P-type ATPase, *Archaeoglobus fulgidus* CopA,<sup>71</sup> have helped to



**Table 1. Coordination Complexes Formed by Solute Binding Proteins (SBPs) from Various Fe(III)-Specific ABC Transporters of Known Structure**

ferric binding protein	coordinating groups	coordinating atoms	coordination number	ref
<i>Hemophilus influenza</i>	His <sup>9</sup> Glu <sup>57</sup> Tyr <sup>195</sup> Tyr <sup>196</sup> H <sub>2</sub> O PO <sub>4</sub> <sup>3-</sup>	NO <sub>5</sub>	6	91
<i>Neisseria gonorrhoeae</i>	His <sup>9</sup> Glu <sup>57</sup> Tyr <sup>195</sup> Tyr <sup>196</sup> H <sub>2</sub> O PO <sub>4</sub> <sup>3-</sup>	NO <sub>5</sub>	6	1D9Y
<i>Mannheimia hemolytica</i>	Tyr <sup>142</sup> Tyr <sup>198</sup> Tyr <sup>199</sup> CO <sub>3</sub> <sup>2-</sup>	O <sub>5</sub>	5	406
<i>Yersinia enterocolitica</i>	His <sup>9</sup> Glu <sup>57</sup> Tyr <sup>195</sup> Tyr <sup>196</sup> H <sub>2</sub> O	NO <sub>5</sub>	6	95
<i>Campylobacter jejuni</i>	His <sup>14</sup> Tyr <sup>15</sup> Tyr <sup>146</sup> Tyr <sup>202</sup> Tyr <sup>203</sup>	NO <sub>4</sub>	5	93
<i>Synechocystis 6803</i>	His <sup>54</sup> Tyr <sup>55</sup> Tyr <sup>185</sup> Tyr <sup>241</sup> Tyr <sup>242</sup>	NO <sub>4</sub>	5	94

place transition metal transport in a structural and mechanistic context (Figure 3). The following sections highlight recent structural insights into how a particular transporter interacts specifically with a particular metal ion, arranged by metal-ion type.

## 2.1. Acquisition of Iron

Iron is an essential element for nearly all organism, notable exceptions being the human pathogen *Borrelia burgdorferi*, the causative agent of Lyme disease,<sup>72</sup> *Lactobacillus plantarum*,<sup>73</sup> and *Streptomyces suis*.<sup>74</sup> Each of these organisms has a very high intracellular requirement for Mn(II), which may well fulfill many of the roles played by Fe(II) in other bacteria. An excess of free iron, particularly Fe(II), is lethal because it can produce radicals in the presence of dioxygen or peroxides.<sup>75</sup> Iron is generally a growth-limiting factor for many prokaryotes due to the low solubility of Fe(III) in water at neutral pH but is required for a number of essential enzymes, including the cytochromes, ribonucleotide reductase, and Fe–S cluster biogenesis.<sup>76</sup> As such, multicellular hosts exercise strict control over the availability of iron to infectious microorganisms via chelation by lipocalins and the use of other high-affinity transport proteins<sup>77</sup> to control infectious disease.<sup>76,78</sup> Thus, the free or bioavailable pool of iron in virtually any microenvironment is much lower than what is necessary for Fe-requiring bacteria to survive. Nonetheless, the total concentration of iron is 100-fold higher in *E. coli* vs a chemically defined minimal medium,<sup>14</sup> demonstrating an impressive concentration of iron within the bacterial cell. Indeed, bacteria have evolved a multiplicity of specialized ways to import, store, and sequester iron.<sup>76</sup>

Iron acquisition can occur by either direct uptake of host iron- or heme-containing proteins or iron binding chelators called siderophores.<sup>77</sup> In Gram-negative bacteria, high-affinity outer membrane (OM) receptors first bind lactoferrin, ferritin, siderophores (ferrichrome, FhuA),<sup>79</sup> or other low molecular weight Fe chelates, e.g., Fe–citrate (FecA),<sup>80</sup> and mediate the transport of iron through the OM into the periplasm.<sup>81,82</sup> These receptors are 22-stranded  $\beta$ -barrel proteins that contain extracellular loops that bind substrates and an N-terminal region or plug that folds into the barrel near the periplasmic surface. Since there are no ion gradients to energize the OM, transport across the OM is coupled to the proton motive force of the cytoplasmic membrane via a periplasm-spanning complex composed of TonB, ExbB, and ExbD (Figure 1).<sup>77,83</sup> The reversible association of TonB with an interacting domain in the N-terminal plug region of the OM transporter, the Ton box,<sup>84</sup> mediates at least part of this energetic coupling, although the mechanistic details remain the subject of ongoing investigation.<sup>85</sup> Once in the periplasm, the uptake of Fe(III) or Fe(III) chelates occurs through the transmembrane channel of ATP binding cassette (ABC) transporters<sup>49,50</sup> found in the plasma membrane in a process mediated by ATP hydrolysis of the cytosolic ATPase subunits. In Gram-

positive organisms, ABC transporters are found in the plasma membrane just underneath the cell wall.<sup>82,86</sup> In both cases, the specificity of this transport is mediated by the solute binding protein (SBP) component of the transporter. The SBP is freely diffusible in the periplasm of Gram-negative bacteria (see Figure 1) (and thus are equivalently denoted periplasmic binding proteins or PBPs) but is covalently anchored to the plasma membrane in Gram-positive bacteria. The soluble portion of the lipid-anchored SBP adopts an identical fold to periplasmic binding proteins, both of which dock on the cognate transmembrane channel of the transporter for metal delivery (Figures 1 and 3). In some bacteria, e.g., *Helicobacter pylori*, iron can be transported across the plasma membrane as Fe(II) or Fe(III) with the high-affinity FeoB transporter specific for Fe(II).<sup>87</sup>

There are many excellent reviews that focus in depth on the mechanisms of bacterial iron transport.<sup>77,82,88–90</sup> As such, we limit our discussion to the metal selectivity of Fe(III)-transporting SBPs as to their coordination number and nature of ligand donor atoms as revealed by high-resolution structural studies. Crystallographic structures of six Gram-negative Fe(III) binding SBPs have now been determined.<sup>77</sup> Each employs at least four oxygen atoms to coordinate the Fe(III) atom and have a coordination number (n) of 5 or 6 (Table 1). The Fe(III) binding SBPs of *N. gonorrhoeae* and *H. influenza* are homologous and reveal that iron binds to two consecutive tyrosine residues, one glutamic acid, one histidine, a water molecule, and a phosphate ion to give a coordination sphere of NO<sub>5</sub> and a coordination number of 6 (Table 1; Figure 4).<sup>91</sup> The structures of these proteins are interesting because they mimic the binding of iron by transferrin,<sup>92</sup> which binds iron with a coordination sphere of Tyr92, Tyr192, His253, Asp60, and a bidentate bicarbonate anion. In transferrin, the two tyrosine residues are found in opposite domains of this two-domain protein, a structural feature that controls the capture of Fe(III); in contrast, all of the Fe(III) SBP structures contain two adjacent tyrosine residues as ligands to the Fe(III).<sup>77</sup>

The crystallographic structures of Fe(III) SBPs from *Y. enterocolitica*, *C. jejuni*, and *Synechocystis* are unique in that they do not contain an exogenous coordinating anion,<sup>93–95</sup> an obligate ligand in transferrin.<sup>92</sup> How Fe(III) is stripped from transferrin and lactoferrin and brought into the periplasm in Gram-negative bacteria for binding by SBPs<sup>77</sup> is the subject of current studies. In *N. gonorrhoeae* this is believed to occur through the proteins TbpB and TbpA.<sup>96,97</sup> TbpB is thought to bind transferrin initially, while TbpA extracts the Fe(III) atom from the transferrin, likely via a ligand exchange mechanism. A similar pair of proteins (LbpA/LbpB) is thought to have an analogous function in extracting Fe(III) from lactoferrin.<sup>77</sup>

Many bacteria can also obtain Fe(III) from hemoproteins and siderophores that the bacteria themselves secrete and directly uptake these Fe(III) complexes into the cytosol

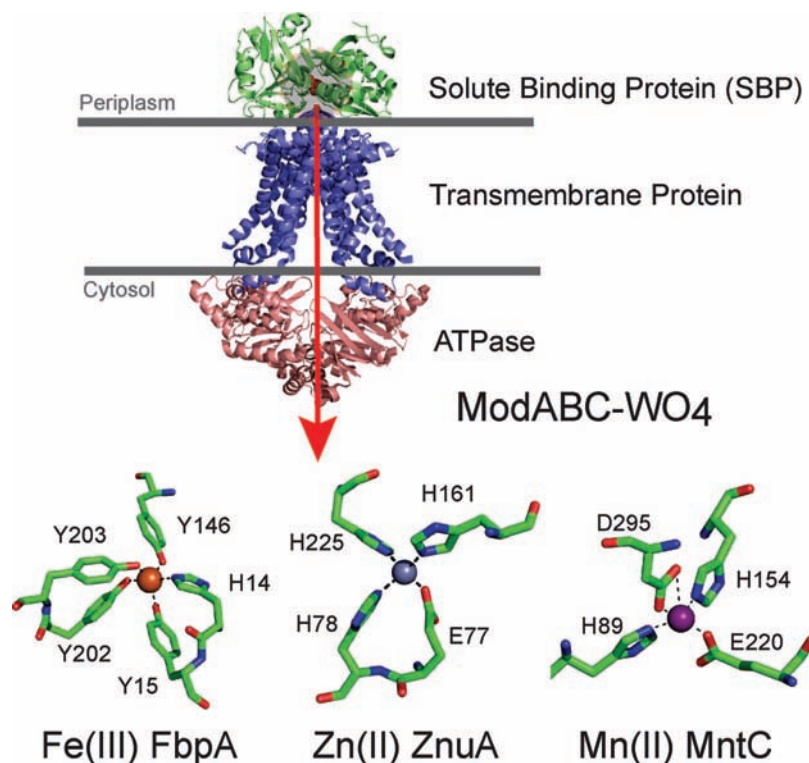


**Figure 4.** Structure of a representative ABC importer, *E. coli* ModABC<sup>408</sup> with the direction of transport shown by the red arrow. The green subunit ModA is the solute binding protein (SBP), with the position of the  $\text{WO}_4^{2-}$  anion shaded red and highlighted in the gray circle. Other SBPs adopt a global structure similar to ModA but feature distinct metal coordination sites as shown for Fe(III)-, Zn(II)-, and Mn(II)-specific SBPs (lower part of figure). Coordination sites are shown for the Fe(III)-specific SBP *Campylobacter jejuni* FbpA (1Y4T),<sup>93</sup> a Zn(II)-SBP *E. coli* ZnuA (2O5V),<sup>410</sup> and the Mn(II)-SBP *Synechocystis* 6803 MntC (1XVL).<sup>122</sup>

before degrading them (Figure 1). Thus, the mechanism for transport of Fe(III) across the plasma membrane does not involve the direct coordination of Fe(III); nonetheless, the mechanism for uptake is analogous to that employed for uncomplexed Fe(III). The structures of these proteins and their functions have been reviewed in detail elsewhere.<sup>77</sup> Specialized membrane transporters are also required to export the Fe(III)-free siderophores from the cytosol to the extracellular milieu. In the majority of characterized systems in both Gram-negative and model Gram-positive organism, *B. subtilis*, these transporters are from the Major Facilitator Superfamily (MFS);<sup>63,67</sup> however, in at least a few cases, ABC transporters have also been shown to perform this role.<sup>98</sup>

## 2.2. Acquisition of Zinc and Manganese

Zinc is one of the most abundant transition metals in any given bacterium, reaching an apparent concentration of  $10^{-4}$  M in *E. coli*, compared to  $10^{-7}$  M in a rich growth medium, Luria-Broth.<sup>14</sup> However, most Zn(II) is bound to nearly 100 different proteins or enzymes<sup>99</sup> with the current evidence consistent with the idea that bacterial cells possess an overcapacity to chelate zinc, rendering the pool of “bioavailable” zinc vanishingly small.<sup>14</sup> The same may well be true for Cu(I) but for different reasons (see section 2.3). Zinc can play a structural, regulatory, or catalytic role in proteins. Structural Zn(II) stabilizes proteins or protein domains from unfolding and can be considered an inorganic analog of disulfide bonds in the reducing environment of the cytosol.<sup>100</sup> Prominent examples of structural Zn(II) include two of the most abundant macromolecular assemblies in bacterial cells, RNA polymerase<sup>101</sup> and the ribosome, where Zn(II) is a structural component of several ribosomal proteins.<sup>102</sup> There

is some evidence to suggest that tetrathiolate ( $\text{S}_4$ ) structural Zn(II) complexes in proteins can also perform a regulatory role via reversible oxidation of the coordinating Cys residues and displacement of the bound Zn(II),<sup>103</sup> although the significance of this in the cell is not fully resolved.

The principal catalytic role of Zn(II) is as nature’s primary Lewis acid where it activates a water molecule to cleave covalent bonds, e.g., in zinc metalloproteases<sup>78</sup> and a wide range of other hydrolytic enzymes. Zinc proteins are involved in DNA replication, glycolysis, pH regulation, and the biosynthesis of amino acids,<sup>99</sup> extracellular peptidoglycan,<sup>104</sup> and low molecular weight thiols, and as a result, zinc status is linked to maintenance of the intracellular redox buffering of the cell.<sup>105,106</sup> Like iron, there is a lower concentration of zinc outside of the cell than there is inside, and zinc availability may well be limiting in many microenvironments, although likely not to the same degree as iron.<sup>14</sup>

Manganese is also a required transition metal for most bacteria, and the evidence is compelling that Mn(II) homeostasis plays a significant role in virulence and pathogenesis of many human microbial pathogens.<sup>23,53,107</sup> Although the total Mn(II) concentration in *E. coli* is comparable to that of Cu(I) and  $\sim 10$ -fold lower than that of Zn(II) and Fe(II), there may be considerably more weakly bound Mn(II) relative to Zn(II), as required by the Irving–William series.<sup>2,3,108</sup> Bacterial manganese superoxide dismutases encoded by *sodA* are ubiquitous, but every organism also has other specific roles that have been evolved for manganese.<sup>109</sup> For instance, manganese is thought to be a required cofactor in two presumed Ser/Thr/Tyr protein kinases (YniA/YcfN) in *S. typhimurium*.<sup>53</sup> In addition, manganese plays a role in carbon metabolism as enolase, pyruvate kinase, lactate dehydrogenase, phosphoenolpyruvate (PEP) carboxylase, and



**Table 2. Coordination Complexes Formed by Solute Binding Proteins (SBPs) from Various Zn(II)- and Mn(II)-Specific ABC Transporters of Known Structure**

organism, metal binding protein	proposed metal bound	coordinating groups	coordinating atoms	coordination number	ref
<i>Synechocystis</i> 6803, ZnuA	Zn	His <sup>83</sup> His <sup>179</sup> His <sup>243</sup> H <sub>2</sub> O	N <sub>3</sub> O	4	121
<i>E. coli</i> , ZnuA	Zn	His <sup>60</sup> His <sup>143</sup> His <sup>207</sup> H <sub>2</sub> O	N <sub>3</sub> O	4	123
<i>Streptococcus pneumoniae</i> , AdcAII	Zn	His <sup>71</sup> His <sup>147</sup> His <sup>211</sup> Glu <sup>286</sup>	N <sub>3</sub> O	4	120
<i>Treponema pallidum</i> , TroA	Zn/Mn	His <sup>68</sup> His <sup>133</sup> His <sup>199</sup> Asp <sup>279</sup>	N <sub>3</sub> O <sub>2</sub>	5	124
<i>Streptococcus pneumoniae</i> , PsaA	Mn <sup>a</sup>	His <sup>67</sup> His <sup>139</sup> Asp <sup>280</sup> Glu <sup>205</sup>	N <sub>2</sub> O <sub>2</sub>	4	114
<i>Synechocystis</i> 6803, MntC	Mn	His <sup>89</sup> His <sup>154</sup> Glu <sup>220</sup> Asp <sup>295</sup>	N <sub>2</sub> O <sub>3</sub>	5	122
<i>Synechocystis</i> 6803, MncA	Mn	His <sup>101</sup> His <sup>103</sup> His <sup>147</sup> Glu <sup>108</sup> H <sub>2</sub> O	N <sub>3</sub> O <sub>2</sub>	5	2

<sup>a</sup> Crystallized with Zn rather than Mn.

PEP carboxykinase are enzymes that are either manganese dependent or highly activated by manganese.<sup>53</sup> Manganese is also a required cofactor for the biosynthesis of the extracellular capsule of *Streptococcus pneumoniae* through the activity of a Mn(II)-dependent tyrosine phosphatase.<sup>110</sup>

In some bacteria, the hyperaccumulation of low molecular weight Mn(II) complexes is hypothesized to directly protect microorganisms, e.g., *Deinococcus radiodurans*, from oxidative stress and radiation damage to DNA as a result of minimizing the production of iron-dependent reactive oxygen species.<sup>111</sup> The generality of this mechanistic hypothesis to other bacteria has not yet been established, and recent studies in *E. coli* suggest that Mn(II) import [through MntH (see below), which itself is activated by the H<sub>2</sub>O<sub>2</sub> sensor OxyR (section 3.8.1)] protects hydrogen peroxide-stressed cells by metallating mononuclear Fe(II)-containing enzymes that will minimize protein oxidation under these conditions.<sup>112</sup> In any case, the protective effect of Mn(II) is unlikely to be traced to nonenzymatic superoxide dismutation activity or as a chemical quencher of hydrogen peroxide.

Like iron, zinc and manganese are transported into the cytosol by ABC transporters with the metal selectivity of this process thought to be dictated largely by the SBP component of the transporter (Figures 1 and 3). In addition, many bacteria import manganese using a second transporter, MntH, which are Nramp proteins similar to those found in mammalian macrophages.<sup>53,113,114</sup> The concentrations of Zn(II) and Mn(II) in the periplasm are not known, but Zn(II) availability may well be limiting. For example, when cells are stressed by low (sub-micromolar) zinc, periplasmic *E. coli* Cu, Zn superoxide dismutase (encoded by *sodC*) has no activity; it is only when cytosolic uptake by the ABC transporter ZnuABC is inhibited that significant SodC activity is observed.<sup>78</sup> This suggests the possibility that zinc chaperones may be necessary to compete with ZnuA for Zn(II) in this compartment under zinc-depleted conditions. Alternatively, excess intracellular zinc may occur as a result of oxidative stress which would liberate Zn(II) from thiol-containing complexes; as a result, periplasmic SodC would be metalated only under conditions that could provide protection against oxidative stress. In any event, there is as yet no documented Zn(II) chaperone that is specific for metalation of a particular zinc enzyme, as described for Cu-metalloenzymes.<sup>115</sup> One candidate for such an activity is *E. coli* YodA (ZinT),<sup>116,117</sup> a periplasmic Zn(II)/Cd(II) binding protein that adopts a fold<sup>118</sup> reminiscent of Fe-sequestering lipocalins.<sup>119</sup> Recent work<sup>12</sup> shows that YodA is weakly upregulated under zinc-depleted concentrations and that the  $\Delta yodA$  strain shows a reduced growth phenotype. These data suggest that YodA may function as a periplasmic chaperone to the zinc transporter ZnuABC under these conditions (see Figure 1).<sup>12</sup> Interestingly, in the Gram-

positive organism, *S. pneumoniae*, a YodA domain is fused directly to AdcA, the SBP-containing subunit of the high-affinity Zn(II) transporter AdcCBA in that organism. The role of the YodA domain in zinc uptake has not yet been established.

Numerous high-resolution structures of SBPs from ABC transporters thought to be specific for zinc or manganese are now available (Table 2). These include *S. pneumoniae* PsaA<sup>114</sup> and AdcAII<sup>120</sup> from Gram-positive organisms and *Synechocystis* ZnuA,<sup>121</sup> *Synechocystis* MntC,<sup>122</sup> *E. coli* ZnuA,<sup>123</sup> and *Treponema pallidum* TroA from Gram-negative bacteria.<sup>124</sup> PsaA<sup>114</sup> and MntC<sup>122</sup> are proposed manganese binding proteins, while AdcAII and ZnuA are zinc binding proteins. The metal selectivity of TroA remains unclear,<sup>124</sup> though based on the sequence homology and metal coordination environment it appears to be a manganese-specific SBP.<sup>120</sup> A comparison of these structures reveals that, in general, Mn(II) binding proteins have higher metal–ligand donor coordination numbers than zinc binding proteins, and this may be a primary criterion for metal selectivity in these systems (Table 2; Figure 4).

*S. pneumoniae* AdcAII (Table 2) is an orphan SBP of unknown function located on the cell surface of many Gram-positive pathogens that is not an obligatory component of any ABC transporter.<sup>120</sup> AdcAII is unique in that it is regulated by the same metalloregulatory protein that controls the expression of the zinc transporter AdcCBA, AdcR (Figure 2; section 3.8.2).<sup>125,126</sup> Zn(II) binds to SBP domain of AdcAII in a tetrahedral coordination geometry formed by three histidines and one glutamic acid,<sup>120</sup> a coordination sphere that is conserved among known Zn(II)-selective SBPs.<sup>121,123</sup> An interesting characteristic of Zn(II)-selective SBPs is that they possess a loop insertion rich in histidine and acidic amino acids positioned near the entrance to the metal binding site.<sup>120</sup> This loop has been shown to possess low affinity for zinc and may function as a “sensor” for extracellular zinc and/or help guide Zn(II) into its high-affinity metal binding site.<sup>127</sup> A loop specifically rich in histidines is observed in nearly all solute binding proteins from ABC transporters that are proposed to bind zinc, with the exception of the orphan SBP AdcAII.<sup>120</sup>

In striking contrast, known manganese-specific SBPs including PsaA in *S. pneumoniae* and MntC in *Synechocystis* (Figure 4) do not possess a His-rich loop region.<sup>114,120</sup> In addition, these SBPs appear to be less selective for their cognate metal Mn(II). For instance, TroA in *Treponema pallidum* has been linked to Zn, Fe, and Mn transport,<sup>120,124</sup> while SitA in *E. coli* has also been linked to both Mn and Fe transport.<sup>128</sup> Furthermore, *S. pneumoniae* PsaA was crystallized with zinc in its metal binding site,<sup>114</sup> although in vivo studies with *psaA* mutants have demonstrated that it is clearly responsible for manganese transport in vivo. As

expected, TroA, MntC, and MncA all have a coordination number of 5, with extra oxygen ligands from what is found in the zinc binding proteins.

The intrinsic selectivity, as defined by the relative thermodynamic affinities of a solute binding protein from an ABC transporter for Zn(II) over Mn(II), has not been extensively experimentally documented in any of these cases. The Irving–Williams series<sup>108</sup> predicts, however, that Zn(II) will bind more tightly than Mn(II) to virtually any SBP; this prediction has been borne out by experiment for the Mn(II) sensor MntR (section 3.6.2) but has not been rigorously tested to our knowledge for any member of this large family of metal binding SBPs. In fact, even the biological metal selectivity of Mn(II) vs Zn(II) can be difficult to establish from sequence alone; for example, the AdcCBA uptake system is thought to be selective for Zn(II) in *S. pneumoniae*<sup>126</sup> but has been reported to be Mn(II) specific in the related dental-plaque-causing bacterium *S. gordonii*.<sup>129</sup> Thus, while it remains a compelling hypothesis that coordination number is the principal origin of molecular specificity of Zn(II) relative to Mn(II) [and Fe(II)] in SBPs, direct support for this remains lacking.

In addition to ABC transporters, Mn(II) is known to be brought into the cell through a number of other transporters. The second most common prokaryotic Mn(II) transporter is MntH, a member of the Nramp family of proton-coupled divalent metal ion transporters, found in both prokaryotes and eukaryotic systems.<sup>51,113,130</sup> In mammalian systems, Nramp or solute carrier 11 (SLC11) transporters are widespread and play critical roles in Mn(II) import/efflux and Fe mobilization.<sup>52</sup> The apparent specificity of MntH for Mn(II) seems low<sup>130</sup> since iron, nickel, cobalt, and zinc can also be transported by Nramps in various bacteria (Figure 3).<sup>51,52</sup> There are no atomic resolution structures of any bacterial or eukaryotic Nramp,<sup>52</sup> although recent evidence suggests a common transport channel of 11 or 12 membrane-spanning helices.<sup>52</sup> In some specialized cases, e.g., in some *Lactobacilli*,<sup>131</sup> manganese can also be transported into bacterial cells via P-type ATPases; it is important to note these bacteria have a very high intracellular requirement for Mn(II). Finally, a low-affinity manganese transporter has been identified in *E. coli* that shares sequence similarity to the eukaryotic zinc- and iron-specific transporter family ZIP.<sup>132</sup> Since the structures and biochemical characterization of these proteins remain to be determined, the molecular basis of their metal selectivities is as yet unresolved.

### 2.3. Acquisition of Copper

The total copper concentration in an *E. coli* cell is low ( $10^{-6}$  M) but still higher than the concentration of copper outside of the cell ( $10^{-8}$  M).<sup>14</sup> With the exception of the photosynthetic cyanobacteria, e.g., *Synechocystis*, which contain an intracellular organelle called the thylakoid which hosts the Cu-requiring process, photosynthesis, there are no known bacterial species that express a cytosolic enzyme that absolutely requires copper.<sup>7,133</sup> All known copper-containing enzymes in Gram-negative bacteria are either periplasmic enzymes or embedded in the cytoplasmic membrane.<sup>7</sup> For example, *E. coli* synthesizes a copper, zinc superoxide dismutase (SodC) and an amine oxidase (MaoA) that are both trafficked to the periplasm and NADH dehydrogenase and *bo3*-type quinol heme-copper oxidase, each embedded in the cytoplasmic membrane, the latter of which orients its copper binding site toward the periplasm.<sup>133</sup>

The periplasm is more oxidizing than the cytosol, which, in turn, stabilizes the cupric form of copper. Periplasmic methionine-containing proteins that are capable of binding both Cu(I) and Cu(II) are found here, e.g., *E. coli* PcoC and *P. syringae* CopC.<sup>9,134–136</sup> These proteins either sequester the metal or traffic it to copper binding proteins or to the extracellular space<sup>9</sup> via an RND family copper efflux system (Figures 1 and 3; section 2.6.3).<sup>40</sup> Indeed, a large fraction of copper detoxification and sensing in Gram-negative bacteria grown under aerobic conditions likely occurs in the periplasm before the metal makes its way into the cytosol. Here two-component sensor-kinase systems, e.g., *E. coli* cusRS, *P. syringae* copRS, and plasmid-encoded *pcoRS* two-component systems, sense excess copper, while multicopper oxidases, e.g., *E. coli* CueO,<sup>137</sup> catalyze the oxidation of Cu(I) to the less toxic Cu(II) form. The most abundant Cu(II) binding periplasmic proteins in *Synechocystis* is CucA (copper cuprin A), a quercetin 2,3-dioxygenase, which sequesters ~2500 atoms of Cu(II) per cyanobacterial cell.<sup>2</sup>

Thus, in striking contrast to iron, zinc, and manganese, the copper requirements of the cytosol are likely to be quite low in most bacteria, with copper toxicity becoming acute at relatively small changes in cytosolic Cu(I) availability. This explains the requirement for Cu(I) chaperones that traffic the metal in the cytosol<sup>138,139</sup> and may also explain the extraordinarily high equilibrium Cu(I) binding affinity that characterizes Cu(I) sensor proteins that upregulate cytosolic Cu(I) efflux systems in response to Cu(I) stress.<sup>34,140</sup> A recent report reveals that *M. tuberculosis* expresses a Cu binding metallothionein, MymT, that protects the organism from copper toxicity (Figure 1) that is strongly induced by copper, cadmium, and oxidative and nitrosative stress.<sup>19</sup> Indeed, the cellular response to Cu(I) toxicity in pathogenic mycobacteria and other organisms often strongly resembles an oxidative stress response.<sup>141,142</sup> This is consistent with the need to minimize the potential for Cu(I)/Cu(II) redox cycling and Fenton chemistry, reminiscent of iron chemistry.<sup>15</sup>

Given its toxicity and a low intracellular requirement for Cu(I), copper uptake into the cytosol in bacteria is not well characterized, a situation that contrasts sharply with that of lower and higher eukaryotes.<sup>143–145</sup> In two cases, copper uptake has been shown to be mediated by a Cu(I)-specific P-type ATPase (see section 2.6.2), *Enterococcus hirae* CopA<sup>146</sup> and *Synechocystis* CtaA. Interestingly, insertional inactivation of the *copA* gene does not protect *Enterococcus* against copper toxicity but does protect against silver toxicity.<sup>146</sup> The same findings characterize the deletion mutants of the copper-importer *ctaA* in *Synechocystis*.<sup>60</sup> This lack of protection is likely due to an alternative, as yet uncharacterized, copper import system.<sup>146</sup> One candidate for such an uptake system is *P. syringae* CopD and related homologues, e.g., *E. coli* PcoD, reached on the basis of a recent report that describes the characterization of *B. subtilis* YcnJ. YcnJ harbors a N-terminal extracytoplasmic domain that is homologous to the periplasmic Cu(II)/Cu(I) binding protein of Gram-negative bacteria, CopC,<sup>147</sup> and a C-terminal transporter domain that is homologous to CopD.<sup>148</sup> Biochemical studies are consistent with the idea that YcnJ is a plasma membrane-localized Cu importer.

It is interesting to note that copper uptake into the cytosol can also be attenuated through other mechanisms, one of which occurs in *Synechocystis*, where copper import by CtaA is partially blocked by a periplasmic iron binding protein FutA2.<sup>149</sup> Deletion of *futA2* leads to low copper-dependent

cytochrome oxidase activity in the plasma membrane. In addition, the copper content of the soluble fraction of a whole cell extract is lower in a *futA2* mutant compared to the wild-type strain;<sup>149</sup> instead, these mutants hyperaccumulate copper in the periplasm. The mechanism by which FutA2 is thought to impact copper uptake into the cytosol is by chelation of Fe(III), which may limit the adventitious association of iron with the copper-transporting sites on CtaA.<sup>149</sup> The generality of this finding in other Gram-negative bacteria is unknown but supports the hypothesis that homeostasis systems for individual metals may strongly influence one another. Another example of this is the origin of cobalt toxicity in *E. coli*, where it has been shown that Co(II) competes out Fe(II) during the biogenesis of [Fe-S] clusters.<sup>150</sup>

Methane-oxidizing bacteria, such as *Methylosinus trichosporium* and *Methylococcus capsulatus*, also uptake copper, but they employ small siderophore-like compounds called methanobactins to do so.<sup>151</sup> The active site of methane monooxidase (MMO) is proposed to bind methanobactin directly; alternatively, methanobactin may scavenge copper from the environment and supply MMO with copper from the periplasm.<sup>151</sup>

## 2.4. Acquisition of Cobalt and Nickel

Both cobalt and nickel are found at total concentrations near the limit of detection for ICP-MS in *E. coli* grown aerobically,<sup>14</sup> in the low to sub-micromolar range. This is consistent with a low nickel metalloenzyme expression under these growth conditions as well as their presence in only a few metalloenzymes relative to Fe-, Zn-, and Mn-containing enzymes. Nickel has been identified as an essential cofactor for nine different enzymes, including NiFe-hydrogenase, Ni-superoxide dismutase, and urease.<sup>152</sup> Cobalt has been confirmed to be found only in the corrin ring of coenzyme B<sub>12</sub>.<sup>153</sup> Despite their low intracellular concentrations, both Ni(II) and Co(II) are concentrated by the cell as well, consistent with some mode of active transport into the cytosol. In Gram-negative bacteria, both Ni(II) (likely as a metallophore of some kind) and cobalamin (vitamin B<sub>12</sub>) bind to a specific outer membrane (OM) receptor, e.g., *E. coli* BtuB<sup>85</sup> and *H. pylori* FrpB4,<sup>154</sup> respectively, and are brought into the periplasm in a TonB/ExbB/ExbD-activated process (Figure 1). This is exactly analogous to the uptake of Fe-dicitrate or Fe-siderophore complexes through OM receptors FecA and FrpB, respectively (Figure 1). FrpB4 in the OM allows *H. pylori* to successfully colonize the stomach by mediating the high-affinity uptake of Ni(II) at low pH; under Ni(II)-replete conditions, this high-affinity system is bypassed with Ni(II) entering the periplasm via low-affinity porins.<sup>154</sup>

Once in the periplasm, two major mechanisms have been identified to import nickel and cobalt into the cytosol: ABC transporters<sup>152</sup> and NiCo-permeases.<sup>153</sup> The ABC transporter, NikABCDE in *E. coli*, is the most well-studied nickel transporter to date,<sup>152</sup> and recent functional studies suggest that in *E. coli*, this transporter is largely dedicated to the metalation of Ni,Fe-hydrogenases.<sup>24</sup> NikA is the periplasmic nickel binding protein (SBP), NikB and NikC form a heterodimeric transmembrane pore, while NikD and NikE are the ATPase subunits in the cytosol. The first crystallographic structure of NikA<sup>155</sup> revealed the surprising finding that the bound Ni(II) was not coordinated to any amino acid side chain but was instead coordinated to five water molecules,<sup>155</sup> a result consistent with an O<sub>5-7</sub> coordination sphere

but inconsistent with N-O bond lengths measured by X-ray absorption spectroscopy.<sup>156</sup> A subsequent structure revealed that NikA binds Fe(III)EDTA(H<sub>2</sub>O)<sup>-</sup>,<sup>157</sup> and follow-up work done by the same group identified a NikA/butane-1,2,4-tricarboxylate complex. These studies taken collectively suggest that NikA may transport a Ni(II)-metallophore rather than the free Ni(II) ion,<sup>158</sup> a hypothesis with clear parallels to the Fe-siderophore uptake systems. More work is needed to identify and chemically characterize a metallophore of bacterial origin that is essential for Ni(II) transport across the membrane. Other ABC systems encoded within gene clusters for coenzyme B<sub>12</sub> biosynthesis are predicted to be involved in cobalt uptake,<sup>153</sup> although biochemical studies have yet to be performed to confirm this. However, it is known that cobalt enters the cytosol as cobalamin or vitamin B<sub>12</sub> through the ABC transporter BtuFC<sub>2</sub>D<sub>2</sub>,<sup>159</sup> in which BtuF is the SBP component of the transporter.<sup>160</sup> Indeed, this ABC transporter, among others, has served as a model system for probing the mechanism of ligand-activated ATP-dependent transport by this ubiquitous family of transporters.<sup>50,161</sup>

Bacterial cells also import Ni(II) and Co(II) through nickel-cobalt transporters (NiCoT),<sup>153,162</sup> integral membrane permeases composed of eight transmembrane  $\alpha$ -helices (TM1-VIII) of unknown structure and oligomerization state.<sup>162</sup> *H. pylori* NixA is a well-studied representative of this class of proteins that supplies Ni(II) for urease.<sup>163,164</sup> The metal specificity of individual transporters for Ni(II) vs Co(II) appears to vary in a way that is correlated by the physical location of the gene within the genome, although the mechanism of metal discrimination is not yet known. For example, the gene encoding a NiCoT that selectively transports cobalt is typically found near genes encoding enzymes required for coenzyme B<sub>12</sub> biosynthesis. Mutational studies reveal that TMII contains an essential, conserved sequence rich in metal coordinating residues—RHA(V/F)DADHI—that is found in both nickel-specific, e.g., *Cupriavidus necator* H16 HoxN and cobalt-preferred *Rhodococcus rhodochrous* J1 NhlF NiCoTs.<sup>162,165</sup> Substitution of the first histidine residue in this sequence with a nonliganding residue lowers the affinity of both HoxN and NhlF for nickel and/or cobalt,<sup>165</sup> while replacement of the second histidine residue in NhlF completely inactivates nickel transport. Replacement of either the second histidine or the preceding aspartic acid inactivates HoxN metal transport.<sup>165</sup> It thus seems likely that these residues are involved in metal coordination during transport, perhaps from a single TM helix. How NiCoTs preferentially transport Co(II)/Ni(II) while failing to transport other more abundant divalent ions, Zn(II) and Cu(II), remains unclear, but the possibility exists that Ni(II) and Co(II) chelates or metallophores, rather than the uncomplexed ions, may represent the actual substrates for these transporters.

Both nickel and cobalt may also enter the cytosol through a member of the CorA family of transporters, which are also known to transport Mg(II) (Figure 1).<sup>166</sup> The crystallographic structure of the divalent metal ion transporter CorA from *Thermatoga maritima* reveals a funnel-shaped homopentamer, each protomer of which contains two transmembrane helices (TM1 and TM2), with the ring of TM1 helices creating the inner cavity through which ions pass. Interestingly, the channel does not appear to contain a metal binding site in the membrane,<sup>167</sup> thus suggesting that the metal ions observed on the cytosolic side of the structure may serve



more of a regulatory role during transport. Indeed, it is believed that the ions pass through the channel as fully hydrated ions since the amino acid residues found inside the channel are not negatively charged, as would be expected for a bona fide ion transporting channel.<sup>166</sup>

## 2.5. Acquisition of Molybdenum and Tungsten

Molybdenum and tungsten are the only second- and third-row transition metals, respectively, that have known roles in biological systems.<sup>168</sup> The most widespread use of molybdenum in bacterial enzymes is in the FeMo-cofactor in nitrogenase; however, another ubiquitous form of Mo is as molybdopterin cofactor.<sup>169</sup> Tungsten-containing enzymes have only recently been purified and characterized and include formate dehydrogenases, formylmethanofuran dehydrogenases, aldehyde-oxidizing enzymes, and acetylene hydratases in a number of unusual organisms.<sup>170</sup> The minimal requirements of *E. coli* and other bacteria for these metals has yet to be determined but are likely to be small.

Molybdenum and tungsten are both transported into *E. coli* via the ABC transporter ModABC as MoO<sub>4</sub><sup>2-</sup> and WO<sub>4</sub><sup>2-</sup> oxyanions rather than as free ions (Figures 3 and 4). ModA is the periplasmic SBP component of this transporter, and its structure has been solved in the presence of both molybdate and tungstate.<sup>171</sup> ModA binds both molybdate and tungstate through seven hydrogen bonds between the protein and the anion and obviously lacks direct metal–ligand coordination bonds. These hydrogen bonds are derived from four main-chain NH groups and three side-chain OH groups (Ser12, Ser39, and Tyr120) that stabilize the oxyanion in an otherwise positively charged pocket.

Interestingly, a recent crystallographic structure of *Methanosarcina acetivorans* molybdate/tungstate ABC transporter (*Ma* ModBC) reveals that the transporter is locked into an “open” trans-inhibited state (Figure 4), thereby suggesting another level of regulation of molybdate uptake.<sup>172</sup> A regulatory domain positioned at the C-terminus of the cytosolic nucleotide binding domains (NBDs) of *Ma* ModC is very similar in structure to the molybdate binding domain in ModE, which in *E. coli* represses the transcription of the molybdate transporter operon *modABCD* by binding to the operator–promoter DNA in the oxyanion-bound state (section 3.8.1).<sup>173</sup> A similar post-translational regulation is observed in *Ctr1* in *Saccharomyces cerevisiae*, where deletion of the C-terminal tail of the copper transporter leads to hypersensitivity to copper.<sup>174</sup> These findings provide molecular insight into a level of regulation beyond transcriptional control (section 3) which would allow the cell to sense elevated metal in the cytosol and thus alter metal homeostasis using a post-translational mechanism.

## 2.6. Efflux of Heavy Metal Ions

In order to affect metal homeostasis (Figure 1), all cells require the transport machinery to efflux metal ions when a certain “set point” of toxicity is reached. Analogous systems are used to efflux heavy metal xenobiotics including cadmium, lead, mercury, and arsenic, which play no biological role. It is worth emphasizing that it is not known with certainty what this set point is for any metal in any cell type, except to say that it likely varies dramatically for individual transition metal ions. For example, specific efflux systems have been described and well characterized for Cu(I), Zn(II), Ni(II), and Co(II) as discussed below. In contrast, only

recently have efflux systems been described for Mn(II), *S. pneumoniae* MntE, and Fe(II), *E. coli* YiiP/FieF,<sup>175</sup> the latter of which has been biochemically shown to transport Zn(II) and Cd(II) but not Fe(II).<sup>176</sup> Fe is a “precious” metal, and when intracellular Fe toxicity is encountered, Fe is mineralized as ferric oxide polymers in multimeric bacterioferritins and Dps-like proteins in the cytosol in a form that is accessible under conditions of Fe scarcity rather than being effluxed from the cell.<sup>21,177–179</sup>

### 2.6.1. Metal Efflux by Cation Diffusion Facilitators

Levels of zinc are thought to vary dramatically in host organisms during the course of a bacterial infection; as such, many bacterial pathogens have evolved methods of exporting Zn(II) from the cytosol.<sup>99,180</sup> At high levels of zinc, most bacteria efflux the extra metal through P-type ATPases (to be discussed in section 2.6.2) or through H<sup>+</sup> antiporters from the cation diffusion facilitator (CDF) family of transporters (Figure 3).<sup>54</sup> CDFs are also prevalent in eukaryotes, and seven CDF proteins, ZnT1–7 (zinc transporter 1–7), have been characterized in mammals that play roles in effluxing zinc across the plasma membrane or into various intracellular compartments.<sup>181–183</sup> The most extensively characterized bacterial CDF is YiiP from *E. coli*.<sup>68,176,184</sup> Functional homologues include *E. coli* ZitB,<sup>185</sup> *Ralstonia metallodurans*, *S. pneumoniae*, and *B. subtilis* CzcD,<sup>180,186–188</sup> and *T. thermophilus* and *S. aureus* CzrB.<sup>189,190</sup> The recent 3.8 Å crystallographic structure of the metalated YiiP homodimer,<sup>191</sup> although at modest resolution, reveals the architecture of the dimer in the membrane and four distinct zinc binding sites per monomer (eight per dimer) designated Z1–Z4 (Figure 5).<sup>68</sup> Z2–Z4 are found associated with a cytosolic, independently folded dimeric domain (Figure 5)<sup>190</sup> that is projected to be regulatory for transport, while Z1 is found in the middle of the lipid bilayer.<sup>68</sup> Biochemical studies reveal that only site Z1 is absolutely required for efflux of zinc across a bilayer.<sup>68</sup>

Four protein-derived ligands coordinate Zn(II) in the Z1 metal site of YiiP to form a pseudotetrahedral coordination geometry (Figure 5). YiiP appears to be capable of discriminating between zinc/cadmium and other essential metals (calcium, magnesium, nickel, cobalt, and manganese) on the basis of this low  $n = 4$  coordination number in a manner analogous to SBPs of ABC transport uptake systems (section 2).<sup>68</sup> However, it is not yet known the degree to which other CzcD-like proteins are capable of this discrimination since many are known to protect cells from Ni(II) and Co(II) toxicity as well.<sup>186,188</sup> Mutational analysis in ZitB in *E. coli*<sup>192</sup> and CzcD in *Ralstonia metallidurans* (both YiiP homologues<sup>68</sup>) and in *E. coli* YiiP<sup>176</sup> confirm that substitution of metal-donor atoms in the transmembrane Z1 site, in particular Asp157 in TM5 (Figure 5), either influences the ability to bind and/or transport Zn(II)/Cd(II) or, alternatively, abolishes formation of the obligate protein homodimer.<sup>193</sup>

The functional significance of the remaining cytosolic metal sites in YiiP and CzrB (Z2–Z4) is not yet known, but they are positioned in such a way that they may allosterically activate the opening of the channel when cytosolic zinc levels rise. It is striking that the high-resolution structure of the soluble, cytoplasmic domain (at 1.80 Å resolution) reveals that metals Z1–Z3 (Z1 and Z2 roughly correspond to Z3 and Z4 in *E. coli* YiiP) form a trinuclear structure which is characterized by two bidentate, or shared, ligands that bridge Z1 with Z2 and Z2 with Z3, positioned at the protomer

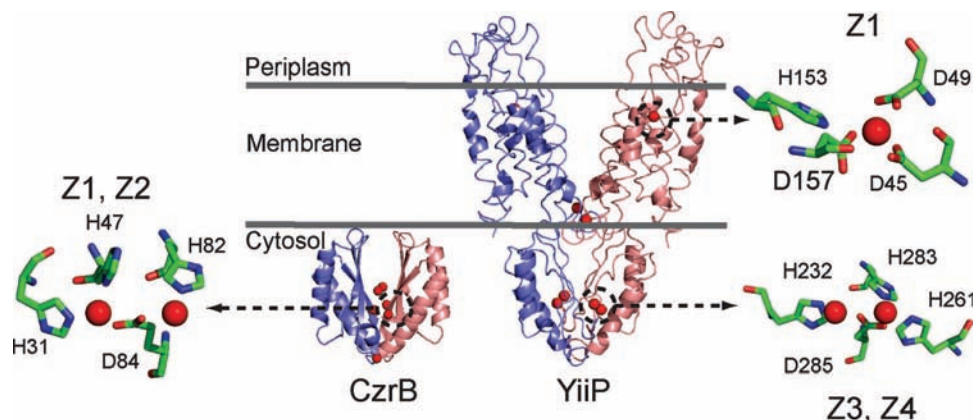


**Figure 5.** Structural comparison of the intact Zn(II) CDF transporter *E. coli* YiiP (2QFI)<sup>68</sup> with the cytosolic domain of the homologue *T. thermophilus* CzrB (3BYR).<sup>190</sup> Each structure highlights the Zn(II) coordination environments for zinc in both YiiP and CzrB. The structures of CzrB and YiiP were refined with three and four Zn(II) ions per protomer, respectively. The cytosolic protein CzrB contains a divalent metal center (Z1 and Z2) that is roughly, but not precisely, analogous to the Z3 and Z4 sites in YiiP. The transmembrane Z1 site in *E. coli* YiiP is also shown with a key ligand D157 highlighted.

interface, the binding of which appears to drive a conformational “closure” of the V-shaped structure (Figure 5). It is not known if all three sites are bound in solution, although isothermal titration calorimetry experiments with the intact YiiP transporter are potentially consistent with this scenario.<sup>194</sup> The regulatory role of these Zn(II) sites may be analogous to that proposed for the N-terminal metal binding domains (MBDs) of P<sub>1B</sub>-type ATPases (see section 2.6.2). It has been speculated that this domain could function as a cytosolic zinc metallochaperone (if somehow liberated from the membrane spanning transport channel) or provide a docking site for a cytosolic zinc metallochaperone itself.<sup>190</sup> There is no experimental support for this one way or the other.

### 2.6.2. Metal Efflux by P-Type ATPases

CDFs are quite common in prokaryotes in general, although they have yet to be identified in photosynthetic cyanobacteria.<sup>195</sup> Here, toxic levels of zinc and other metals, notably copper, are exported from the cytosol by a number of metal-specific P<sub>1B</sub>-type ATPases.<sup>58</sup> As pointed out above, the vast majority of transition metal-transporting P<sub>1B</sub>-subtype ATPases are known or predicted to be efflux pumps that provide resistance to metal toxicity, in which metal ions are moved *from* the cytosolic compartment. This is consistent with the catalytic mechanism in which phosphorylation of the aspartate residue in the P-domain (Figure 6a) occurs upon ATP binding to the N-domain and metal binding to the transmembrane binding site(s) from the cytosolic side of the membrane. This poises the enzyme to change conformations, allowing access of the metal to the extracytoplasmic side of the membrane, metal release, and subsequent enzyme dephosphorylation.<sup>58</sup>

Although there are as yet no atomic resolution structures of an intact heavy-metal ion-transporting P<sub>1B</sub>-ATPase, the basic architecture of the core transporter is homologous to the extensively structurally characterized sarcoplasmic reticulum Ca(II)-ATPase.<sup>69,70</sup> This is confirmed by a recent cryoelectron microscopy reconstruction experiment of intact apo *A. fulgidus* (*Af*) CopA,<sup>71</sup> a Cu(I)-transporting ATPase, individual domains of which have been structurally characterized at high resolution by X-ray crystallography (Figure 6b).<sup>196–198</sup> *Af* CopA has also been the subject of extensive biochemical studies as well.<sup>16,55,199</sup> *Af* CopA is characterized

by eight transmembrane (TM) helices that form the channel for metal transport (Figure 6a). TM6 bears the CPx signature sequence, which has long been implicated in conjunction with other residues in the membrane helices to coordinate the metal during transport.<sup>200,201</sup> CPx can be CPC (as indicated in Figure 6a for *Af* CopA), CPH, or SPC in P<sub>1B</sub>-ATPases; for example, *E. hirae* CopA possesses a CPC motif, whereas CopB, suggested to transport Cu(II), possesses a CPH motif.<sup>146</sup> In Cu(I) transporters specifically, the CPC motif is immediately followed by a conserved ALGL motif. Large cytoplasmic loops are folded into actuator (A-domain) and ATP binding subdomains (N- and P-domains) (Figure 6).

X-ray absorption spectroscopy and biochemical studies provide the first direct spectroscopic evidence that the CPC motif binds Cu(I) in any Cu(I)-transporting P<sub>1B</sub>-ATPase.<sup>16</sup> These studies reveal that *Af* CopA binds 2 mol equivalents of Cu(I) to two distinct transmembrane binding sites, one coordinated by the two cysteines in the CPC motif in TM6 and a tyrosine residue in TM7,<sup>16</sup> with the second Cu(I) coordinated by invariant Asn, Met, and Ser residues in the second site positioned between TM7 and TM8 (Figure 6a).<sup>16</sup> Substitution of any of these six conserved residues results in loss of copper binding and transport.<sup>16</sup> Each site adopts a trigonal planar coordination geometry, and each binds Cu(I) independently with affinities in the 10<sup>15</sup> M<sup>-1</sup> range. It is interesting to note that these transmembrane binding sites are positioned such that they at least partially superimpose on the two crystallographically defined Ca(II) binding sites found in the inner TM4–TM5–TM6 and TM8 helices of the vertebrate Ca(II)-ATPase.<sup>69,70</sup> In addition, a Zn(II) binding site in *E. coli* ZntA has been mapped by mutagenesis experiments to the CPC motif in TM6 and conserved residues in TM7 and TM8.<sup>201,202</sup> These findings taken collectively are consistent with the idea that metal specificity of a P<sub>1B</sub>-type ATPase is governed by the coordination chemistry of transmembrane binding sites, although more work is required to further substantiate this proposal.

In addition to the transmembrane metal binding site(s), many prokaryotic P<sub>1B</sub>-ATPases contain one or several tandemly linked ferredoxin fold-like  $\beta\alpha\beta\beta\alpha\beta$  metal binding domains (MBDs) usually found N-terminal to the first TM helix (TM1) (Figures 6a and 7). *Af* CopA is unusual among Cu(I)-transporting ATPases in that it contains a single MBD at both the C- and N-terminal ends of the molecule, both



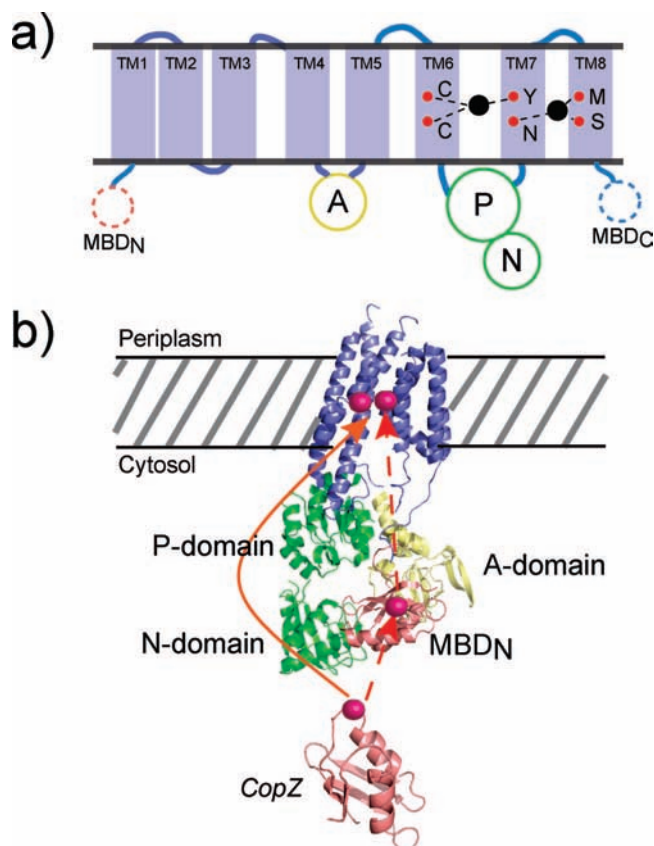


**Figure 6.** (a) Schematic representation of the topology of a heavy metal P<sub>1B</sub>-type ATPase transporter. TM, transmembrane helix; MBD, metal binding domain; A, actuator domain; P, phosphorylation domain; N, nucleotide binding domain; red spheres, approximate positions of mapped residues important for Cu(I) transport by *A. fulgidus* CopA;<sup>199</sup> black spheres, metal ion bound to the transmembrane binding site(s) in a manner consistent with X-ray absorption studies.<sup>16</sup> (b) Models for Cu(I) delivery to the transmembrane metal binding sites in the CopA P-type ATPase from *A. fulgidus*.<sup>16</sup> A ribbon diagram of a CopA monomer modeled on the cryo-EM structure of the CopA dimer.<sup>71</sup> Transmembrane helices are shown in slate, P/N domains are shown in green,<sup>197</sup> and the A domain<sup>196</sup> is colored yellow. The N-terminal MBD is shown in salmon. The Cu(I)-chaperone CopZ ribbon diagram in shaded salmon is based on the structure of *Enterococcus hirae* CopZ (PDB code 1CPZ).<sup>411</sup> The dashed red line symbolizes the intermediate transfer of Cu(I) from CopZ to the N-MBD, to the transmembrane metal binding site(s). The red solid line represents the direct delivery of Cu(I) in CopZ to the transmembrane metal binding site of CopA. The locations of the bound Cu(I) ions are for schematic purposes only. Adapted with permission from ref 199. Copyright 2008 National Academy of Sciences U.S.A.

positioned in the cytosol and proximal to TM8 and TM1, respectively (Figure 6a). TM1 is thought to correspond to the “bent” helix that is critical for substrate translocation across the membrane as the pump cycles through its well-defined transport cycle.<sup>203</sup> The presence of cytosolic MBDs represents a significant point of departure from other classes of P-type ATPases, including the Ca(II)-ATPase, and the functional role(s) of the MBDs remains the subject of ongoing investigation.<sup>199</sup> In Cu(I)-translocating ATPases, an MBD harbors a single metal binding site as part of GMTCCxC Cu(I) binding loop but minimally consisting of two Cys residues to create a linear digonal, trigonal planar, or equilibrium structure between the two (Figure 7).<sup>138</sup> For example, the Wilson’s and Menkes disease Cu/Ag-specific ATPases ATP7A and ATP7B, respectively, have six tan-

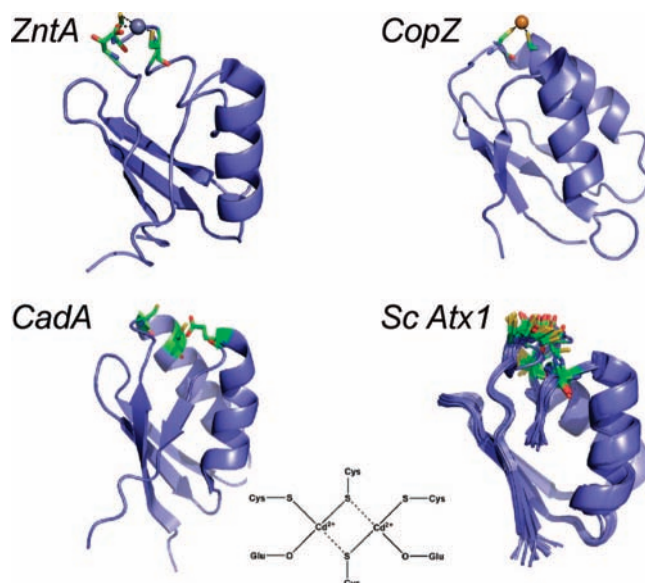


**Figure 7.** Ribbon diagrams of the N-terminal MBDs of the P-type ATPases *E. coli* ZntA<sup>213</sup> and *Listeria monocytogenes* CadA compared to representative bacterial Cu(I) metallochaperones from the N-terminal domain of CopZ from *B. subtilis*<sup>412</sup> and ScAtx1 from *Synechocystis* PCC 6803 (an NMR bundle).<sup>221</sup> A schematic rendering of the dimeric, binuclear Cd(II) complex adopted by CadA is also shown.<sup>214</sup>

demly linked MBDs, while those from lower eukaryotes and most prokaryotes have zero, one, or two MBDs.

MBDs are structurally homologous to cytosolic Cu(I) chaperones (Figure 7) that are responsible for trafficking Cu(I) in the cytosol for delivery to a particular Cu(I) metalloenzyme or Cu(I)-specific P<sub>1B</sub>-type ATPase. MBDs are known to provide docking sites for Cu(I) chaperones that allow Cu to be handed off via a series of intermolecular metal–ligand exchange reactions mediated by transient electrostatically stabilized protein–protein interactions to partner MBDs without dissociation of the metal into bulk solution (Figure 8).<sup>204–207</sup> This provides strong support for the central tenet of the Cu-trafficking hypothesis.<sup>208</sup>

Metal coordinating residues outside of the Cys-X<sub>2</sub>-Cys metal binding loop in MBDs as well as the precise structure a MBD adopts when bound to different metal ions<sup>209</sup> appears to influence the metal specificity of the associated transporter or metallochaperone, although the origin of this effect is not entirely clear. For example, the canonical Cu(I)-MBDs of P<sub>1B</sub>-type ATPases *B. subtilis* CopA and *S. cerevisiae* Ccc2a and their cognate Cu(I) chaperones, CopZ and Atx1, respectively, possess either a digonal S<sub>2</sub> coordination site or one that readily takes up an exogenous thiol ligand from solvent (Figure 7).<sup>210,211</sup> In another Cu(I) metallochaperone, *Synechocystis* Atx1 (ScAtx1), a distorted trigonal S<sub>2</sub>N complex seems to be found, where a His derived from loop 5 between helix α<sub>2</sub> and strand β<sub>4</sub> is a metal ligand (Figure 8).<sup>212</sup> Interestingly, that His moves away from the Cu(I) ion in the docked intermediate complex between ScAtx1 and the target N-terminal MBD of PacS, which ultimately imports Cu(I) into the thylakoid (Figure 8).<sup>207</sup> For the Zn/Cd/Pb transporter *E. coli* ZntA, a conserved Asp just N-terminal to the first Cys (DCXXC) has been proposed to drive three or four coordination of Zn(II),<sup>213</sup> in contrast, for the Cd/Pb-selective transporter *Listeria monocytogenes* CadA, a conserved Glu in loop 5 appears to form a coordination bond to the Cd(II) in a binuclear homodimeric subunit bridging



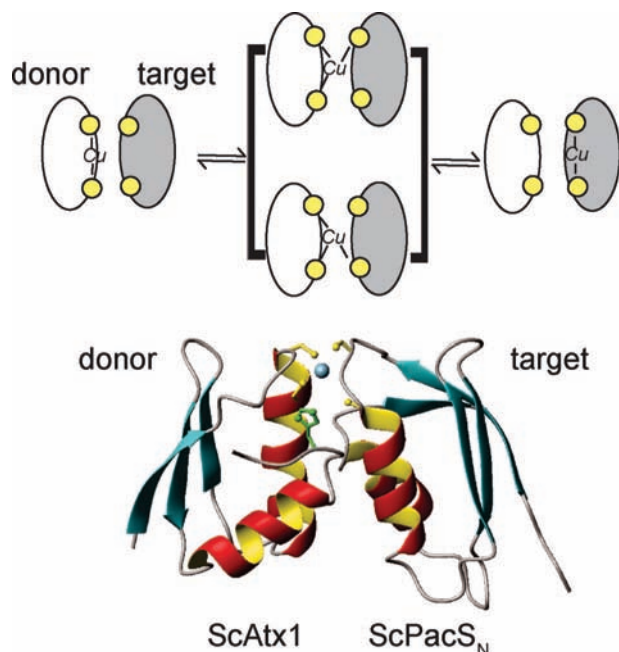


**Figure 8.** (a) Schematic model of Cu(I) exchange between a Cu(I) donor metallochaperone and a Cu(I) target protein, e.g., the MBD of P-type ATPases. The structural intermediate shown in brackets is a transiently formed Cu(I) cross-linked intermolecular complex,<sup>138</sup> a three-dimensional NMR-based model of which is shown in b for the complex between the Cu(I) chaperone ScAtx1 and the N-terminal MBD of PacS from *Synechocystis* PCC 6803.<sup>207</sup> Adapted with permission from ref 206. Copyright 2006 National Academy of Sciences U.S.A.

structure (Figure 7).<sup>214</sup> The functional role of these MBDs has not yet been determined,<sup>209,215</sup> since there are no known zinc chaperones in the cytosol.

The precise function of the MBDs in metal transport is not fully established and may differ for different transporters. It is known, however, that metal binding to the MBD of various Cu(I)- and Zn(II)/Cd(II)-transporting ATPases cannot be an obligatory transport intermediate for subsequent transfer to the transmembrane binding site(s), since deletion of the MBD has no influence on the intrinsic ability of the pump to transport metal ions, although maximal rates in some *in vitro* reconstituted systems are lower. For *Af* CopA, the C-terminal MBD is completely functionally dispensable, unlike the N-terminal MBD.<sup>203</sup> Recent biochemical studies reveal that the Cu(I) chaperone *Af* CopZ can indeed transfer Cu(I) to the N-terminal MBD of *Af* CopA as predicted by the Cu-trafficking model (Figure 8).<sup>199</sup> However, this transfer intermediate is apparently *not* competent to transfer Cu(I) to the transmembrane sites; in fact, CopZ seems capable of transferring Cu(I) to the transmembrane sites directly under nonturnover conditions,<sup>199</sup> consistent with their reported relative equilibrium affinities for Cu(I)<sup>16</sup> (Figure 6b). Similar differences in zinc binding affinities between the N-terminal MBD and the transmembrane metal binding site of the Zn(II) efflux P-type ATPase pump, *E. coli* ZntA, are consistent with either a regulatory or a directional transfer role.<sup>215,216</sup>

These biochemical studies with *Af* CopA<sup>199</sup> are consistent with a model in which the N-MBD plays a regulatory role in modulating the transport rate. This model may well be consistent with the low-resolution structural model of *Af* CopA lacking one or both terminal MBDs determined by cryoelectron microscopy (Figure 6b).<sup>71,217</sup> Difference cryoelectron density maps permitted the authors to confidently position the N-terminal MBD between the nucleotide binding

(N) and actuator (A) domains which are conserved in all P-type ATPases of similar structure (Figure 6b).<sup>196–198</sup> Although one must be cautious in extracting mechanistic detail from what is intrinsically a low-resolution model, the remarkable feature of the model is that the Cu(I) binding loop of the MBD interacts with the A- and N-domain, near the ATP binding site, optimally positioned to perform a regulatory or allosteric function, and is thus consistent with the biochemical studies.<sup>199</sup> Previous studies of the Ca(II) ATPase show that there is a large rotation of the A-domain that mediates coupling between the transmembrane ion binding and catalytic sites during the transport cycle, which allows the N-domain to pivot upon ATP binding and phosphorylation.<sup>218</sup> The structure suggests that the N-terminal MBD would restrict this movement which is rate limiting for Cu(I) transport, in the metal-free or inactivated state.<sup>58,217</sup> Interestingly, the  $\alpha$ -helical surface of the MBD is exposed to solvent where it can engage in direct protein–protein interactions with CopZ, as previously defined for other related Cu(I)-translocating ATPases; subsequent metal transfer might allow displacement of the MBDs from this site, thereby activating the transporter.<sup>206,207,210</sup> It will be interesting to see how this structure accommodates N-terminal domains with multiple tandem MBDs but certainly provides a structural rationale for biochemical findings that suggest that the membrane-proximal MBDs have distinct functional roles relative to other MBDs,<sup>209</sup> while more distal MBDs may well interact more strongly with the metallochaperone.<sup>205,219</sup>

The fact that *A. fulgidus* CopA adopts a 2-fold symmetric homodimer in these tubular crystals also deserves mention. Although the Ca(II) ATPase is thought to function as a monomer, P-type ATPases are known to exist in both monomeric and dimeric quaternary structural states, both of which are functional. In any case, it is interesting to note that the metal binding loops of the MBDs from individual protomers within the low-resolution CopA dimer may be close enough to form metal-bridged structures so often observed in isolated MBDs when metal ions are added;<sup>214,220,221</sup> the functional significance of these cross-linked structures has not been established.

### 2.6.3. Other Efflux Mechanisms

There are many other ways that organisms control the toxic effects of high intracellular metal concentrations. For example, export of the heavy metal(oid) arsenic is accomplished through multiple mechanisms. The first is a two-component membrane-associated system comprised of the proteins ArsA and ArsB.<sup>222–224</sup> ArsA functions as an arsenate-stimulated ATPase, while ArsB is the transmembrane protein that allows for transport of the metal or metalloid out of the cytosol. The mechanism of As(III)/Sb(III) stimulation involves the direct binding of these metals to trigonal planar coordination sites in the ATPase domains. Metals can be exported by ArsB functioning independently as a chemiosmotic transporter.<sup>222–224</sup> The ArsAB system is remarkably efficient in *E. coli*, allowing for an internal concentration of arsenic of 1 nM in a prevailing external concentration as high as 1 mM.<sup>223</sup>

As discussed above for copper detoxification (section 2.3), the periplasm of Gram-negative bacteria can be used either as an intracellular compartment that provides for storage of biologically required metal ions separate from the cytosol or under conditions of acute toxicity to clear metals from the periplasm to the outside of the cell. This latter process is accomplished by transenvelope “efflux guns”<sup>225</sup> that span

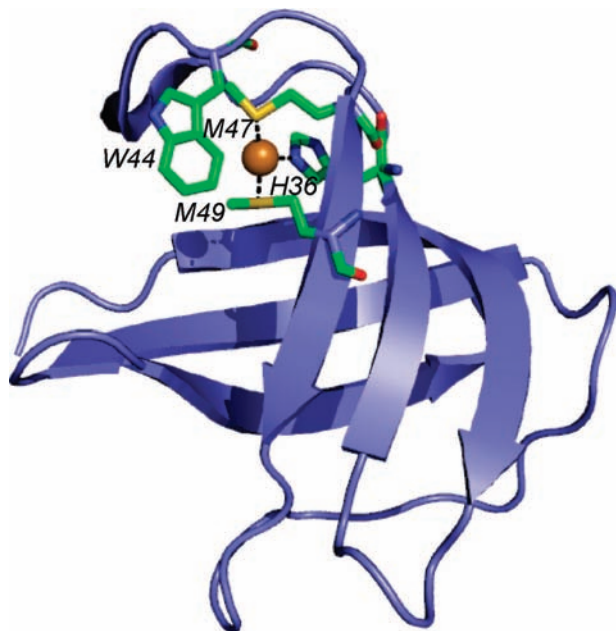


**Figure 9.** Ribbon representation of *E. coli* CusF highlighting the tetragonal distortion of the Met-His-Met trigonal Cu(I) plane by the indole ring of W44 which forms a classical cation- $\pi$  interaction with the Cu(I) ion.<sup>230,231</sup>

the periplasmic space between the cytoplasmic and outer membranes and is carried out by members of the resistance-nodulation-cell division (RND) protein family (Figure 1).<sup>222</sup> RND proteins are integral membrane proteins, and biochemical studies of the prototype member, *R. metallodurans* CzcA (cadmium-zinc-copper), reveals that CzcA is cation/H<sup>+</sup> antiporter with a topology of 12 membrane spanning helices;<sup>226</sup> many other RND proteins are involved in multidrug resistance (drug export) in bacteria.<sup>227</sup> CzcA and CnrA (cobalt-nickel resistance) are the two RND protein systems chiefly responsible for heavy metal export of the indicated metal ions; however, other RND systems for heavy metal transport are known.<sup>228,229</sup> CzcA is found as part of a tripartite CzcCBA efflux protein complex, and the same is predicted for CnrCBA; the B protein bridges the periplasm and connects the permease in the cytoplasmic membrane with CzcC (CnrC) embedded in the outer membrane.<sup>222</sup>

A similar efflux system, CusCFBA, is also induced by copper toxicity under anaerobic conditions in *E. coli*.<sup>40</sup> Here, a periplasmic Cu(I) binding protein, CusF, which forms an unusual tetragonally distorted His-Met<sub>2</sub>-Trp  $\pi$ -cation complex with Cu(I) (Figure 9),<sup>230,231</sup> is predicted to deliver metal directly to the CusB transperiplasmic oligomer, for which there is now experimental evidence.<sup>8</sup> These studies would seem to indicate that the source of copper to be transported to the outside of the cell is 2-fold, either directly from the cytosol through the permease CusA or from within the periplasm itself via CusF, deposited there via some other route, i.e., by a P-type ATPase or a CDF protein [in the case of Zn(II)]. The crystallographic structure of all three parts of the acridine (Acr) efflux system from *E. coli*, including the trimeric RND protein AcrB,<sup>232–234</sup> the outer membrane cylindrical protein TolC,<sup>235</sup> and the periplasmic spanning protein AcrA,<sup>236</sup> shed considerable molecular detail on this process, specifically as it relates to the extrusion of small molecule drugs, bile acids, and detergents from the cell.<sup>227</sup> In particular, most mechanistic models suggest that the AcrAB system functions as an A<sub>3</sub>B<sub>3</sub> heterohexamers, which docks onto the TolC OM channel for drug export (Figure

3). The MexA-MexB-OprM tripartite system is the analogous RND drug efflux system in *Pseudomonas aeruginosa*,<sup>237</sup> whose transcription is regulated by the MarR family regulator (Figure 2) MexR (section 3.8.2).<sup>238,239</sup> The molecular determinants of metal selectivity of the Czc, Cnr, and Cus systems are completely unexplored and may be dictated by protein-protein interactions in the periplasm as well as the intrinsic metal specificity of the permease in the cytoplasmic membrane.

## 2.7. Metal Transporters: Summary

Several points can be made that speak to the specific determinants of metal selectivity of uptake and efflux systems in bacteria. First, the selectivity of an ABC transporter for the “right” metal ion would seem to be dictated largely by the first metal coordination shell in the SBP component of the transporter (Tables 1 and 2; Figure 3). However, it could be argued that formation of a cognate coordination complex is necessary but not sufficient to establish the required degree of specificity. Clearly, the “cognate” transmembrane (TM) component of the channel could reinforce the metal selectivity of the SBP by driving a conformational change that leads to rapid dissociation of the ligand from the SBP into the aqueous channel, *only* when a fully cognate protein-protein-metal complex is assembled.<sup>159</sup> A similar mutually reinforcing system of metal selectivity may also characterize P-type ATPases. Here, the cytosolic MBDs, which may well have low intrinsic metal selectivity (Figure 7), might “enforce” an enhanced selectivity of the transmembrane site(s) by inducing a conformational change in the transporter *only* when the cognate metal is bound to the MBD(s); formation of a noncognate coordination complex would not allow the MBDs to play a proposed regulatory (activating) role.<sup>209</sup> Finally, the general concept of regulatory metal sites positioned on the cytosolic side of the membrane that either downregulate uptake or stimulate efflux by a specific transporter may well become the rule rather than the exception. As described below, metal sensor proteins exploit the same “two-step” strategy in which specific features of the coordination chemistry of the metal-sensing site(s) are amplified or reinforced by downstream conformational changes that are themselves more strongly tied to biological regulation.

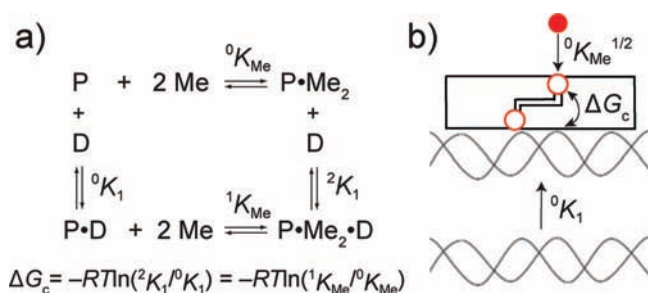
## 3. Prokaryotic Metal Sensor Proteins

Prokaryotes typically contain a panel of metalloregulatory proteins that collectively manage metal ion homeostasis in the cell. These specialized “metal receptor proteins” function as transcriptional regulators of genes that encode membrane-bound transporters that mediate metal ion uptake and metal efflux from the cytosol (section 2) and to a lesser degree genes that encode intracellular chelators, e.g., metallothioneins,<sup>240</sup> and bacterioferritins<sup>20</sup> and, in the case of Hg and As, metal detoxification enzymes (Figure 1).<sup>241,242</sup> These systems globally coordinate homeostasis of individual metal ions in the cytosol. Seven major transcriptional regulator families have thus far been structurally and/or functionally characterized in some detail,<sup>22</sup> with new ones (at least three more) emerging from other transcriptional regulator families in which the majority of members play no role in metal homeostasis (Figure 2).<sup>22</sup>

Transcriptional regulators from different sensor families (Figure 2) sometimes regulate the expression of genes with identical functions in different organisms, consistent with a



## Scheme 1



“mix-and-match” approach for the evolution of metal-sensing operons or regulons in a particular organism, perhaps aided by horizontal gene transfer and subsequent convergent evolution.<sup>243</sup> For instance, a set of Cu(I)-specific effluxing P-type ATPases that share high pairwise sequence similarity are regulated by CsoR in *M. tuberculosis*,<sup>244</sup> CueR (a MerR family member) in *E. coli*,<sup>245</sup> and CopY in *E. hirae*,<sup>246</sup> which, as described below, are characterized by distinct mechanisms of metalloregulation of transcription. Even in the same organism, *E. coli*, the transcription of functionally orthologous metal uptake transporters, e.g., ABC transporters specific for Ni(II) and Zn(II), are regulated by metal sensor proteins from distinct structural families, which are NikR<sup>247</sup> and Zur (a Fur family member),<sup>248</sup> respectively. The functional equivalent of Zur from Gram-negative proteobacteria is hypothesized to be a MarR family member AdcR in at least some Gram-positive organisms (section 3.8.2).<sup>4</sup>

As discussed below, general features of the molecular details by which an individual metalloregulatory protein selectively responds to one or a small overlapping subset of metal ions remain elusive due largely to a lack of high-resolution structures of all the functionally relevant “allosteric” states (Scheme 1). For example, in some instances, we have quite a lot of information about the first coordination shell of ligands around a regulatory metal ion and in other cases structural insight into how coordination complexes with the “wrong” noninducing metal ion compare with that of the “right” metal ion; the recent data will be summarized below. What is generally lacking, aside from *E. coli* NikR and DtxR/IdeR from Actinobacteria, is how the structure of these coordination chelates changes or “enforces” a conformation of the regulator when bound to, or dissociated from, the DNA operator.

### 3.1. ArsR/SmtB Family

The ArsR/SmtB family is the most extensively studied and likely the largest and most functionally diverse metalloregulatory protein family.<sup>36,37</sup> The ArsR/SmtB (or ArsR) family is named for its founding members, *E. coli* As(III)/Sb(III) sensor ArsR<sup>249</sup> and *Synechococcus* PCC 7942 Zn(II) sensor SmtB.<sup>250</sup> Many bacterial genomes across virtually every bacterial taxonomy encode at least one ArsR family regulator as annotated by the NCBI Cluster of Orthologous Groups (COG0640) and the number of unique ArsR/SmtB-encoding genes is conservatively in excess of 500.<sup>37</sup> Notably, the Actinobacteria *Mycobacterium tuberculosis* and *Streptomyces coelicolor* encode 10 and 13 ArsR/SmtB proteins, respectively, the majority of which have not yet been functionally characterized. Detailed comparative studies of ArsR/SmtB sensors therefore provide an excellent opportunity to investigate how nature employs the same protein fold to create proteins with distinct or orthologous functions.<sup>26,37,251–253</sup>

The ArsR/SmtB family includes proteins responsible for sensing a wide variety of metal ions, ranging from essential metal ions Zn(II) and Ni(II) to toxic metal pollutants such as As(III), Cd(II), and Pb(II) (Figure 2). Genes regulated by ArsR/SmtB family proteins are usually responsible for effluxing, scavenging, or detoxifying excess metal ions found in the cytosol. As transcriptional repressors, apo ArsR/SmtB proteins bind to a DNA operator that physically overlaps the promoter where they repress transcription of downstream genes. Metal binding induces a low-affinity conformation that mediates dissociation from the DNA and thus drives transcriptional derepression. One striking aspect of ArsR/SmtB family proteins is that diverse metal ion binding sites have evolved at structurally distinct places on what is likely the same protein fold (Figure 10, left). These are designated  $\alpha 3\text{N}$  (also referred to as metal site 1 in *S. aureus* pI258 CadC),  $\alpha 3$ ,<sup>36</sup>  $\alpha 4\text{C}$  (as in *M. tuberculosis* CmtR),<sup>243,251</sup>  $\alpha 5$  (or site 2 in *S. aureus* pI258 CadC),  $\alpha 5\text{C}$ , and  $\alpha 5\text{--}3$ .<sup>36,37</sup> This nomenclature derives from the secondary structural element, e.g., the  $\alpha 3$  helix, or the N- or C-terminal “tail” region that are known or projected on the basis of mutagenesis experiments to provide ligand donor atoms to the metal ion in each case (Figure 10, right). These metal-coordinating residues are also highlighted on a multiple sequence alignment of representative ArsR family sensors discussed here (Figure 11).

#### 3.1.1. Structural Studies

Several metal-free (apo) and metal-bound structures have been solved for individual ArsR repressors by X-ray crystallography or NMR spectroscopy. These include crystallographic structures of two  $\alpha 5$ -site sensors in the apo- and Zn(II)-bound state, *Synechococcus* SmtB<sup>254</sup> and *S. aureus* CzrA,<sup>254</sup> the apo-structure of  $\alpha 3\text{N}$  Cd(II)/Pb(II) sensor *S. aureus* CadC,<sup>255</sup> and a solution structure of Cd(II)-bound  $\alpha 4\text{C}$  Cd(II)/Pb(II) sensor *M. tuberculosis* CmtR.<sup>256</sup> As shown on the structure of a representative ArsR/SmtB repressor, *S. aureus* pI258 CadC,<sup>255</sup> all ArsR/SmtB proteins are dimeric and possess a similar fold with a winged helix–turn–helix motif ( $\alpha 3$ –turn– $\alpha 5$ ) used for DNA binding (Figure 10, right). The structures of CadC and *Synechococcus* SmtB can be described as “flat” or “open”, with the winged helical domain being an integral part of the dimer. The primary interface of the dimer is formed by the N-terminal  $\alpha 1$  and C-terminal  $\alpha 5$  helices; in CadC, the N-terminal  $\alpha 0$  helix also packs against the winged helix domain (Figure 10). In other metal sensor families (Figure 2), the winged helix domain constitutes a folded subdomain within the molecule.

Metal binding residues in ArsR family sensors are nearly always derived from opposite protomers within the homodimer to form pairs of symmetry-related metal sites. For example, the metalloregulatory  $\alpha 5$  sites employ ligands from across the adjacent N- and C-terminal regions of the  $\alpha 5$  helix (Figure 12). Likewise, the  $\alpha 3\text{N}$  and  $\alpha 4\text{C}$  Cd/Pb binding sites employ Cys thiolates derived from the distinct  $\alpha$ -helices within the core of the molecule ( $\alpha 3$  or  $\alpha 4$ ) and the N-terminal and C-terminal tails, respectively, of the opposite protomer. Positioning such sites across the dimer interface is optimal for driving quaternary structural transitions in the dimer that may well be critical for driving allosteric negative regulation of DNA operator binding by inducing metal ions. One recently reported exception to this is *Acidithiobacillus ferrooxidans* ArsR (*Af* ArsR), in which inspection of a homology model seemed to suggest that three cysteines from



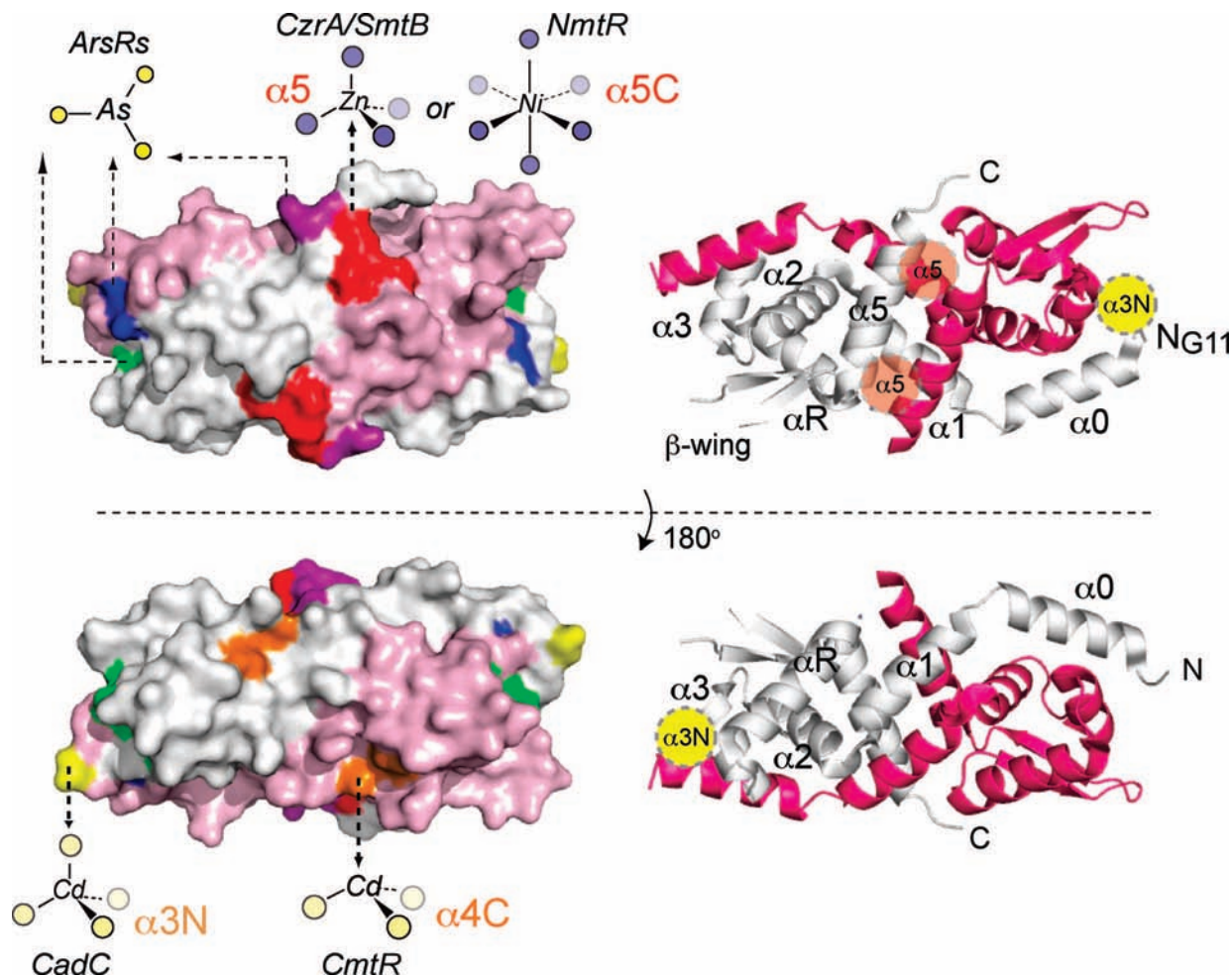


**Figure 10.** Summary of the known metal binding sites of ArsR/SmtB family repressors on the structure of *S. aureus* pI258 CadC homodimer.<sup>255</sup> (Left) Space-filling models of two views of CadC adapted from ref 267 with ribbon representations of the same view shown on the right. One protomer is shaded pink and the other gray, with the  $\alpha$ -helices labeled consecutively from the N-terminus  $\alpha 0$ – $\alpha 5$  of the ribbon diagrams (which correspond to  $\alpha 1$ – $\alpha 6$  in the Ye et al. structure), along with schematic locations of the  $\alpha 3N$  (yellow) and  $\alpha 5$  (shaded red) sensing sites on each view of the dimer.<sup>255</sup> The approximate locations and schematic renderings of representative coordination complexes of distinct sensing sites are shown on the left and correspond to *S. aureus* pI258 CadC (yellow,  $\alpha 3N$ ), *E. coli* plasmid R773 ArsR (green,  $\alpha 3$ ), *S. aureus* CzrA/*Synechococcus* SmtB and *M. tuberculosis* NmtR (red,  $\alpha 5$  and  $\alpha 5C$ , respectively), *M. tuberculosis* CmtR (orange,  $\alpha 4C$ ), *C. glutamicum* ArsR1 (blue), and *A. ferrooxidans* ArsR (purple). The  $\alpha 5$ – $3$  metal site characterized in the Ni/Co sensor *M. tuberculosis* KmtR<sup>37</sup> is not explicitly shown but partially overlaps the  $\alpha 5$  site. See text for details and Figure 11 for a multiple sequence alignment that highlights these metal sensor sites in the ArsR/SmtB family.

the C-terminus of one protomer could coordinate As(III); the degree to which this characterizes the actual structure is not known.<sup>253</sup>

Homodimeric ArsR/SmtB family repressors can exist in one of four allosteric states or configurations: the free apoprotein dimer (denoted P), the metalated repressor ( $P \cdot Me_2$ ), the apo-repressor-DNA complex ( $P \cdot D$ ), and the “ternary” metalated protein–DNA complex ( $P \cdot Me_2 \cdot D$ ) (Scheme 1).<sup>22</sup> In the simplest model of metalloregulation, metal binding drives a quaternary structural conformational transition that stabilizes a low DNA binding affinity of the repressor, i.e., the  $P \cdot Me_2$  complex is significantly different from that of the  $P \cdot D$  complex. There is, as yet, no high-resolution structure of the DNA-bound complex state ( $P \cdot D$ ) for any ArsR/SmtB metal sensor, thus making it difficult to understand the nature of this anticipated conformational change. In addition, the extent of the conformational change required to effect regulation may well vary for different ArsR family repressors given the distinct location of metal-sensing sites on individual sensors (Figure 10). We recently solved the quaternary structure of the paradigm  $\alpha 5$  sensor *S. aureus* CzrA bound to a *czr* operator DNA fragment using NMR

methods, and this structure provides new insights into the conformation and dynamics of the repressor–DNA complex, particularly when compared to the CzrA– $Zn_2$  complex.<sup>257,258</sup>

### 3.1.2. Metal Selectivity

One interesting feature of well-characterized individual ArsR/SmtB family members is that regulatory metal binding sites of a characteristic metal–liganding donor set are found in distinct places, both in the primary structure (Figure 11 for a multiple sequence alignment) as well as on what is known or projected to be common secondary, tertiary, and quaternary structural fold (Figure 10). For example, the  $\alpha 3$ / $\alpha 3N$  and  $\alpha 4C$  metal binding sites nearly exclusively utilize cysteine residues to coordinate metal ions, and as a result, thiophilic or “soft”, highly polarizable metals such as Cd(II), Pb(II), and As(III) bind here (Figures 10 and 11). In three cases where Zn(II) is known to bind to the  $\alpha 3N$  sites to carry out regulation, e.g., in the cyanobacterial Zn(II) sensors *Anabaena* AzrR,<sup>259</sup> *O. brevis* BxmR,<sup>38</sup> and *Synechocystis* ZiaR,<sup>260</sup> a His residue replaces one of the Cys to create a  $S_3N$  donor set. This donor set is distinguished from the  $S_3$

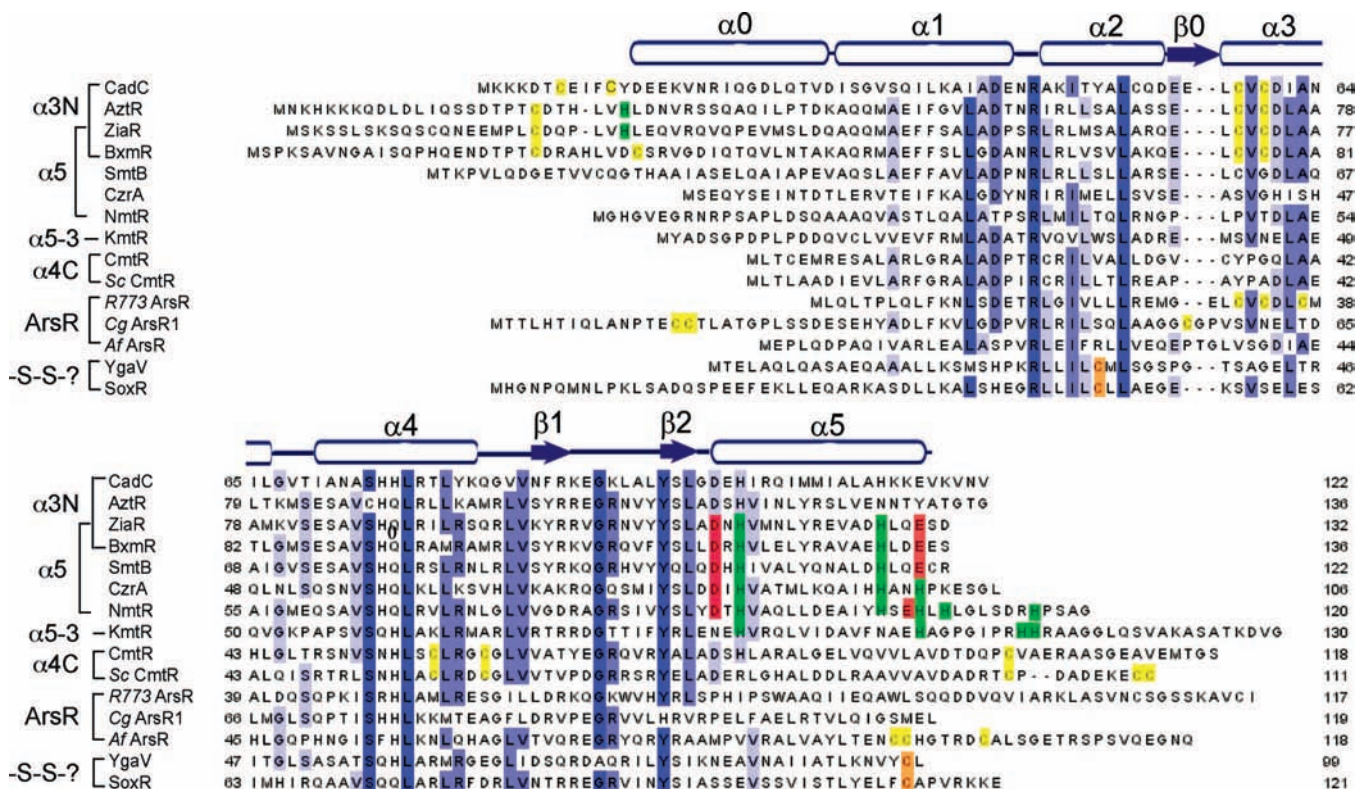


**Figure 11.** Multiple sequence alignment of ArsR/SmtB family repressors discussed here with the secondary structural units of apo-CadC shown.<sup>255</sup> These secondary structural units align well with those known for *S. aureus* CzrA and *Synechococcus* SmtB.<sup>254</sup> The residues known to coordinate *regulatory* metal ions in each sequence are shaded yellow (Cys), green (His), or red (Asp/Glu) in each sequence, with degree of residue-specific conservation at each position in the alignment indicated by the blue shading. See text for details.

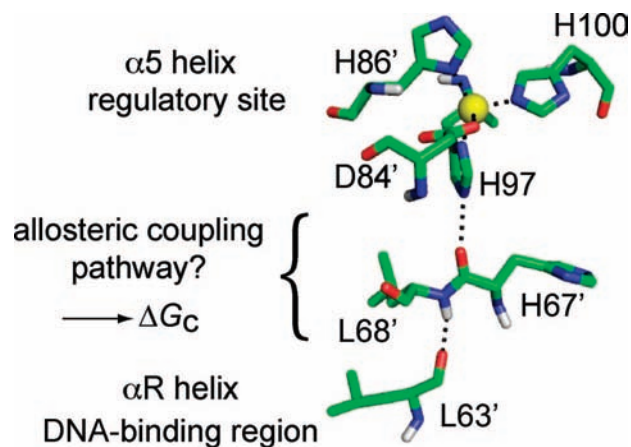


**Figure 12.** Proposed hydrogen-bonding network in Zn(II)-bound CzrA that links the  $\alpha 5$  regulatory sites to that of the DNA binding helices, which is thought to contribute directly to the magnitude of  $\Delta G_c$  (see Scheme 1).<sup>22,254</sup>

[Pb(II)] and  $S_4$  [Cd(II)] donor sites of the related Cd(II)/Pb(II) sensor, *S. aureus* CadC (Figure 11).<sup>261–263</sup> Finally, what appears to distinguish a trigonal As(III)  $\alpha 3$ -sensing site<sup>264</sup> from the Cd(II)/Pb(II)-sensing  $\alpha 3N$  site is metal coordination by a key Cys residue from the N-terminal region of the opposite subunit, Cys7 in *S. aureus* CadC (Figure 11). Cys7 is a key allosteric residue for Cd(II), Pb(II), and Bi(III), substitution of which greatly diminishes the ability of CadC to sense Cd(II) *in vitro*<sup>261,265</sup> and *in vivo*.<sup>266</sup> Bona fide ArsRs related to *E. coli* plasmid R773 ArsR lack this N-terminal region, and regulation by As(III) in a DNA binding assay is insensitive to the presence or absence of Cys7 (Busenlehner and Giedroc, unpublished observations).

Recent work reveals that As(III)-sensing ArsRs have evolved a range of regulatory binding sites that are structurally distinct from the canonical *E. coli* R773 ArsR and provide support for the hypothesis that the ArsR/SmtB family protein matrix is particularly adaptable or evolutionarily “plastic” relative to the nature and number of regulatory metal binding sites. This is projected to occur as a result of convergent evolution in response to environmental pressures.<sup>267</sup> For example, in *Corynebacterium glutamicum* ArsR1, As(III) is coordinated by three cysteine residues in a trigonal  $S_3$  coordination complex at a site distinct from the canonical  $\alpha 3$ - or  $\alpha 4C$ -sensing sites in linking two consecutive Cys from the N-terminal  $\alpha 0$  helix and single Cys in the opposite protomer just N-terminal to the CVC sequence of *E. coli* R773 ArsRs and *S. aureus* CadC (Figure 11).<sup>267</sup> Thus, while reminiscent of the  $S_4$  Cd(II)-sensing site of CadC, it is clearly structurally distinct, consistent with the independent evolution of this metal site.

A recently characterized ArsR/SmtB family repressor, BxmR from the cyanobacterium *O. brevis*, provides an illustration of the evolution of *functional* diversity and redundancy of metal binding sites within a single family member (Figure 11). BxmR regulates the expression of metallothionein and P-type ATPase in response to both Cu(I)/Ag(I) and Zn(II)/Cd(II) as well as the thiol-specific oxidant diamide, all novel properties.<sup>38,268,269</sup> BxmR, like its closest ortholog, *Synechocystis* ZiaR, retains all the metal binding residues in both the  $\alpha 3N$  and  $\alpha 5$  sites (Figure 11). The  $\alpha 3N$  site is capable of binding Cd(II), Ag(I), and Cu(I), the latter through formation of a binuclear  $Cu_2S_4$  cluster analogous to that of *E. hirae* CopY (see section 3.4), while the  $\alpha 5$  site is capable of binding only Zn(II) with high affinity. Unlike CadC, which binds a structural Zn(II) ion at the  $\alpha 5$  site with



no regulatory function,<sup>255,261,270</sup> metal binding to either the  $\alpha 3\text{N}$  or the  $\alpha 5$  site in BxmR is capable of negatively regulating operator DNA binding. Strikingly, however, the functional metal specificity profile of each site differs. The cysteine-rich  $\alpha 3\text{N}$  adopts a range of coordination structures that mediate metalloregulation of DNA binding by all metals that induce gene expression in the cell, including Cd(II), Zn(II), Ag(I), and Cu(I); in contrast, the  $\alpha 5$  site is uniquely capable of driving Zn(II) regulation.<sup>38</sup> Thus, BxmR exhibits the novel property of possessing a relaxed metal response and has retained a functional redundancy in its ability to sense Zn(II). The biological significance of these findings is not yet known.

The C-terminal  $\alpha 5$  helical region of ArsR/SmtB family repressors has also been subjected to evolutionary modification in a way that changes the metal specificity of a particular sensor. For example, the canonical  $\alpha 5$ -sensing site, first characterized in *Synechococcus* SmtB<sup>254,271</sup> and *S. aureus* CzrA,<sup>26,254</sup> adopts an evolutionarily conserved tetrahedral  $\text{N}_2\text{O}_2$  or  $\text{N}_3\text{O}$  coordination geometry reminiscent of the Zn(II) binding sites of SBPs associated with high-affinity Zn(II)-specific ABC transporters (Figure 4; Table 2). In contrast, the Ni(II)/Co(II)-sensing site of *M. tuberculosis* NmtR<sup>272</sup> forms an octahedral N/O-rich coordination complex that incorporates the same four Zn(II) site  $\alpha 5$  ligands but adds two additional ligands thought to be donated by the C-terminal tail in NmtR but missing in SmtB/CzrA to create an  $n = 6$  complex optimized for Ni(II)/Co(II) sensing (Figures 10 and 11).<sup>26</sup> A preliminary model of apo-NmtR based on an analysis of the one-bond backbone amide  $^1D_{\text{NH}}$  residual dipolar coupling constants (RDCs)<sup>273</sup> reveals that the global quaternary structural core is very similar to that of apo-CzrA with disordered N- and C-terminal extensions, including those residues proposed to coordinate Ni(II) in the allosterically inhibited state (Reyes and Giedroc, unpublished observations). Interestingly, KmtR, a second Ni(II)/Co(II) sensor in *M. tuberculosis* that functions independently of NmtR in the cell, may also form an octahedral histidine-rich coordination site for Ni(II) and Co(II) but with a different set of ligating residues relative to NmtR in a metal site designated  $\alpha 5-3$  (Figures 10 and 11).<sup>37</sup> Finally, *Af* ArsR forms a trigonal  $\text{S}_3$  As(III) coordination site derived from consecutive Cys that align with the C-terminus of the  $\alpha 5$  helix and a third more C-terminal Cys (Figure 11).<sup>253</sup>

How do these structural and functional characteristics of individual ArsR/SmtB family members help us to understand the origin of metal selectivity in this large protein family? One conclusion that seems to emerge is that there are two “hot spots” for evolutionary diversity of metal sites in ArsR/SmtB sensors. One is on or just N-terminal to the  $\alpha 3$  helix, while the other is within the C-terminal  $\alpha 5$  helical region, each of which exploits the more divergent N-terminal and C-terminal “tails”, respectively, to create new binding sites for metal ions (Figures 10 and 11). There are also clear trends in coordination number, geometry, and ligand donor type that make it possible to narrow down the subset of metal ions or metalloids that might be sensed by a particular ArsR family sensor in the cell.<sup>26,272</sup>

### 3.1.3. Mechanism of Allosteric Regulation

All of these data taken collectively are consistent with the hypothesis that coordination number is most closely linked to the specificity of metalloregulation in the cell rather than metal binding affinity or other characteristics.<sup>26</sup> The far more

difficult challenge is to understand the molecular basis of this “selectivity”, which must be dictated by interactions outside of the first coordination shell, i.e., second-shell interactions, that energetically “link” or couple the metal site to the DNA binding site to effect allosteric negative regulation of operator binding. This is embodied in the model-independent thermodynamic quantity,  $\Delta G_c$  (Scheme 1), and requires high-resolution structural and dynamical information to understand in molecular terms. For example, the crystallographic structures of the apo- and Zn(II)-bound forms of SmtB and CzrA along with solution NMR studies suggest a quaternary structural switching model for allosteric regulation (Figure 12).<sup>254</sup> This model involves a hydrogen-bonding network formed upon metal binding, which connects the metal binding  $\alpha 5$  helix and the DNA binding domain. Opposite sides of the imidazole ring of the key allosteric residue His117 in SmtB (His97 in CzrA) function in both the first and second coordination shells (Figure 12). The  $\text{N}^{\delta 1}$  atom donates a coordination bond to the metal ion, while the  $\text{N}^{\epsilon 2}$  donates a hydrogen bond to the main-chain carbonyl oxygen of Arg87' (His67' in CzrA) across the protomer interface. Formation of this hydrogen bond sets up a network that is further propagated to L83 (L63 in CzrA) in the DNA binding motif through main-chain–main-chain hydrogen-bond interactions (Figure 12). Although it has been proposed that this hydrogen-bonding pathway substantially contributes to the large observed coupling free energy  $\Delta G_c$  of ca. +6 kcal/mol,<sup>26</sup> the origin of the driving force for this allosteric switch remains unclear. Clearly, thermodynamic studies in conjunction with high-resolution structural studies of all four allosteric states (Scheme 1) will be required to fully understand this fundamental aspect of allostery in metal sensor proteins and how this pathway and underlying energetics may differ for an  $\alpha 5\text{C}$  Ni(II) sensor relative to the  $\alpha 5$  Zn(II) sensor or for an  $\alpha 3\text{N}$  sensor vs an  $\alpha 5$  sensor.<sup>22</sup>

Indeed, aside from apo-CadC and Cd(II)-bound CmtR, there are no other high-resolution structures of non- $\alpha 5$  site-sensing ArsR/SmtB family repressors; as a result, a detailed mechanistic understanding of allosteric negative regulation by these sensors is not yet known. This is likely to be interesting since the measured allosteric coupling free energies vary dramatically for different subfamilies of ArsR/SmtB regulators, from ca. +1 kcal/mol for CmtR<sup>243</sup> to ca. +3 kcal/mol for CadC<sup>261</sup> to ca. +6 kcal/mol for CzrA.<sup>26</sup> Recent data from BxmR shows significantly different coupling free energies for the two metal sites, with ca. 1.6–1.9 kcal/mol when sensing Cu(I) and Ag(I) through the  $\alpha 3\text{N}$  site and  $\geq 3.2$  kcal/mol when sensing Zn(II) via the  $\alpha 5$  site.<sup>38</sup> Although the relative magnitudes of  $\Delta G_c$  cannot be rigorously compared since different models were used to resolve  $\Delta G_c$  in each case, the trends are clear and reveal that the allosteric coupling free energy is largest for the metal site farthest from the DNA binding site ( $\alpha 5$ ) and smallest for the metal sites predicted to be closer to the DNA in the complex ( $\alpha 3\text{N}$  and  $\alpha 4\text{C}$ ). Indeed, the  $\alpha 3\text{N}$  metal site defines the N-terminal edge of the  $\alpha 3$ -turn- $\alpha \text{R}$  DNA binding heads and may even form part of the protein–DNA interface.<sup>258</sup>

### 3.1.4. Putative Nonmetal Ion-Sensing ArsR/SmtB Sensors

Although most ArsR/SmtB family proteins are proposed to be metalloregulatory repressors, some family members have been reported to regulate genes involved in other cellular processes. For example, *Vibrio cholerae* HlyU regulates the expression of the hemolysin gene *HlyA*, and



its homologue has been proposed to function as a master transcriptional regulator for virulence in *Vibrio vulnificus*.<sup>274</sup> *Pseudaminobacter* SoxR is the regulator of a cluster of genes required for sulfur oxidation,<sup>275</sup> which is induced by reduced sulfur compounds, e.g., thiasulfate, by these chemolithotrophic  $\alpha$ -proteobacteria. *Xylella fastidiosa* BigR regulates the transcription of genes related to biofilm formation,<sup>276</sup> while *E. coli* YgaV represses the expression of the *ygaVP* operon encoding a membrane-associated protein YgaP that displays sulfur transferase (rhodanese) activity.<sup>277</sup> Each of these proteins are predicted to be ArsR/SmtB family repressors with a similar fold (Figure 11) but clearly lack all of the known metal binding sites thus far characterized.

In most of these cases, only limited in vivo and in vitro data are available and the natural inducers and their mechanism of induction of these transcriptional regulators remain unknown. Interestingly, tributyltin (TBT) is capable of inducing the *ygaVP* operon via YgaV in vivo. Although TBT may not be the natural inducer, upregulation of the YgaP rhodanese activity, often associated with cyanide detoxification via cysteine persulfide chemistry, may be required to mitigate the effects of oxidative stress induced by TBT.<sup>277</sup> Thus, *Pseudaminobacter* SoxR and *E. coli* YgaV may represent two ArsR/SmtB proteins primarily involved in regulating sulfur metabolism. It is interesting to note that a multiple sequence alignment of each of the nonmetal-sensing ArsR/SmtB regulators mentioned above reveals conservation of two Cys positioned in the predicted  $\alpha 2$  and  $\alpha 5$  helices (shaded orange in Figure 11), the functional importance of which remains unexplored.

### 3.2. MerR Family

The mercuric ion resistance regulator, MerR, first studied in transposons Tn501 from *P. aeruginosa*<sup>278</sup> and Tn21 from *Shigella flexneri* R100 plasmid,<sup>241</sup> is the prototype metalloregulatory protein upon which the word “metalloregulatory” was originally coined.<sup>279</sup> The Hg(II) sensor MerR is now known to be the founding member of a large class of MerR family regulators (COG0789) that function nearly exclusively as transcriptional activators<sup>280,281</sup> of the expression of genes required for metal efflux or detoxification or in some cases defense against oxidative stress and drug resistance.<sup>282</sup> MerR proteins collectively possess very similar N-terminal winged helical domains comprised of a helix–turn–helix– $\beta$ -hairpin structure followed by a long dimerization helix but quite divergent C-terminal effector binding domains (Figure 13). The structural diversity in the C-terminal region makes it possible for individual MerR family proteins to sense not only various metal ions, including Zn(II) by ZntR,<sup>283</sup> Cu(I) by CueR,<sup>34</sup> Hg(II) by MerR,<sup>284</sup> Au(I) by GolS,<sup>285</sup> Cd(II) by CadR,<sup>286</sup> and Pb(II) by PbrR,<sup>287</sup> but also oxidative stress by SoxR via an [2Fe–2S]<sup>2+</sup> cluster and small molecule drugs in the case of BmrR<sup>288</sup> and MtaN (Figure 2).<sup>289</sup>

#### 3.2.1. Metal Selectivity

Insights into the coordination chemistry of MerR regulators was first determined in MerR itself by <sup>199</sup>Hg NMR spectroscopy and site-directed mutagenesis experiments to adopt a subunit-bridging trigonal planar Hg(II) coordination site formed by three cysteine residues.<sup>290,291</sup> In contrast to ArsR/SmtB family repressors which have evolved an impressive panel of regulatory metal binding sites at distinct locations

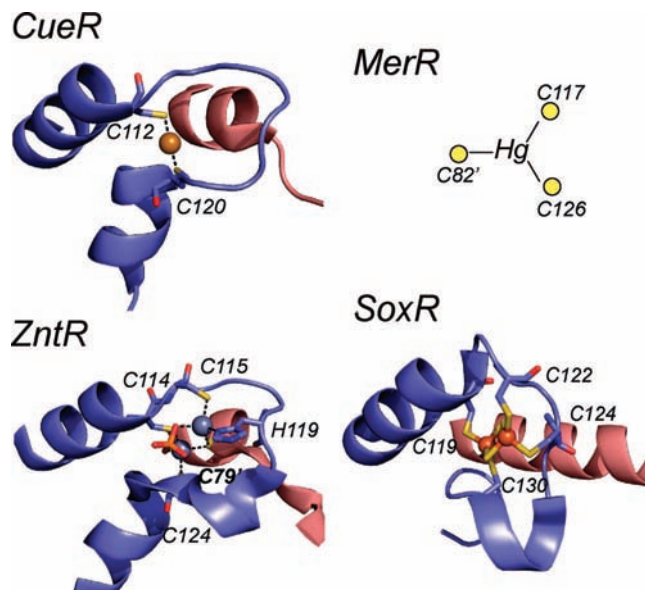


**Figure 13.** Ribbon representations of the metal binding loops of various MerR family metalloregulators. In all cases, only one of the two symmetry-related metal sites are shown with one protomer shaded blue and the other red; annotated metal-donor ligands shown in stick. The structures shown are the Cu(I)-bound form of *E. coli* CueR,<sup>34</sup> the Zn(II)<sub>2</sub> sulfate anion (shown in red/orange)-bridged binuclear structure of *E. coli* ZntR,<sup>34</sup> and the [2Fe–2S]<sup>2+</sup> center of *E. coli* SoxR.<sup>296</sup> A schematic of the single subunit-bridging Hg(II) site of Tn501 MerR consistent with spectroscopic and functional data<sup>290,291</sup> but of unknown structure is also shown for comparison.

as a means to evolve metal selectivity, the metal binding sites in individual MerR family proteins are all composed of residues derived from two symmetry-related metal binding loops at the periphery of the dimer, positioned just C-terminal to the long dimerization helix, which itself is followed by a short C-terminal helix (Figure 13). This single metal binding site region in MerR proteins has evolved to sense a wide range of divalent as well as monovalent metal ions, each of which is characterized by a signature disposition of metal ligands (Cys/His) in the metal binding loop and elsewhere (Figure 13).<sup>34,282</sup> Previous crystallographic structures of *E. coli* CueR bound to Cu(I), Ag(I), and Au(I) and ZntR bound to Zn(II) reveal how MerR proteins distinguish between divalent and monovalent metal ions,<sup>34</sup> while more recent studies on *Salmonella typhimurium* GolS illustrates how a MerR protein can be finely tuned for preferential sensing of Au(I) over Cu(I).<sup>285</sup>

A comparison between Cu(I)-bound *E. coli* CueR and Zn(II)-bound *E. coli* ZntR structures reveals several key determinants for metal specificity of monovalent metal ions (CueR) over divalent metal ions (ZntR). One conserved residue at the N-terminus of the dimerization helix from the opposite protomer in the dimer plays a critical role in this specificity switch. All monovalent metal ion MerR sensors have a conserved serine (Ser77 in CueR) in this position, while all divalent metal ion MerR sensors contain a conserved cysteine (Cys79' in ZntR) (Figure 13). Ser77 in CueR stabilizes the metal binding loop in helping to form a shielded, hydrophobic environment for the Cu(I) ion. In contrast, Cys79' in ZntR directly coordinates one of the two Zn(II) ions bound in the metal binding loop, thus providing an additional ligand for the metal and resulting in a higher coordination number optimal for binding Zn(II) relative to Cu(I). Furthermore, significant charge neutralization mediated

by the partial positive charge of the helix dipole of the C-terminal short  $\alpha$ -helix as well as other proposed charge–charge and hydrogen-bonding interactions also play important roles in stabilizing a buried and novel linear dithiolate or digonal  $S_2$ –Cu(I) coordination complex.<sup>292</sup> It is important to point out that the linear dithiolate complex in CueR is also suitable for coordinating Hg(II). However, the near optimal neutralization of the net negative charge arising from the two thiolate anions and one +1 charged Cu(I) ion is predicted to enhance the binding of monovalent Cu(I) relative to divalent Hg(II) on electrostatic grounds.<sup>34</sup> The structure of Hg(II)–MerR remains unknown, but the same two Cys from the metal binding loop (Cys112 and Cys120) are combined with a third Cys analogous to Cys79 in ZntR (Cys82') to create a trigonal planar  $S_3$  site (Figure 13).<sup>290</sup>

Although the structure of CueR provides a structural rationale for understanding the molecular basis for the ability of CueR to discriminate between divalent and monovalent ions, biochemical studies have shown that CueR is poor at distinguishing between similar monovalent metal ions such as Cu(I), Ag(I), and Au(I);<sup>293</sup> in fact, their crystallographic structures are isomorphous.<sup>34</sup> A recent report on GolS, a MerR protein which is about 100-fold more sensitive to Au(I) than Cu(I) and Ag(I), provides another opportunity to understand how a simple dithiolate metal coordination chemistry can be finely tuned to be biologically selective for Au(I). Small differences in the metal binding loop region are solely responsible for this metal specificity since a simple surgical replacement of the GolS metal binding loop by that of CueR gives rise to the significant Cu(I)-dependent response *in vivo*.<sup>285</sup>

In short, these findings reveal that while coordination number and geometry are important determinants of metal selectivity in MerR family members, the precise details of the immediate coordination environment, e.g., electrostatics and perhaps other more subtle features, can be used to tune the selectivity of what is a *single* metal binding site. Additional structural information on other MerR family proteins will provide new details as to how small changes in the metal binding pocket can lead to distinct metal specificity profiles. For example, it will be particularly interesting to understand how Cd(II)-sensing CadR distinguishes Cd(II) over Pb(II)/Zn(II) and how Pb(II)-sensing PbrR detects Pb(II) over Cd(II)/Zn(II). If lessons from *S. aureus* CadC are any indication,<sup>261</sup> it seems likely that the Pb(II) complex in PbrR may be optimized to make a trigonal  $S_3$  coordination complex but one in which the protein matrix exploits the stereochemically active lone pair of 6s electrons to create a binding site that stabilizes a hemidirected, highly distorted  $S_3$  complex. The second shell in CadR may not do this and thus would dictate a preference for Cd(II) over Pb(II). Structural studies on these two MerR regulators alone may greatly expand the principals learned from inspection of the metal-bound CueR and ZntR structures (Figure 13).<sup>34</sup>

### 3.2.2. Transcription Activation

MerR family proteins are unique in the mechanism of transcription activation among all the metalloregulatory proteins.<sup>281</sup> The DNA sequences MerR proteins recognize have one common feature: a long 19- or 20-bp spacer between the –35 and –10 promoter elements, which results in poor RNA polymerase binding affinity and transcription initiation efficiency.<sup>294</sup> As originally determined for MerR itself,<sup>295</sup> both the apo- and effector-bound forms are capable

of binding to their cognate operator DNA sequences with similar affinities. However, only the effector-bound form can significantly unwind and distort the DNA helix, bringing the –35 and –10 elements to the same side of the DNA helix in a position optimized for RNA polymerase binding and ultimately transcriptional activation.<sup>294</sup> Thus, both RNA polymerase and the effector-bound MerR family member are predicted to be bound to the promoter simultaneously. This mechanism of allosteric modulation of the DNA structure was first documented at high resolution by the crystallographic structure of a multidrug efflux regulator *B. subtilis* BmrR bound to a small lipophilic drug, tetraphenylphosphonium (TPP), in complex with its cognate 22-base pair DNA operator; this was followed by several other multidrug transporter regulator–DNA complex structures.<sup>288</sup> Unfortunately, there is yet no high-resolution structure for any MerR family metal sensor in complex with DNA. However, the recently published structure of the oxidative stress sensor *E. coli* SoxR–DNA complex sheds considerable light on this. SoxR contains an oxidized  $[2Fe-2S]^{2+}$  cluster coordinated by four cysteines from the metal binding loop (Cys119, Cys122, C124, and Cys130) that is analogous to that found in metal-sensing MerR proteins (Figure 13).<sup>296</sup>

*E. coli* SoxR activates the transcription of SoxS in response to superoxide, nitric oxide, and other redox-cycling agents;<sup>297</sup> indeed, the reduced SoxR  $[2Fe-2S]^+$  cluster reacts with low molecular weight NO donors, e.g., *S*-nitrosoglutathione, *in vitro* and *in vivo* to form dinitrosyl–iron complexes that are capable of activating *soxS* expression.<sup>298,299</sup> SoxS, a member of the AraC family of transcriptional activators, then activates the expression of genes such as superoxide dismutase SodA, outer membrane drug effluxer TolC, and DNA repair-related endonuclease IV.<sup>297,300,301</sup> These studies suggest that the *soxRS* regulon plays essential roles in oxidative stress sensing and resistance. Interestingly, recent work has uncovered another MerR family protein NmlR from *Streptococcus pneumoniae* that is proposed to function as an NO stress sensor.<sup>300,301</sup> Although the mechanism remains unclear, it is possible that NmlR senses NO by forming an *S*-nitrosyl thiol adduct on its lone cysteine residue, thereby altering the conformation of DNA-bound NmlR, leading to transcriptional activation analogous to that which has been observed in *E. coli* OxyR;<sup>302</sup> this would represent a sensing mechanism that is completely distinct from that of *E. coli* SoxR.

The activated, oxidized  $[2Fe-2S]^{2+}$  form of SoxR bound to DNA uncovers at high resolution what may be a general structural mechanism of activation from a 20-bp spacer promoter, which is most commonly found in the cognate operator–promoter sequences for many metal ion sensors in the MerR family, including MerR, ZntR, and CueR (Figure 14).<sup>296</sup> This structure is distinct from the previously reported BmrR–DNA and MtaN–DNA complexes, each of which is characterized by a 19-bp spacer in the promoter.<sup>288</sup> In the SoxR–DNA structure, the long dimerization helix ( $\alpha 5$ ) exhibits the largest differences relative to the drug–BmrR–DNA structures in that it is twisted into a unique position relative to BmrR and stabilized by hydrophobic interactions. The DNA in the complex is also significantly more bent ( $\sim 65^\circ$ ) than that in BmrR– and MtaN–DNA complexes ( $\sim 47$ – $50^\circ$ ) (Figure 14a), resulting in further shortening of  $\sim 3.4$  Å, which compensates for the additional 1-bp spacer in the DNA relative to the 19-bp spacer DNA for the BmrR and MtaN complexes. Base-specific interactions by the residue at position 26 (Ser for SoxR, Glu for MerR, and Lys for CueR,



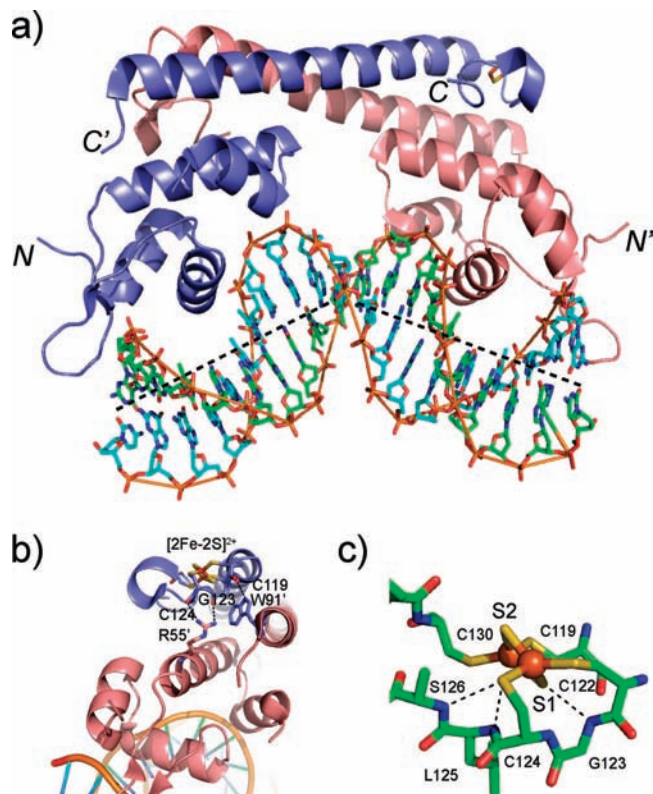
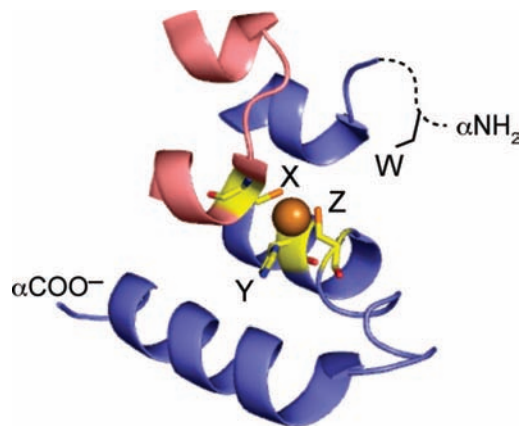


**Figure 14.** Crystallographic structure of the oxidized (activated) *E. coli* SoxR-DNA complex.<sup>296</sup> (a) Overall view of the structure of SoxR-DNA complex showing a significant bend ( $\sim 65^\circ$ ) in the *sox* operator DNA. The DNA strands are colored green and cyan and shown in stick representation; the two protomers of the SoxR homodimer are shown as ribbon structures and shaded as in Figure 15. (b) Intersubunit hydrogen-bonding interactions that link main-chain carbonyl oxygen atoms from G123 and C124 in the metal binding loop that coordinates the  $[2\text{Fe}-2\text{S}]^{2+}$  cluster with the side chain of R55' from the DNA binding domain of the opposite protomer. A main-chain-side-chain hydrogen bond between C119 and W91' from the dimerization helix of the opposite protomer is also shown. (c) Close-up view of the  $[2\text{Fe}-2\text{S}]^{2+}$  cluster revealing how electrostatic interactions around the bridging  $\text{S}^{2-}$  anion S1 may facilitate the conformational change upon reversible reduction/oxidation of the cluster.<sup>296</sup>

etc.) may play an important role for each individual MerR protein to recognize their own operator sequences. Furthermore, signal transduction between the sensing domain and the DNA binding domain is proposed to be mediated by direct interactions between the two domains.<sup>296</sup> Hydrogen-bonding interactions between the backbone carbonyl oxygens of Gly123 and Cys124 in the  $[2\text{Fe}-2\text{S}]^{2+}$  binding loop and a conserved Arg55' in the  $\alpha 3'$  helix from the opposite protomer is proposed to be crucial in driving a quaternary structural conformational change coupled to DNA distortion (Figure 14b). An analogous set of interactions is also found in the recent drug-bound BmrR-DNA complex to be crucial for transcription activation and may well be common to all MerR family regulators.<sup>303</sup>

The SoxR-DNA structure also suggests a plausible mechanism by which reversible oxidation of the reduced  $[2\text{Fe}-2\text{S}]^+$  cluster may drive an interdomain reorganization that is required to allosterically induce DNA distortion upon oxidation. However, without a high-resolution structure of the transcriptionally inactive  $[2\text{Fe}-2\text{S}]^+$  form of SoxR bound to DNA, these suggestions are speculative. In any case, it is interesting to note that the oxidized  $[2\text{Fe}-2\text{S}]^{2+}$  cluster, while nearly completely exposed to solvent, is asymmetrically



Fingerprint:	W-X-Y-Z
Cu(I) CsoR:	x-C-H-C
Ni(II) RcnR:	H-C-H-H
Redox (?):	x-C-x-C
FrmR (redox):	x-C-H-x

**Figure 15.** Schematic representation of the W-X-Y-Z “fingerprint” of individual CsoR/RcnR family repressors adapted from ref 309. The X-Y-Z region of the fingerprint is defined by the ligands to the Cu(I) ion in Cu(I)-sensing CsoRs, corresponding to C36, H61', and C65' in opposite protomers of *M. tuberculosis* CsoR (shaded red and blue, respectively).<sup>244</sup> W corresponds to H3 in *E. coli* RcnR, which must occupy the third position relative to the M1  $\alpha\text{NH}_2$  group.<sup>309</sup> The invariant Cys in the X position is shaded red.

disposed relative to the immediately surrounding charge distribution of the metal binding loop (Figure 14c).<sup>296</sup> In particular, the S1 bridging sulfide anion lies in a region of partial positive electrostatic potential, contributed by three main-chain amide nitrogens from Gly123, Lys125, and Ser126 in the metal binding loop (Figure 14c). Reduction of the cluster (addition of an  $e^-$ ) would therefore remove a patch of significant electrostatic repulsion around S1, and pull “up” on the loop, which in turn would pull “up” on Arg55' and thereby alter the conformation of the DNA binding domain.

Observations gleaned from the structure of the oxidized SoxR-DNA complex provide significant insight into the allosteric mechanism of transcriptional activation by other metal ion sensors in the MerR family. This is a consequence of the similarities in the DNA sequence used for the structural studies, i.e., a 20-bp spacer between the  $-10$  and  $-35$  regions of the promoter and the effector binding domains, and because SoxR and the MerR family metal ion sensors are known to utilize overlapping subsets of residues from the metal binding loop to sense different stresses.

### 3.2.3. Beyond the SoxR-SoxS Paradigm

*E. coli* SoxR was originally discovered as a major factor, along with the LysR family transcriptional regulator (LTTR) OxyR (section 3.8.1), required to mediate resistance against oxidative stress, in particular by hydrogen peroxide and superoxides.<sup>304</sup> As discussed above, in *E. coli*, SoxR regulates transcription of a single gene, *soxS*, by binding to the *sox* operator, the product of which upregulates the entire *soxRS* regulon. A recent bioinformatics analysis has uncovered a large fraction of bacterial organisms, including the proteobacterium *P. aurigenosa* and the soil-dwelling *Streptomyces coelicolor*, harbor a “solo” *soxR* gene<sup>305</sup> and lack the gene



encoding the master regulator, SoxS.<sup>306</sup> In these bacteria, SoxR regulates a handful of genes not directly associated with oxidative stress but instead are involved in transport, via the *mexGHI-opmD* RND efflux pump (see section 2.6.3), and the metabolism of small molecules, including redox-active antibiotics (as chemical weapons against competing organisms) and endogenous pigments, e.g., the highly fluorescent phenazine pyocyanin in *P. aureginosa*.<sup>306</sup> Pyocyanin is a quorum-sensing molecule that regulates biofilm formation in pseudomonas and coordinates and organizes bacterial community growth. Pyocyanin activates the *soxR* regulon in *P. aureginosa*, although the mechanism has not yet been worked out.<sup>307</sup> It is the case, however, that in the presence of molecular oxygen, pyocyanin can generate superoxides, which can in turn oxidize the [2Fe–2S]<sup>+</sup> cluster of SoxR in the normal fashion. Indeed, recent electrochemical studies reveal that the reduction potentials *E. coli* and *P. aureginosa* SoxRs bound to the *sox* operator are approximately the same, +200 mV vs the normal hydrogen electrode, a value that is shifted dramatically (by +490 mV) relative to the free protein.<sup>308</sup> The origin of shift is likely derived from the large conformational distortion induced by reduced SoxR bound to the DNA. This redox potential means that in the highly reducing conditions of the cytosol the DNA-bound forms of both *E. coli* and *P. aureginosa* SoxR will be in their reduced states and are thus poised to sense oxidative stress generated via multiple pathways.

### 3.3. CsoR/RcnR Family

The CsoR/RcnR family is the most recently structurally characterized family among all major metalloregulatory protein classes. *M. tuberculosis* CsoR is representative of a subfamily of Cu(I) sensors,<sup>244</sup> while *E. coli* RcnR is representative of a subset of Ni(II)/Co(II) sensors.<sup>309,310</sup> The classification of different subfamilies is dependent on the conserved residues in several signature positions, herein designated W-X-Y-Z, in a multiple sequence alignment (Figure 15). Cu(I)-sensing CsoRs contain a conserved W-X-Y-Z x-Cys-His-Cys sequence (where x is any amino acid) as a “fingerprint”, and RcnR proteins contain a His-Cys-His-His W-X-Y-Z fingerprint in the precisely corresponding positions.<sup>309</sup> Other subfamilies have distinct fingerprint features and include the formaldehyde repressor from *E. coli*, FrmR, which has yet to be biochemically characterized. Other CsoRs may be involved in oxidative stress resistance or sensing of small molecules, speculation based on common genomic neighborhoods, and conservation of only two Cys in the X and Z positions of the fingerprint (Figure 15); none of these have been functionally characterized as yet.<sup>309</sup>

#### 3.3.1. CsoR-Like Cu(I) Sensors

Unlike other Cu(I) sensors such as *E. coli* CueR and *E. hirae* CopY which are largely confined to the Proteobacteria and Firmicutes, respectively, genes encoding CsoRs are widely distributed through most major bacterial species.<sup>244</sup> As the founding member, *M. tuberculosis* CsoR (*Mtb* CsoR) has been characterized using biological, biophysical, and structural methods. CsoR is the transcriptional repressor of the *cso* (Cu-sensitive operon) which encodes CsoR itself, a gene of unknown function but limited to mycobacteria (*rv0968* in *Mtb*), and a Cu(I)-effluxing P-type ATPase CtpV. Apo-CsoR binds to the operator–promoter region upstream of the *csoR* gene with the addition of Cu(I) but not other

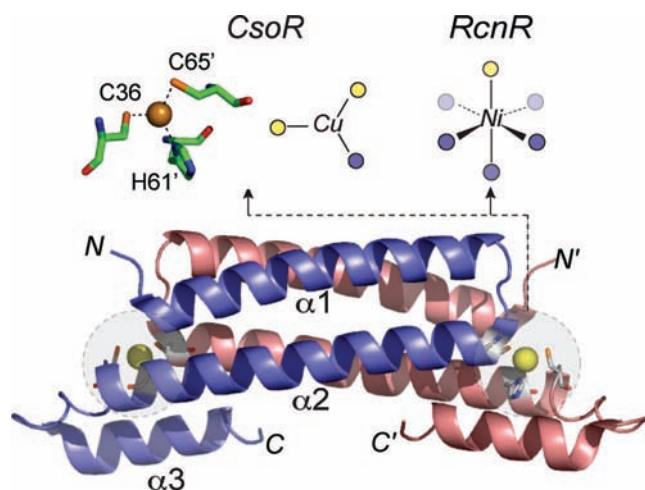


**Figure 16.** Ribbon representation of the 2.6 Å crystallographic structure of the Cu(I)-bound *M. tuberculosis* CsoR homodimer.<sup>244</sup> The crystallographically defined structure of the Cu(I) coordination complex is shown in stick representation, while schematic representations of Cu(I) and Ni(II) complexes of CsoR and *E. coli* RcnR,<sup>309</sup> respectively, are also shown. Cys sulfur ligands are shaded yellow, while N/O ligands are given by the blue spheres. The  $\alpha$ -helices of the blue protomer in CsoR are labeled  $\alpha 1$ – $\alpha 3$ .

divalent metals, resulting in derepression of transcription. Physiological Cu(I) stress induces the expression of a relatively small number of genes in *M. tuberculosis*, and it is not known as yet how many of these are regulated by CsoR.<sup>142</sup> It is also not known as yet if the Cu(I) binding metallothionein MymT<sup>19</sup> is regulated by CsoR.

The 2.6 Å crystallographic structure of Cu(I)-bound CsoR reveals a homodimeric structure with a core antiparallel four-helix bundle ( $\alpha 1$ ,  $\alpha 1'$ ,  $\alpha 2$ ,  $\alpha 2'$ ) and the short C-terminal  $\alpha 3$  helix stacked against the base of the molecule, proximate to  $\alpha 2'$  helix of the opposite protomer (Figure 16). The Cu(I) ion is coordinated to an intersubunit metal binding site formed by two conserved cysteines (Cys36 and Cys65) and one conserved histidine (His61) with very high affinity (C36, H61, and C65 define the X, Y, and Z positions of the fingerprint; Figure 15).<sup>244</sup> Due to the lack of a classical DNA binding motif such as the winged helix–turn–helix domain commonly found in other metalloregulatory proteins (Figure 2), how apo-CsoR binds to its cognate DNA operator remains unclear as is the mechanism by which Cu(I) binding induces allosteric negative regulation of operator DNA binding.

*B. subtilis* CsoR is another CsoR homologue that has been functionally characterized and shown to regulate expression of the *copZA* operon in a manner similar to that of *Mtb* CsoR.<sup>311</sup> Recent in vitro experiments reveal that *B. subtilis* CsoR also binds Cu(I) with very high affinity and forms a trigonal S<sub>2</sub>N coordination site.<sup>140</sup> Interestingly, *B. subtilis* CsoR is also capable of binding Ni(II), Zn(II), and Co(II) with high affinity but adopts non-native metal coordination complexes in each case. Binding of these divalent metal ions does not strongly inhibit *copZA* operator DNA binding, which is consistent with the theme that emerges from the study of ArsR/SmtB and MerR family members that metal–ligand coordination geometry plays the key role in establishing metal selectivity rather than metal binding affinity.<sup>13,26,35</sup>

Another interesting question is how these Cu(I) sensors actually acquire Cu(I) ion in the cytosol since it is commonly accepted that there is little free or bioavailable Cu ions in the cytosol due to its toxicity.<sup>138</sup> Cytosolic copper chaperones

usually play essential roles in mediating Cu-trafficking via ligand transfer reactions (Figures 7 and 8).<sup>312</sup> In *B. subtilis*, CsoR regulates the expression of not only the Cu(I)-effluxing ATPase but also the Cu(I) chaperone CopZ. Although the experimental evidence is not yet in, it is reasonable to hypothesize that CopZ donates Cu(I) to CsoR, analogous to that which has been documented to occur in *E. hirae*, where CopZ delivers Cu(I) to the Cu(I) sensor CopY (see section 3.4). It is as yet not clear how general this model is going to be since in many bacteria, including the model organisms *M. tuberculosis* and *E. coli*, an obvious functional homologue of the Cu(I) chaperones CopZ or Atx1 is not readily identified; as a result, it is not clear how *M. tuberculosis* CsoR and *E. coli* CueR acquire their metal under copper stress. On the other hand, such a chaperone may not be needed since CsoRs from both *B. subtilis* and *M. tuberculosis* as well as *E. coli* CueR possess extraordinarily high Cu(I) binding affinities<sup>34,140,244</sup> and thus may be capable of scavenging essentially all cytosolic Cu(I) under these conditions. It is also interesting to note that Cu(I) stress induces a second Cu(I)-CsoR homologue of the three total<sup>244</sup> (the third contains an x-C-x-C fingerprint; Figure 15) in *M. tuberculosis* whose function remains undefined.<sup>142</sup>

### 3.3.2. RcnR-Like Co(II)/Ni(II) Sensors

*E. coli* RcnR is a Co(II)/Ni(II) sensor that regulates the expression of a nickel and cobalt efflux protein RcnA (Figure 1).<sup>310</sup> RcnA is proposed to be a member of the major facilitator superfamily (MFS) family of membrane permeases that is unrelated to NiCoT permeases.<sup>65</sup> Although RcnR shares very low sequence similarity with CsoR, it is predicted to be an all  $\alpha$ -helical protein with a fold similar to that of CsoR; thus, RcnR and CsoR are considered to be distantly related orthologs that represent two major subfamilies in this new metalloregulatory protein family.<sup>309</sup>

Unlike Cu(I)-sensing CsoRs, RcnRs possess a His-Cys-His-His W-X-Y-Z metal binding fingerprint (Figure 15); recent Ni(II) and Co(II) binding experiments coupled with characterization by electronic and X-ray absorption spectroscopies reveal that RcnR binds both Ni(II) and Co(II) with a 6-coordinate octahedral geometry, clearly distinct from Cu(I)-CsoR complex (Figure 16). Although the Ni(II) and Co(II) coordination spheres may differ slightly, they both include all four of the signature residues conserved in RcnR-like proteins with a fifth ligand donated from the  $\alpha$ -amino group at the N-terminus which would be in close proximity. The identity of the sixth ligand remains unknown, with possible recruitment of a backbone amide or a solvent molecule into the first coordination shell.<sup>309</sup> The obvious differences between coordination geometries of Cu(I)-bound CsoR and Ni(II)-bound RcnR reinforce the notion that coordination geometry controls metal selectivity with a higher coordination number being far more favorable for Ni(II) and Co(II) relative to Cu(I).

In a striking parallel with ArsR/SmtB  $\alpha$ 5-site sensors as well as MerR family sensors, a comparison of CsoR and RcnR illustrates the degree to which metal sites with distinct selectivities can be evolved from a common "core" of primary coordinating residues, which in this case likely corresponds to the Cys pair across the protomer interface, Cys36 and Cys65' in *M. tuberculosis* CsoR (Figure 15). Metal binding here, or even reversible disulfide bond formation or derivatization of one or both Cys (see below), might be anticipated to alter the structure of the dimer (or

oligomer), which in turn might be necessary, albeit not sufficient in the case of CsoR and RcnR, to drive allosteric negative regulation of DNA binding. The characterization of putative nonmetal ion-sensing CsoRs is thus of interest (section 3.3.3).

### 3.3.3. Putative Nonmetal-Sensing CsoR/RcnR Regulators

An extensive multiple sequence alignment of CsoR/RcnR family proteins (formerly annotated as DUF156; now COG1937)<sup>244</sup> reveals other members with "fingerprint" residues distinct from the x-Cys-His-Cys and His-Cys-His-His W-X-Y-Z residues of CsoR and RcnR, respectively (Figure 15).<sup>309</sup> For example, *E. coli* FrmR is characterized by a x-Cys-His-x fingerprint and has been reported to regulate genes related to formaldehyde resistance and degradation.<sup>313</sup> Formaldehyde is representative of a class of  $\alpha,\beta$ -unsaturated aldehydes, highly toxic naturally occurring carbonyl-containing electrophiles that are generated from oxidation of amino acids, lipids, and carbohydrates; formaldehyde itself is an intermediate in the metabolism of C<sub>1</sub> compounds by some bacteria.<sup>314</sup> Methylglyoxal is another toxic carbonyl electrophile that occurs as a consequence of triose-phosphate intermediates generated by glycolysis, reacts with low molecular weight thiols, and is detoxified by the consecutive action of glyoxalases I and II.<sup>315</sup> Both formaldehyde and methylglyoxal react with cysteine thiols to create thioesters or thiol-S-alkylated products. In this context, the earlier discovery of the single-Cys-containing CsoR family member, FrmR,<sup>313</sup> takes on added significance given the recent demonstration that a key regulator of the formaldehyde detoxification system in *B. subtilis* is AdhR (formaldehyde dehydrogenase regulator), a MerR family regulator (section 3.2) that is related to the putative nitric oxide stress sensor in *S. pneumoniae* NmlR.<sup>300</sup> Like FrmR, AdhR (and NmlR) contains a single Cys residue that has been shown to be required for formaldehyde sensing, and the hypothesis is that activation of the expression of *adhA* occurs via derivatization of the single Cys by thiol-S-alkylation.<sup>316</sup>

Other CsoR/RcnR family members contains x-Cys-x-Cys W-X-Y-Z fingerprints; note that these are unlikely to be Cu(I) sensors given that substitution of the Cu(I) ligand His renders CsoR inactive as a Cu(I) sensor.<sup>244</sup> Instead, these putative CsoR/RcnR orthologs are proposed to be involved in some way in oxidative stress sensing or antibiotic resistance based on the immediate genomic neighborhood.<sup>309</sup> However, there is no evidence as yet that these CsoRs actually bind DNA, but this seems likely. For example, we note that in two Gram-positive pathogens, *S. pneumoniae* and *S. aureus*, x-Cys-x-Cys CsoR/RcnR family members are found near genes encoding a rhodanese homology domain protein and/or a putative glyoxalase I. In *S. aureus*, in fact, this putative CsoR is upstream of a gene encoding a rhodanese, superficially analogous to the organization of the *E. coli* *ygaVP* operon regulated by a two-Cys-containing, nonmetal-sensing ArsR family regulator YgaV discussed above (see Figure 11).<sup>277</sup> This genomic neighborhood implicates these x-Cys-x-Cys CsoRs in oxidative stress sensing, detoxification of carbonyl electrophiles, or sulfur trafficking. Inspection of the structure of *M. tuberculosis* CsoR reveals that these two conserved cysteine residues in a x-Cys-x-Cys CsoR are predicted to be in close proximity, which makes it possible for these residues to undergo reversible disulfide bond formation under oxidative stress. Such a mechanism has been shown to be operative in other antibiotic and redox-sensing repressors,



as exemplified by the MarR family member *Pseudomonas aeruginosa* MexR (section 3.8.2).<sup>238</sup> However, to qualify as a cytosolic redox sensor, the reduction potential of this cysteine pair must be tuned in a way that tracks with changes in that potential that occur under conditions of oxidative stress. Therefore, both functional biological and biochemical studies will be required to understand this nonmetal-sensing subgroup of this newly discovered metalloregulatory protein family.<sup>244,309</sup>

### 3.4. CopY Family

CopY represents a family of copper-specific metalloregulatory proteins restricted largely to the Firmicutes<sup>244</sup> and was first characterized in *E. hirae*.<sup>246</sup> It is proposed to be a member of MecI/BlaI family due to the high sequence similarity in the N-terminal DNA binding domain and the fact that CopY and MecI/BlaI recognize identical cognate DNA sequences (Figure 2).<sup>317</sup> *E. hirae* CopY regulates the transcription of the *copyZBA* operon which encodes two copper-specific P-type ATPases (CopA and CopB) thought to be involved in copper uptake and efflux, respectively, and the copper chaperone CopZ. It has been shown that Zn(II)-bound CopY binds to the operator–promoter region of the *copyZBA* operon and represses the transcription; Cu(I)-bound CopZ then transfers Cu(I) to Zn(II)-bound CopY, forming Cu(I)–CopY, which dissociates from the DNA and leads to transcriptional derepression of the operon.<sup>318</sup> Most CopYs possess a conserved CXCXXXXCXC motif close to the C-terminus, and spectroscopic studies reveal that each CopY protomer within the dimer is capable of binding two equivalents of Cu(I) per monomer to form a highly luminescent binuclear  $S_4$ -Cu<sub>2</sub> cluster<sup>318</sup> exactly analogous to Cu(I) formed by the ArsR/SmtB family regulator BxmR.<sup>318</sup>

Recent functional and structural studies of the CopY family Cu sensor *Lactococcus lactis* IL1403 CopR provides new insights into the CopR regulon as well as the high-resolution structure of the N-terminal winged helix DNA binding domain.<sup>141,319</sup> Expression profiling experiments reveal that the CopR regulon consists, as expected, of Cu-homeostasis-related genes including *copB* and the *copRZA* operon but also genes related to oxidative stress resistance, e.g., lactate oxidase (*lctO*), nitroreductase (*ytjD*), and glyoxalase I (*yaiA*).<sup>141</sup> Similar findings characterize *M. tuberculosis*<sup>142</sup> and are consistent with the physiological scenario in which excess Cu(I) may be capable of engaging in redox cycling and generation of reactive oxygen species (see section 2.3).<sup>15</sup> The solution structure of the CopR N-terminal DNA binding domain monomer has recently been solved by NMR methods and reveals, as anticipated, a winged helix–turn–helix domain similar to the N-terminal domain of *S. aureus* MecI and BlaI, respectively, the regulators of the genes encoding the penicillin binding protein and  $\beta$ -lactamase whose crystal structures with and without DNA bound have been previously reported.<sup>319,320</sup> Further biophysical and structural characterization of the C-terminal Cu(I) binding domain in the context of the intact homodimeric repressor, however, will be required to fully understand how Cu(I) is capable of mediating an allosteric or regulatory response upon DNA binding while Zn(II) is not.

### 3.5. Fur Family

The Fur family of metalloregulatory proteins is named for the founding member *E. coli* Fe-regulated uptake repressor

Fur and encoded in the genomes of virtually every Gram-negative bacterium,<sup>20</sup> with the notable exception of the plant symbiont *Rhizobium* and other closely related  $\alpha$ -proteobacteria (section 3.5.2).<sup>321</sup> In *E. coli*, Fur is a global transcriptional regulator of well over 90 genes encoding both proteins and noncoding RNAs and involved in iron homeostasis as well as oxidative stress and acid tolerance.<sup>20</sup> A handful of Fur orthologs have now been extensively characterized and include sensors for other transition metal ions, e.g., the Zn(II) sensor Zur,<sup>322,323</sup> the Mn(II)/Fe(II) sensor Mur,<sup>324</sup> the Ni(II) sensor Nur,<sup>325</sup> as well as those that sense hydrogen peroxide (H<sub>2</sub>O<sub>2</sub>), PerR.<sup>326</sup> Fur proteins are typically transcriptional repressors when bound to their cognate metal ion effectors, with the apoprotein possessing low or negligible affinity for the DNA operator. There may well be exceptions to this model, however, since *H. pylori* Fur has been shown to repress transcription of a ferritin gene and an *sodB*-encoded superoxide dismutase in its iron-free apo form and functions as an activator when bound to Fe(II).<sup>327</sup> However, many of the activating functions of Fur appear mediated indirectly through Fur-dependent repression of the expression of an antisense regulatory small RNA.<sup>328,329</sup>

#### 3.5.1. Structural Studies

The crystallographic structures of *P. aeruginosa* Fur,<sup>330</sup> *B. subtilis* PerR,<sup>331,332</sup> *S. coelicolor* Nur,<sup>333</sup> and *M. tuberculosis* Zur<sup>322</sup> (formerly annotated as FurB) reveal a similar protein fold with an N-terminal winged helix DNA binding domain linked to a C-terminal dimerization domain by a flexible linker. The number and function of metal sites in individual Fur family members seem to differ, but consensus may well be emerging on a single metalloregulatory site or region likely shared by all Fur proteins capable of adopting a range of coordination geometries dictated by metal type.<sup>22,334</sup> Many Fur family repressors contain what is now known to be a structural Zn(II) site that adopts a tetrahedral S<sub>4</sub> coordination complex formed by four cysteine residues derived exclusively from the dimerization domain; *P. aeruginosa* Fur does not possess this structural site (Figure 17).<sup>22,322</sup> NMR studies on *E. coli* Fur suggest that Zn(II) bound at this tetrathiolate site strongly stabilizes the functional dimer.<sup>335</sup> The crystallographic structure of *M. tuberculosis* Zur reveals the S<sub>4</sub> site as well as two additional bound Zn(II) ions that correspond roughly to the location of the two sites found in the Zn(II)-complexed structure of the Fe(II) sensor *P. aeruginosa* Fur.<sup>322</sup> Biochemical and spectroscopic experiments of *E. coli* Zur, however, reveal just two metal sites, the structural S<sub>4</sub> sites which could only be removed by protein denaturation, and a regulatory Zn(II) site which adopts a tetrahedral mixed S–N/O coordination complex.<sup>336</sup> This site is likely analogous to the regulatory site in PerR which brings residues from both N- and C-terminal domains, which are distantly separated in the apo-repressor (Figure 17), in close proximity. This is consistent with a model in which metal binding orients the relative dispositions of the two DNA binding domains (Figure 17), creating a conformation with high DNA binding affinity.<sup>322</sup> Such a model may not hold for all Fur proteins since *H. pylori* Fur and Irr (see below) are capable of binding to operator DNA in the absence of a bound metal ion. A recent study has shown that apo-Fur binding to DNA may be dependent on a single nucleotide change in the DNA sequence.<sup>327</sup> Additional structural and biochemical studies are required to understand



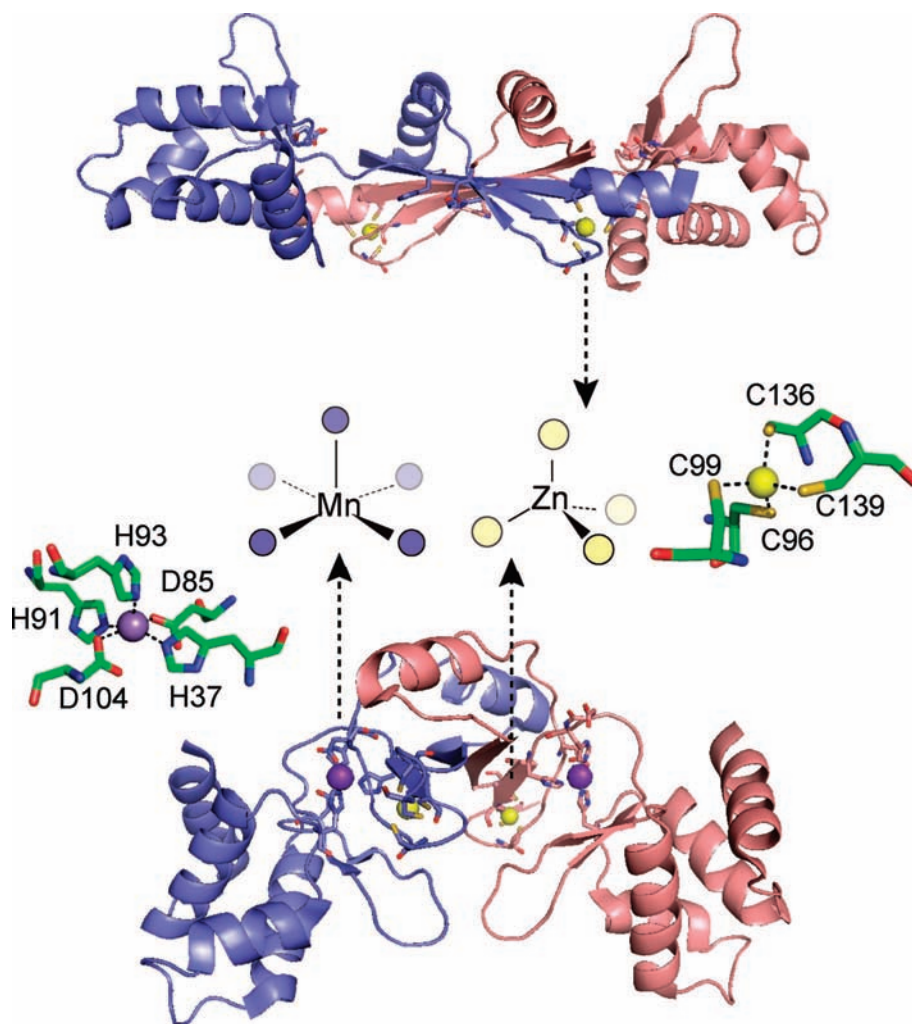


**Figure 17.** Ribbon diagrams of two crystallographic structures of *B. subtilis* PerR with the subunits shaded blue and red.<sup>332</sup> (Top) Oxidized form of PerR, designated PerR-Zn-ox, in which the regulatory metal sites are empty and H37 and H91 are modeled as 2-oxo-histidine residues.<sup>332</sup> Each of the two structural Zn(II) ions are bound to the homodimer in a tetrathiolate, tetrahedral coordination complex that is conserved in some but not all Fur family members.<sup>329</sup> (Bottom) Mn(II)-activated PerR, denoted PerR-Zn-Mn, in which the H<sub>2</sub>O<sub>2</sub>-sensing or regulatory site is formed by a square pyramidally coordinated Mn(II) or Fe(II) atom by H37 from the winged helical DNA binding domain (on the periphery of the homodimer), D85 from the connecting linker, and H91, H93, and D104 from the dimerization domain (middle), all from the same protomer. The symmetry-related metal ligands are also shown on the opposite subunit. H37 is oxidized to 2-oxo-His in PerR-Zn-oxo (shown), as is H91.<sup>326,332</sup> The structural model of PerR-Zn-ox (top) superimposes on apo-PerR-Zn.<sup>331</sup>

the mechanism underlying this DNA binding mode by Fur family regulation.

The H<sub>2</sub>O<sub>2</sub> sensor *B. subtilis* PerR also contains the anticipated structural S<sub>4</sub> Zn(II) site and binds Fe(II) or Mn(II) to a regulatory site that bridges the N- and C-terminal domains; the recently reported crystal structures of an oxidized PerR (PerR-Zn-ox) and PerR-Zn-Mn complex further support this allosteric regulation mechanism proposed for *M. tuberculosis* Zur (Figure 17).<sup>332</sup> The formation of a pentacoordinate, square pyramidal Mn(II) coordination complex in the regulatory site “locks down” the structure of the dimer into a conformation suitable for high-affinity DNA binding while at the same time creating an open coordination site for H<sub>2</sub>O<sub>2</sub>. Unlike other oxidative stress sensors that employ cysteine residues or [Fe-S] clusters to sense H<sub>2</sub>O<sub>2</sub>, sensing by PerR is mediated by a unique Fe(III)-catalyzed oxidation reaction in which one of two histidine residues in the regulatory metal site, either His37 from the DNA binding domain or His91 from the dimerization domain, is converted to 2-oxo-His, resulting in an oxidized protein incapable of binding DNA (Figure 17).<sup>326</sup> Interestingly, both this protein, designated PerR-Zn-His37ox, and PerR-Zn-His37A are

still capable of binding Mn(II) with micromolar affinity or just 20-fold lower than wild-type PerR; this suggests His37 from the DNA binding domain is a key allosteric residue,<sup>22,35</sup> substitution or modification of which results in a failure to properly orient the N- and C-terminal domains for DNA binding.<sup>332</sup> In contrast, oxidation of His91 simply lowers the affinity of Mn(II)/Fe(II) binding to nearly undetectable levels, resulting in metal dissociation and subsequent dissociation from the DNA operator.<sup>332</sup> The newly reported PerR-Zn-Mn complex structure also reveals a structural rationale as to why His37 and His91 are subject to Fe(III)-catalyzed oxidation, while the other Mn(II) ligand His93 is refractory. His93 occupies an axial position directly opposite an open coordination site that will be bound by H<sub>2</sub>O<sub>2</sub> and is therefore completely inaccessible to the locally generated hydroxyl radical.<sup>334,337</sup>

### 3.5.2. Iron Sensing without Fur

Many plant symbiotic  $\alpha$ -proteobacteria, including *Rhodospirillum capsulatus*, *Rhizobium leguminosarum*, *Bradyrhizobium japonicum*, and *Agrobacterium tumefaciens* do not

encode a bona fide Fe(II) repressor Fur but instead seem to employ two novel regulatory proteins of unknown structure to sense intracellular Fe status and mediate iron homeostasis.<sup>321</sup> These are RirA,<sup>338</sup> a member of the Rrf2 family of the winged-helical repressors, and Irr, a Fur family ortholog (see Figure 2) that possesses the unusual property of undergoing heme-dependent degradation under Fe(heme)-replete conditions. RirA belongs to the same protein family that contains NsrR, a nitric oxide sensor,<sup>339</sup> and IcsR, a repressor of the *Isc* genes in *E. coli* required for Fe–S protein biogenesis and recently tied to iron-dependent regulation of biofilm formation.<sup>340</sup> NsrR has been shown to contain a 2Fe–2S cluster which activates operator–promoter binding;<sup>341</sup> as a result, the holoform of NsrR is a transcriptional repressor, and this property is projected to be common among other Rrf2 family regulators. *Bradyrhizobium japonicum* Irr, on the other hand, functions as a repressor under Fe-deplete conditions and thus likely binds as an apoprotein to its DNA operator;<sup>342</sup> under conditions of high intracellular heme, heme is thought to bind to a short N-terminal heme regulatory motif (HRM) which leads to degradation of Irr via an as yet unknown mechanism and dissociation from the DNA.<sup>343</sup> It is interesting to note that these same  $\alpha$ -proteobacteria sometimes encode one additional Fur ortholog, which limited data suggest is either the Mn(II)-uptake regulator Mur<sup>324</sup> or alternatively a minor Fe–Fur.<sup>321</sup> It will be interesting to understand the structural details of Irr and Mur function in the context of Fur family regulators in general as well as that of Rrf2 proteins, about which very little is known.

### 3.6. DtxR Family

The DtxR family of metalloregulatory proteins includes two major subfamilies: Fe(II) sensors and Mn(II) sensors. *Corynebacterium diphtheriae* DtxR is the founding member of the first subgroup and named for its function in regulating diphtheria toxin expression, which is strongly tied to the Fe status of the cell,<sup>20</sup> while *B. subtilis* MntR is the paradigm Mn(II) sensor.<sup>344</sup> DtxR performs a role in Actinobacteria that is functionally analogous to that carried out by Fe(II)–Fur in Gram-negative bacteria.<sup>78</sup>

#### 3.6.1. DtxR-Like Fe(II)-Sensing Repressors

*C. diphtheriae* DtxR and its homologue IdeR from *M. tuberculosis* regulate genes that encode for proteins that mediate iron uptake and storage.<sup>20</sup> These genes are constitutively expressed under iron-limiting conditions, while elevated cytosolic iron results in repression mediated by DtxR/IdeR. This transcriptional response is highly specific for Fe(II) in vivo, while in vitro experiments reveal that Ni(II) or Co(II), but not Mn(II), is also capable of functioning as an activator of DNA binding. Therefore, many in vitro studies, including most of the structural work, have been carried out using Ni(II) or Co(II) as the corepressor.<sup>345</sup> It is important to emphasize, however, that there are no structures of DtxR bound to its cognate inducer Fe(II) and that the Ni(II)-dependent conformational changes discussed below may be necessary but not sufficient to support robust transcriptional regulation in the cell. DtxR/IdeR regulators contain an N-terminal winged helix DNA binding domain followed by a helical dimerization domain and a C-terminal SH3-like domain which is absent in the Mn(II) sensor MntR.<sup>346</sup> This SH3-like domain has been suggested to

enhance the DNA binding affinity by stabilizing intra- and/or intersubunit protein–protein interactions.<sup>347,348</sup>

Two distinct metal binding sites have been characterized in DtxR and are designated the primary (regulatory) and ancillary sites. The ancillary site is made up of ligands (His79, Glu83, His98, and two solvent molecules) derived exclusively from the dimerization helices; in contrast, the primary metal site also incorporates a residue from the N-terminal  $\alpha$ -helix in the DNA binding domain.<sup>349</sup> While metal binding to the ancillary site seems to play a structural role in stabilizing the protein, the involvement of an N-terminal residue(s) in the primary binding site, including direct first-shell coordination to the thioether moiety of Met10 and a water-mediated interaction with Leu4, is thought to drive a helix–coil transition in the  $\alpha$ 1 helix upon metal binding.<sup>346,350</sup> Since this N-terminal unstructured region in the apoprotein is thought to inhibit DNA binding largely on the basis of an unfavorable steric clash, this conformational change in the N-terminal helix is thought to be crucial for Ni(II)-dependent allosteric activation of DNA binding.<sup>346</sup> Metal binding also appears to induce a slight domain closure of the N-terminal DNA binding domains in the dimer, resulting in an optimized conformation for DNA recognition.<sup>346</sup> While compelling, it must be emphasized that the degree to which the global quaternary structural conformations of the Ni(II)-activated and apoprotein states of the DtxR or IdeR dimer differ in solution has not yet been determined; as a result, the extent to which domain closure, akin to that which occurs prominently in PerR<sup>332</sup> and perhaps most other Fur family regulators,<sup>322</sup> contributes to allosteric activation is not yet clear.

#### 3.6.2. MntR-Like Mn(II)-Sensing Proteins

The founding member of this subgroup of DtxR family regulators is *B. subtilis* MntR. MntR regulates the transcription of the high-affinity manganese uptake systems encoded by the *mntABCD* and *mntH* (see section 2).<sup>351</sup> MntR represses the expression when cytosolic Mn(II) levels are high in a manner that is highly specific for Mn(II) and Cd(II) over other divalent metal ions such as Mg(II), Ca(II), Fe(II), Co(II), Ni(II), and Zn(II).<sup>351,352</sup>

While atomic resolution crystallographic studies of wild-type and mutant MntRs bound to a number of metal ions reveal an overall architecture that is very similar to the Fe(II) regulators DtxR and IdeR, many interesting insights into the number, nature, and specificity of metal binding sites have been observed in multiple structures of MntR. The initial Mn(II)-bound MntR structure revealed a binuclear Mn(II) cluster formed by two Mn(II) ions separated by 3.3 Å, named Mn<sub>A</sub> and Mn<sub>B</sub>, each of which adopts an octahedral or distorted octahedral coordination geometry.<sup>353</sup> However, recent crystals grown at room temperature show another conformer with Mn(II) binding sites apart by 4.4 Å, named Mn<sub>A</sub> and Mn<sub>C</sub>.<sup>352</sup> The coordination geometry around the individual Mn(II) ions remains similar, with the major difference in the two structures being the nature of the bridging and bidentate ligands. This new Mn<sub>A</sub>–Mn<sub>C</sub> conformer is more consistent with the Mn(II)–Mn(II) distance determined by solution EPR studies and thus thought to be biologically relevant.<sup>354</sup>

The Ca(II)-, Cd(II)-, and Zn(II)-bound MntR structures have also been solved.<sup>352</sup> Unlike the Mn(II)-bound structure, only one Zn(II) is bound at a site similar to that of Mn<sub>A</sub> but adopts a non-native tetrahedral coordination geometry; this

clearly suggests why Zn(II) is not an effective allosteric activator of operator DNA binding.<sup>352</sup> However, Ca(II) and Cd(II) both form the binuclear  $\text{Me}_A\text{-Me}_C$  (Me = metal) structures structurally analogous to that formed by Mn(II). This seems to explain why Cd(II) is an effector *in vivo* but in the case of Ca(II) seems to contradict the anticipated correlation between coordination geometry and metal selectivity. However, further biochemical studies revealed, as expected for a site characterized by a number of borderline soft imidazole ligands, that 100 mM  $\text{CaCl}_2$  was required to activate just 50% of the MntR dimers to bind to the DNA. Obviously, such a high Ca(II) concentration is likely not biologically attainable in the cell, thus providing an explanation as to why MntR is selective for Mn(II) and Cd(II) but not Ca(II) *in vivo*.<sup>352</sup> These studies of MntR provide a nice illustration of the importance of considering the impact that the prevailing cytosolic concentrations of individual metal ions might have on the biological specificity of a metal sensor in the cell, which may not be revealed by *in vitro* and structural studies alone.<sup>7</sup>

A recently reported structure of apo-MntR allows for a direct comparison with the metal-bound state that is active in DNA binding, and these studies provide insight into a proposed mechanism for allosteric regulation of operator binding of MntR by Mn(II).<sup>355</sup> They reveal that the N-terminal DNA binding domains in the apoprotein dimer are capable of adopting a number of distinct orientations relative to the dimerization domain, and in each case, they are farther apart than those in the activated Mn(II)-bound state; this assessment is further supported by solution EPR studies on spin-labeled MntR. This domain closure is mediated in part by the  $\alpha 4$  helix that connects the two domains and donates several key residues that coordinate both Mn(II) ions. Mn(II) ligands from the N-terminal  $\alpha$ -helix were also found to play an important role in driving this conformational change, which is similar to the proposed model in DtxR and IdeR.<sup>355</sup> Interestingly, the dynamics of MntR as probed by hydrogen–deuterium exchange mass spectrometry reveal that amide groups in the  $\alpha 4$  helix are significantly protected from exchange with solvent upon Mn(II) binding and results in a global rigidification of the entire protein, which presumably reduces the entropic cost of DNA binding.<sup>356</sup> Analogous findings characterize the dynamics of AntR, an MntR homologue from *Bacillus anthracis*. EPR spectroscopy reveals that the mean distance between the two DNA binding helices in the dimer as well as the backbone dynamics are both decreased upon metal binding.<sup>357</sup> Further support for an entropically driven activation mechanism in MntR could be obtained from isothermal titration calorimetry experiments, which would provide a direct determination of the enthalpic and entropic contributions to the allosteric coupling free energy (Scheme 1).<sup>22</sup>

### 3.7. NikR

Initially characterized in *E. coli*, NikR is a transcriptional regulator for the expression of proteins involved in nickel uptake and other nickel-requiring enzymes.<sup>247</sup> The tetrameric NikR contains a central mixed  $\alpha/\beta$  fold flanked by two dimeric ribbon–helix–helix (RHH) domains<sup>358</sup> in which two antiparallel N-terminal  $\beta$ -strands from opposite protomers make a two-stranded antiparallel  $\beta$ -sheet that contacts with the major groove in one-half-site of a 2-fold symmetric DNA operator (Figure 18); NikR is thus described as a dimer of

dimers.<sup>358,359</sup> NikR is the only known metal-sensing member of the bacteriophage P22 Arc repressor RHH superfamily, which includes phage P22 Mnt repressor as well as the methionine repressor *E. coli* MetJ.<sup>360,361</sup> Extensive biochemical and structural studies have been carried out on NikRs from *E. coli*,<sup>24,359,362–367</sup> *H. pylori*,<sup>368,369</sup> and *P. horikoshii*.<sup>370</sup> *E. coli* NikR is the most extensively characterized and unique among all metalloregulatory proteins discussed here in that high-resolution structures of the three major allosteric states (see Scheme 1), i.e., apo-, Ni(II)-, and DNA–Ni(II)-bound conformers are available. In addition, extensive spectroscopic and crystallographic information is also available for various inducing and noninducing metal derivatives of NikR that provide molecular-level insight to metal selectivity by NikR.

#### 3.7.1. Structural Studies

*E. coli* NikR regulates the transcription of the *nik* operon (*nikABCDE*) which encodes a high-affinity nickel-specific uptake ABC transporter (see section 2.4). Ni(II)-bound NikR binds to the *nik* operator–promoter DNA with high affinity and thus represses transcription under Ni(II)-replete conditions; apo-NikR binds weakly and nonspecifically to the operator, revealing that Ni(II) is an obligate corepressor.<sup>363</sup>

The crystal structure of apo-NikR reveals that the C-terminal regulatory domain forms a tetrameric core flanked by canonical N-terminal RHH DNA binding domains (Figure 18).<sup>359</sup> The C-terminal tetrameric regulatory domain is structurally homologous to the ACT (aspartokinase, chorismate mutase, and TyrA) domain, which functions in small molecule effector and amino acid sensing allosterically regulate their enzyme activity. Understanding the mechanism of allosteric regulation of NikR by Ni(II) ions will certainly shed light on any common regulatory features of ACT-domain-containing enzymes and proteins.<sup>371</sup> Biochemical studies establish that NikR contains two sets of Ni(II) binding sites, including one set of high-affinity sites located in the tetrameric C-terminal regulatory domain and another set (or sets) of low-affinity sites, the nature of which remains the subject of ongoing investigation (see below). Ni(II) binding to the four symmetry-related high-affinity sites in the tetrameric ACT domain allosterically activates *nik* operator–promoter binding. The occupancy of the low-affinity site(s) is proposed to orient the two DNA binding domains of the tetramer to a “closed” cis-type conformation, which further enhances the DNA binding affinity, again presumably largely on entropic grounds (Figure 18).

Although the structure of a Ni(II)-bound full-length NikR was initially unavailable, the structure of the isolated C-terminal domain bound to Ni(II) provided much detailed information on the coordination structure of the high-affinity site as well as the conformational change in this domain upon Ni(II) binding.<sup>359</sup> In this structure, Ni(II) adopts an  $\text{N}_3\text{S}$  square planar coordination geometry favored by low-spin  $d^8$  Ni(II), formed by three histidine residues (His87, His89, and His76') and one cysteine residue (Cys95) across the tetramer interface (Figure 18). An extensive hydrogen-bonding network links adjacent nickel binding sites and potentially stabilizes Ni(II) binding in a way that productively drives a conformational change toward an active, DNA binding form. In addition, the  $\alpha 3$  helix is fully formed and stabilized by Ni(II) binding.<sup>359</sup>

The structure of Ni(II)–NikR–DNA complex provides additional insights into Ni(II) regulation, not only as it relates



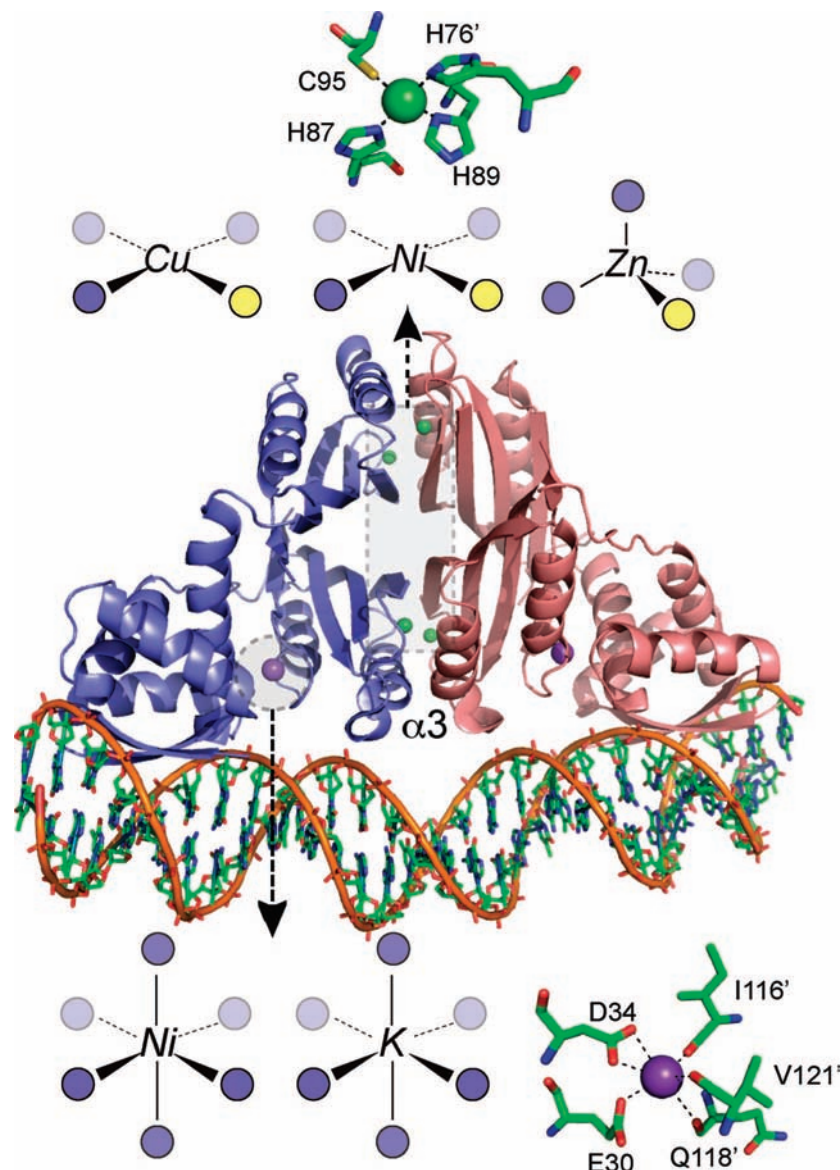


**Figure 18.** Ribbon representation of the crystallographic structure of the *E. coli* NikR–DNA complex with Ni(II) (shaded green) bound at the high-affinity C-terminal sites and  $K^+$  ions (shaded purple) bound at the low-affinity sites in close proximity to the DNA.<sup>362</sup> Schematic representations of the coordination complexes formed by other metal ions bound in each site consistent with recent structural and spectroscopic studies are also shown.<sup>309,373</sup> The  $\alpha 3$  helices are indicated (see text for details).

to plausible mechanisms of allosteric activation, but also on the nature and number of low-affinity Ni(II) sites which enhance the affinity of NikR for the operator.<sup>366</sup> The cocomplex structure together with the structures of Ni(II)-bound full-length NikR and the apoprotein structure clearly show the dramatic conformational changes within the tetramer that links these allosteric states.<sup>362</sup> The allosteric model that emerges is one where Ni(II) binding to the high-affinity square planar sites induces relatively localized structural changes involving loop and helix ( $\alpha 3$ ) formation; these structural changes are necessary but not sufficient to fully activate NikR to bind to the operator. Ni(II) binding to two low-affinity sites on the tetramer–DNA complex, near the DNA–NikR interface as originally proposed on the basis of the *P. horikoshii* NikR structure,<sup>370</sup> induces a dramatic reorientation of the RHH domains to adopt a “closed” cysteine conformation (Figure 18). Interestingly, these low-affinity sites within the NikR–DNA complex structure are characterized by octahedral coordination geometry and filled with potassium ( $K^+$ ) ions instead of expected Ni(II) ions.

The coordination site is very unusual, with ligands derived mostly side-chain and backbone carbonyl oxygens originating from both the C-terminal metal binding domain as well as the N-terminal DNA binding domain; this finding is consistent with a central role played by this site in driving the dramatic conformational change toward an optimized high DNA binding affinity state (Figure 18).<sup>362</sup>

### 3.7.2. Metal Selectivity

Of the two sets of the regulatory metal binding sites in NikR, the high-affinity square planar Ni(II) coordination sites in the C-terminal domain have been studied most extensively. Metal binding studies reveal that the high-affinity site is capable of coordinating many other divalent metal ions with an affinity ranking that roughly follows the Irving–Williams series, i.e.,  $Mn(II) < Co(II) < Ni(II) < Cu(II) \geq Zn(II)$ .<sup>364</sup> It was therefore of great interest to understand the mechanism by which NikR responds specifically to Ni(II) in the cell, given higher affinity complexes formed by two potentially

more abundant divalent ions Cu(II) and Zn(II). As anticipated, coordination geometry, superimposed on metal availability in the “right” oxidation state, once again functions collaboratively as a key determinant for biological metal selectivity.

Recent comprehensive X-ray absorption spectroscopy studies reveal that different metals adopt different coordination geometries in the high-affinity sites, with a square planar coordination geometry formed by Ni(II) and Cu(II), octahedral for Co(II), tetrahedral for Zn(II), and trigonal for reduced Cu(I) (Figure 18).<sup>372</sup> To probe the coordination geometry of the low-affinity sites, bimetallic NikR samples with DNA bound were prepared and characterized. These data clearly reveal that when the high-affinity sites are occupied by Cu(II), the low-affinity sites adopt an average octahedral (N/O)<sub>6</sub> coordination geometry with Ni(II); this is the first direct structural insight into the structure of the low-affinity sites when bound to Ni(II) (Figure 18). Since biochemical studies show that only Ni(II) and to a lesser extent Cu(II), which adopts the same square planar coordination geometry, drive the conformational changes necessary for allosteric activation *in vitro*, they present a compelling correlation between formation of the “right” coordination geometry and a metal-specific allosteric response. The fact that NikR is exquisitely selective for Ni(II) *in vivo* is explained by the fact that under the reducing conditions of the cytosol, any free Cu present will be in the Cu(I) oxidation state with the amount of Cu(II) being vanishingly small. The fact that the availability of Cu(I) is also likely to be extremely low, due to the action of copper chaperones and metalloregulatory proteins that bind Cu(I) with very high affinity, coupled with the fact that Cu(I) adopts a non-native trigonal coordination geometry in NikR, further ensures that NikR will be selective for Ni(II) in the cytosol.<sup>372</sup>

Recent structural studies on Cu(II) and Zn(II) bound to the *E. coli* NikR C-terminal metal binding domain provide further support for these ideas.<sup>373</sup> This study reveals that an ordering of the  $\alpha 3$  helix is also observed in the Cu(II)-bound but not Zn(II)-bound regulatory domain, a finding that further links conformational ordering within the regulatory domain itself with the formation of a square planar Ni(II) coordination chelate.

### 3.8. Other Metalloregulatory and Oxidative Stress-Sensing Proteins

Outside of the seven major families of metalloregulatory proteins previously discussed,<sup>22</sup> biological studies carried out over the last couple of years have uncovered new proteins from other transcriptional regulator families that also appear to function as direct sensors of metal ions, metal oxyanions, or oxidative stress via dithiol–disulfide exchange chemistry. In the latter case, it is well established that such redox sensors can be efficiently tuned to a particular redox potential by adjusting the  $pK_a$  of one or both Cys residues that are linked in some way to a conformational change in the regulator (see section 3.3.3). We discuss three examples here, although in some cases additional biochemical, biophysical, and structural studies will be required to fully elucidate the mechanism by which these regulators function in controlling metal homeostasis.

#### 3.8.1. LysR Family Members ModE and OxyR

The LysR-type transcriptional regulators (LTTRs) are named for the Lys repressor, LysR, the transcriptional activator of the *lysA* gene, which encodes the lysine metabolic enzyme diaminopimelate decarboxylase.<sup>374</sup> LTTRs represent the most prevalent type of transcriptional regulator in bacteria and contain an N-terminal winged helix DNA binding domain followed by a regulatory domain of diverse function.<sup>374</sup> As suggested by these numbers, LTTRs regulate a very wide range of genes including those associated with virulence, quorum sensing, motility, and oxidative stress. Most LTTRs are obligate tetramers which are known or predicted to adopt a dimer-of-dimers structure in a fashion reminiscent of NikR (section 3.7) and bind to a 2-fold symmetric operator sequence in which half sites are separated by 10–15 base pairs.<sup>375</sup>

*E. coli* OxyR is the prototype redox-responsive LTTR that is involved in transcriptional activation of an oxidative stress regulon in response to hydrogen peroxide, superoxide, and nitrosative stress.<sup>304</sup> OxyR contains two conserved Cys residues, Cys199 and Cys208, and early experiments suggested a regulatory model based on reversible disulfide bond formation that is linked to stabilizing the OxyR tetramer on the DNA operator, thereby engaging in a direct protein–protein interaction with RNA polymerase.<sup>376–378</sup> More recent work reveals that a range of oxidative stressors that induce the *oxyR* regulon result in *S*-hydroxylation, *S*-nitrosylation,<sup>379,380</sup> formation of mixed disulfides with low molecular weight thiols, and formation of thioesters as a result of electrophilic attack by carbonyl compounds on regulatory cysteines of OxyR,<sup>381</sup> furthermore, modification of Cys199 appears to be necessary and sufficient for regulation by a wide range of redox agents.<sup>302</sup> These findings, in turn, are consistent with the characterization of OxyR from *Deinococcus radiodurans* as a hydrogen peroxide sensor which harbors a single Cys residue.<sup>382</sup> OxyR is a global regulator, and it is important to point out that the degree to which other oxidative stress-sensing transcriptional regulators respond to a range of inducers in the cell is unknown. In any case, these experiments emphasize the intrinsic complexity of thiol-based redox switching mechanisms,<sup>383–385</sup> which may involve formation of a variety of derivatives depending on the stressor, *i.e.*, one or more modes of regulation may well be operative in the cell, while some may be far more important than others.<sup>386</sup>

The only LTTR family member that is known thus far to be directly involved in metal homeostasis is *E. coli* ModE, which represses the transcription of the molybdate transporter operon *modABCD* by binding to the operator–promoter DNA in the oxyanion-bound form.<sup>173</sup> In contrast to OxyR and the vast majority of LTTRs, ModE appears to function as an obligate dimer rather than a tetramer. Crystal structures of both apo- and molybdate-bound forms of ModE reveal that molybdate is bound in the C-terminal domain through hydrogen-bonding interactions of the oxyanion oxygen with amino acid residues which form the binding pocket. Molybdate binding changes the relative orientation of the N-terminal DNA binding domain in the dimer, stabilizing an active conformation for DNA binding which, in turn, transcriptionally represses  $\text{MoO}_4^{2-}$  uptake into the cytosol (Figure 2).<sup>387</sup>



### 3.8.2. MarR Family Member AdcR

The MarR family of transcriptional repressors is named for the founding member *E. coli* multiantibiotic resistance repressor MarR<sup>388</sup> and comprises a family of winged helix proteins responsible for global regulation, multidrug resistance, and oxidative stress sensing that is widespread in bacteria (Figure 2).<sup>389</sup> There are now seven crystallographic structures of MarR family proteins and one member bound to its DNA operator, *B. subtilis* OhrR<sup>390</sup> (see Figure 2). OhrR is an organic peroxide sensor that represses the expression of a peroxiredoxin OhrA in *B. subtilis*. OhrR harbors a single Cys residue in the  $\alpha$ 1 helix of the dimerization domain which is situated in a hydrophobic pocket containing conserved hydrogen-bonding residues, structural features tied to its intrinsic reactivity. Oxidation of this Cys leads first to a cysteine sulfenate ( $-\text{SOH}$ ) which does not induce DNA dissociation; this is ultimately converted to a mixed disulfide in an *S*-thiolation reaction or a cyclic sulfenamide derivative, both of which lead to derepression of *ohrA* expression.<sup>384</sup> The structural model of the uninduced OhrR–DNA complex suggests a model for derepression whereby cysteine oxidation drives a change in the two-dimensional distance between the DNA recognition helices on opposite protomers in the dimer, thereby lowering the affinity for DNA.

Other biochemically characterized oxidation-sensing MarR family proteins can be divided into single Cys and dual Cys subclasses and include *S. aureus* MgrA,<sup>391</sup> the global regulator *S. aureus* SarA,<sup>392</sup> *S. aureus* SarZ,<sup>385</sup> and the dual Cys sensor, *P. aereginosa* MexR (Figure 2).<sup>239</sup> Recent studies suggest that MexR-mediated derepression of the *mexAB-oprM* RND multidrug resistance operon achieved by a wide range of inducers including  $\text{H}_2\text{O}_2$  and antibiotics occurs via a common mechanism: reversible interprotomer disulfide bond formation (redox potential of  $-155$  mV) which locks the dimeric repressor in a low-affinity DNA binding conformation.<sup>238</sup> The extent to which this mechanism characterizes other antibiotic-sensing MarR regulators is unknown.

The *S. pneumoniae* adhesion competence operon (*ad-cRCBA*) encodes a MarR family regulator AdcR and a Zn(II)-selective ABC transporter that is crucial for the pathogenicity of the organism and whose expression is regulated by AdcR.<sup>125</sup> AdcR also regulates the transcription of a group of pneumococcal histidine triad proteins (PhtA, -B, -D, and -E), zinc binding proteins<sup>393</sup> situated on the cell surface which are collectively required for virulence of *S. pneumoniae*; these are currently used as protective antigens against *Streptococcus pneumoniae* infection.<sup>126,394</sup> AdcR is functionally analogous to *L. lactis* ZitR<sup>395</sup> and proposed to repress the transcription of this operon in a Zn(II)-dependent manner via a corepression model (Figure 2) in which Zn(II)-bound AdcR binds with high affinity to the operator–promoter region and thereby shuts off expression of the uptake system under Zn(II) stress. This anticipated mode of regulation<sup>396</sup> would be unique in the MarR family because virtually all other MarR proteins repress the transcription in their unligated or reduced forms and dissociate from the DNA upon induction.<sup>389</sup>

It is interesting to note that pneumococcal AdcRs and *L. lactis* ZitR are unique among MarR family members in that they specifically harbor a single Cys in the predicted  $\alpha$ 1 helix as well as stretch of six contiguous His/Glu residues in what is predicted to be the  $\alpha$ 5 helix within the C-terminal  $\alpha$ -helical regulatory domain. The analogous region of the  $\alpha$ 5 helix in *B. subtilis* OhrR is known to kink or bend strongly when

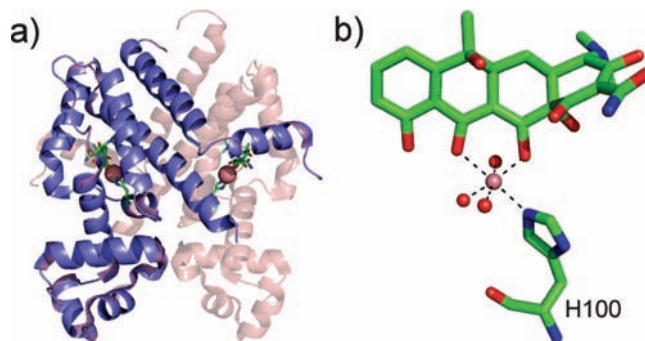


**Figure 19.** (a) Ribbon diagram of a class D tetracycline repressor (TetR) bound to the antibiotic  $[\text{Co7HTc}]^+$  in a very deep pocket in the C-terminal core of regulatory domain (2 VKE). The Co(II) ion is shaded red with the remainder of the antibiotic shown in stick representation. The core domain is at the top of the figure, while symmetry-related DNA binding domains are shown at the bottom of the structure. (b) Conformation of tetracycline (7HTc) bound to the core domain, with Co(II) bound in an octahedral coordination geometry, as indicated. Water molecules are donated by red spheres, while the imidazole  $\text{N}^{\epsilon 2}$  nitrogen of His100 donates the only Co(II)–side-chain coordination bond. Mg(II) is likely the biological metal ion and forms an isostructural complex.<sup>400</sup>

OhrR is oxidized; thus, a parallel, albeit *activating*, regulatory mechanism may well characterize AdcR upon Zn(II) binding. In vitro metal and DNA binding experiments complemented with in vivo metal induction assays with *adcR* mutant strains are required to provide additional insights into this novel metalloregulatory protein of the MarR family.

### 3.8.3. TetR Family Member SczA

The homodimeric tetracycline (tet) repressor TetR in Gram-negative bacteria binds a tetracycline–magnesium complex  $[\text{MgTc}]^+$  in an  $\alpha$ -helical regulatory domain, which mediates transcriptional derepression of the gene encoding TetA, a  $\text{H}^+$  antiporter embedded in the cytoplasmic membrane that effluxes  $[\text{MgTc}]^+$  from the cytosol (Figure 2).<sup>397</sup> The structure of the winged helix TetR–tetO DNA complex is known to high resolution, as is the structure of the TerT– $[\text{MgTc}]^+$  complex, which collectively suggest a plausible allosteric model for lowering the affinity of TetR for its operator DNA sequence.<sup>398,399</sup> It is interesting to note that an octahedrally coordinated Mg(II) ion is an obligate binding partner of tetracycline and links the coordination of the  $\beta$ -diketonate moiety of Tet and the imidazole  $\text{N}^{\epsilon 2}$  atom of an invariant His100 (Figure 19).<sup>400</sup> All first-row transition metal ions are capable of binding isomorphously to that of Mg(II) and negatively regulate DNA binding in vitro.<sup>400</sup>

*S. pneumoniae* CzCD is a cation diffusion facilitator (CDF) responsible for Zn(II) resistance homologous to *S. aureus* CzrB and *E. coli* YiiP (Figure 5).<sup>180</sup> While *S. aureus* CzrB is regulated by an ArsR/SmtB family protein CzrA (see section 3.1), recent studies show that the expression of *S. pneumoniae* CzCD is regulated by a TetR family protein SczA.<sup>401</sup> The genes encoding a novel MerR-like nitric oxide (NO) stress sensor NmlR (see section 3.2.2) and a class 3 Zn(II)-dependent alcohol dehydrogenase AdhC, which catalyzes the NADH-dependent reduction of *S*-nitrosoglutathione (GSNO)<sup>300</sup> just downstream of *czcD*, are also regulated by SczA.<sup>180</sup> Since the *nmlR-adhC* operon is also autoregulated by NmlR in response to NO stress, this dual regulation provides an example of the coupling of oxidative/nitrosative stress resistance to zinc homeostasis in the cell. Biological experiments suggest that Zn(II) binding to SczA will decrease

its binding affinity to the *czcD* operator—promoter and induce transcriptional derepression.<sup>180</sup> It is interesting to note that the His residue that corresponds to His100 in TetR (Figure 19) as well as His64, which makes a hydrogen bond to the bound Tet, are conserved in the Zn(II) sensor SczA. This provides support for the proposal that the regulatory Zn(II) binding site(s) in SczA may well be located in a pocket that at least partially superimposes on the [MgTc]<sup>+</sup> binding site in TetR. The Zn(II) binding affinity, stoichiometry, and coordination chemistry have yet to be systematically investigated in SczA and should provide new insights into the evolution of a metalloregulatory Zn(II) binding site from other inducer sites.

#### 4. Perspectives

In this review, we surveyed our increasingly sophisticated understanding of the degree to which bacterial metal transporters and metal-sensing transcriptional regulators exploit “favorable” coordination chemistries to create metal homeostasis systems that are selective for one or a small group of metal ions. Several important points emerge from this analysis. First, the ability of a metal “receptor” site to adopt a *singular* metal coordination geometry around the regulatory metal ion or ions in a metal sensor protein, e.g., tetrahedral, square planar, octahedral, or other, drives both local and long-range quaternary structural changes that mediate allosteric inhibition or activation of operator DNA binding. Indeed, the structural and dynamical mechanism of allosteric coupling of metal and DNA binding is gaining clarity for the  $\alpha$ 5-site ArsR/SmtB family sensors,<sup>258</sup> at least one member of the MerR family, *E. coli* SoxR,<sup>296</sup> *B. subtilis* PerR,<sup>332</sup> the DtxR family regulators DtxR and MntR,<sup>350,355</sup> and the Ni(II) sensor *E. coli* NikR.<sup>362</sup> Second, the rules that govern the use of favorable metal coordination geometries by metal sensor proteins are recapitulated in metal transporters, although our understanding of these systems is comparatively far less advanced due, in part, to the difficulty of studying integral membrane proteins at atomic resolution. Integrated knowledge obtained from spectroscopic, structural, and biochemical investigations will continue to move this field further, an excellent example of which is the model Cu(I) P-type ATPase effluxer, *Archaeoglobus fulgidus* CopA.<sup>16,71,196,197</sup>

Much has also been learned about the evolution of metal selectivity in metal sensor proteins. Compelling support for convergent or parallel evolution of metal-sensing sites on ArsR/SmtB family repressors is now available<sup>37,267</sup> and leads to a remarkable “scatter-shot” picture of allosteric sites over much of the surface in what is predicted to be a relatively unchanging structural scaffold (Figure 10). This picture of effector site evolution may well be reporting on a “low bar” for “loss-of-function”, e.g., inhibition of DNA binding, in a structurally compact DNA binding protein, and is consistent with the “rule of varied allosteric control” in which protein families evolve seemingly random allosteric control pathways.<sup>402</sup> Such a situation stands in striking contrast to other metal sensor systems discussed here, which seem to exploit rather subtle changes in metal coordination geometry and/or nuclearity in a *single* metalloregulatory site or region to evolve the necessary degree of metal selectivity in the cell.

Global expression profiling, proteome remodeling, and metallomics approaches will play an ever-increasing role in understanding how the cellular environment controls the physiology of metal homeostasis in the cell as well as the

degree to which oxidative stress and antibiotic resistance systems impact metal homeostasis and vice versa.<sup>2,403,404</sup> This is of critical importance for human health given the degree to which metal homeostasis and oxidative stress resistance play in the host—microbial pathogen interactions.<sup>107,405</sup> In this regard, it is interesting to note that essentially all metal sensor protein families are known or projected to harbor one or more nonmetal-sensing orthologs that specifically allow the cell to respond to oxidative, nitrosative, and/or electrophile stress (Figure 2). Our understanding of how these systems are integrated in the intracellular milieu of metal homeostasis is in its infancy<sup>112</sup> but emphasizes the importance of working “holistically” in a single bacterial organism in order to understand the “inorganic chemistry of the cell”.<sup>2,27,316</sup> Future advances will continue to be made at the interface of microbial physiology, analytical and bioinorganic chemistry, and biophysical chemistry and structural biology in order to fully appreciate how cells selectively respond to their environment in a way that maximizes the utility and minimizes the inherent toxicity of metal ions in biological systems.<sup>22</sup>

#### 5. Acknowledgments

The authors thank the U.S. National Institutes of Health for their generous support of our work on metalloregulatory proteins and related topics (R01 GM042569). F.E.J. is the recipient of an NIH postdoctoral fellowship (GM084445). We also acknowledge members of the Giedroc laboratory for their many helpful discussions as well as a critical reading of the manuscript.

#### 6. Note Added in Proof

Fu and coworkers have refined the structure of the *E. coli* YiiP to 2.9 Å resolution (Lu, M.; Chai, J.; Fu, D. *Nat. Struct. Mol. Biol.* **2009**, doi: 10.1038/nsmb.1662). The new model contains three Zn(II) sites, with roles in metal transport (transmembrane) or allosteric activation (cytosolic) largely as discussed here. Two reports describe the crystallographic structure of the intracellular soluble domain of the Fe(II) transporter FeoB, which establishes the molecular basis of FeoB as a G-protein coupled molecular gate (Guilfoyle, A.; Maher, M. J.; Rapp, M.; Clarke, R.; Harrop, S.; Jormakka, M. *EMBO J.* **2009**, *28*, 2677 and Köster, S.; Wehner, M.; Herrmann, C.; Kühlbrandt, W.; Yildiz, Ö. *J. Mol. Biol.* **2009**, *392*, 405). Although the structure of an Nramp-type (Slc11) Fe/Mn transporter remains unavailable, recent findings are consistent with a structural core composed of two sets of five transmembrane helices, with strong similarities to Slc6 family sodium-coupled transporters of known structure, including the prokaryotic leucine transporter, LeuT (Czachorowski, M.; Lam-Luk-Tseung, S.; Cellier, M.; Gros, P. *Biochemistry*, **2009**, *48*, 8422). A recent report reveals that a major intracellular origin of copper toxicity in *E. coli* is the inactivation of, and Fe-release from, metabolic enzymes that contain solvent-exposed iron-sulfur clusters in a process that does not require molecular oxygen (Macomber, L.; Imlay, J. A. *Proc. Natl. Acad. Sci. U.S.A.* **2009**, *106*, 8344). Insights into DNA operator recognition and wrapping by the Ni/Co sensor *E. coli* RcnR suggest that these findings may characterize other CsoR/RcnR family members (Iwig, J. S.; Chivers, P. T. *J. Mol. Biol.* **2009**, doi: 10/1016/j.jmb.2009.08.038). Finally, a recent monograph reviews how metal sensors dictate metal availability and metalloprotein



maturation in cells, with insights drawn from bacteria to lower eukaryotes, flies, and mammals (Waldron, K. J.; Rutherford, J. C.; Ford, D.; Robinson, N. J. *Nature* **2009**, *460*, 823).

## 6. References

- (1) Lippard, S. J.; Berg, J. M. *Principles of Bioinorganic Chemistry*; University Science Books: Mill Valley, CA, 1994.
- (2) Tottey, S.; Waldron, K. J.; Firbank, S. J.; Reale, B.; Bessant, C.; Sato, K.; Cheek, T. R.; Gray, J.; Banfield, M. J.; Dennison, C.; Robinson, N. J. *Nature* **2008**, *455*, 1138.
- (3) Waldron, K. J.; Robinson, N. J. *Nat. Rev. Microbiol.* **2009**, *7*, 25.
- (4) Panina, E. M.; Mironov, A. A.; Gelfand, M. S. *Proc. Natl. Acad. Sci. U. S. A.* **2003**, *100*, 9912.
- (5) Duran, R. V.; Hervás, M.; De La Rosa, M. A.; Navarro, J. A. *J. Biol. Chem.* **2004**, *279*, 7229.
- (6) Finney, L. A.; O'Halloran, T. V. *Science* **2003**, *300*, 931.
- (7) Tottey, S.; Harvie, D. R.; Robinson, N. J. *Acc. Chem. Res.* **2005**, *38*, 775.
- (8) Bagai, I.; Resing, C.; Blackburn, N. J.; McEvoy, M. M. *Biochemistry* **2008**, *47*, 11408.
- (9) Davis, A. V.; O'Halloran, T. V. *Nat. Chem. Biol.* **2008**, *4*, 148.
- (10) Maier, R. J.; Benoit, S. L.; Seshadri, S. *BioMetals* **2007**, *20*, 655.
- (11) Bandyopadhyay, S.; Chandramouli, K.; Johnson, M. K. *Biochem. Soc. Trans.* **2008**, *36*, 1112.
- (12) Graham, A. I.; Hunt, S.; Stokes, S. L.; Bramall, N.; Bunch, J.; Cox, A. G.; McLeod, C. W.; Poole, R. K. *J. Biol. Chem.* **2009**, *284*, 18377.
- (13) Pennella, M. A.; Giedroc, D. P. *BioMetals* **2005**, *18*, 413.
- (14) Outten, C. E.; O'Halloran, T. V. *Science* **2001**, *292*, 2488.
- (15) Singleton, C.; Le Brun, N. E. *BioMetals* **2007**, *20*, 275.
- (16) Gonzalez-Guerrero, M.; Eren, E.; Rawat, S.; Stemmler, T. L.; Arguello, J. M. *J. Biol. Chem.* **2008**, *283*, 29753.
- (17) Scott, J. A.; Karanjkar, A. M. *Biotechnol. Lett.* **1995**, *17*, 1267.
- (18) Blindauer, C. A.; Harrison, M. D.; Robinson, A. K.; Parkinson, J. A.; Bowness, P. W.; Sadler, P. J.; Robinson, N. J. *Mol. Microbiol.* **2002**, *45*, 1421.
- (19) Gold, B.; Deng, H.; Bryk, R.; Vargas, D.; Eliezer, D.; Roberts, J.; Jiang, X.; Nathan, C. *Nat. Chem. Biol.* **2008**, *4*, 609.
- (20) Andrews, S. C.; Robinson, A. K.; Rodriguez-Quinones, F. *FEMS Microbiol. Rev.* **2003**, *27*, 215.
- (21) Bitoun, J. P.; Wu, G.; Ding, H. *BioMetals* **2008**, *21*, 693.
- (22) Giedroc, D. P.; Arunkumar, A. I. *Dalton Trans.* **2007**, *29*, 3107.
- (23) Rosch, J. W.; Gao, G.; Ridout, G.; Wang, Y. D.; Tuomanen, E. I. *Mol. Microbiol.* **2009**, *72*, 12.
- (24) Rowe, J. L.; Starnes, G. L.; Chivers, P. T. *J. Bacteriol.* **2005**, *187*, 6317.
- (25) Yamamoto, K.; Ishihama, A. *Mol. Microbiol.* **2005**, *56*, 215.
- (26) Pennella, M. A.; Shokes, J. E.; Cosper, N. J.; Scott, R. A.; Giedroc, D. P. *Proc. Natl. Acad. Sci. U.S.A.* **2003**, *100*, 3713.
- (27) O'Halloran, T. V. *Science* **1993**, *261*, 715.
- (28) Somerville, R. *Prog. Nucleic Acid Res. Mol. Biol.* **1992**, *42*, 1.
- (29) Daber, R.; Stayrook, S.; Rosenberg, A.; Lewis, M. J. *Mol. Biol.* **2007**, *370*, 609.
- (30) Lewis, M. C. *R. Biol.* **2005**, *328*, 521.
- (31) Ansari, A. Z.; Chael, M. L.; O'Halloran, T. V. *Nature* **1992**, *355*, 87.
- (32) Kullik, I.; Toledano, M. B.; Tartaglia, L. A.; Storz, G. *J. Bacteriol.* **1995**, *177*, 1275.
- (33) Wang, X.; Mukhopadhyay, P.; Wood, M. J.; Outten, F. W.; Opdyke, J. A.; Storz, G. *J. Bacteriol.* **2006**, *188*, 8335.
- (34) Changela, A.; Chen, K.; Xue, Y.; Holschen, J.; Outten, C. E.; O'Halloran, T. V.; Mondragon, A. *Science* **2003**, *301*, 1383.
- (35) Pennella, M. A.; Arunkumar, A. I.; Giedroc, D. P. *J. Mol. Biol.* **2006**, *356*, 1124.
- (36) Busenlehner, L. S.; Pennella, M. A.; Giedroc, D. P. *FEMS Microbiol. Rev.* **2003**, *27*, 131.
- (37) Campbell, D. R.; Chapman, K. E.; Waldron, K. J.; Tottey, S.; Kendall, S.; Cavallaro, G.; Andreini, C.; Hinds, J.; Stoker, N. G.; Robinson, N. J.; Cavet, J. S. *J. Biol. Chem.* **2007**, *282*, 32298.
- (38) Liu, T.; Chen, X.; Ma, Z.; Shokes, J.; Hemmingsen, L.; Scott, R. A.; Giedroc, D. P. *Biochemistry* **2008**, *47*, 10564.
- (39) Tottey, S.; Harvie, D.; Robinson, N. *Acc. Chem. Res.* **2005**, *38*, 775.
- (40) Outten, F. W.; Huffman, D. L.; Hale, J. A.; O'Halloran, T. V. *J. Biol. Chem.* **2001**, *276*, 30670.
- (41) Yamamoto, K.; Ishihama, A. *Biosci. Biotechnol. Biochem.* **2006**, *70*, 1688.
- (42) Gardner, A. M.; Gessner, C. R.; Gardner, P. R. *J. Biol. Chem.* **2003**, *278*, 10081.
- (43) D'Autreaux, B.; Tucker, N. P.; Dixon, R.; Spiro, S. *Nature* **2005**, *437*, 769.
- (44) Aono, S. *Dalton Trans.* **2008**, *24*, 3137.
- (45) Outten, F. W.; Theil, E. C. *Antioxid. Redox Signal.* **2008**, *11*, 1029.
- (46) Outten, F. W. *Nat. Chem. Biol.* **2007**, *3*, 206.
- (47) Crack, J. C.; Jervis, A. J.; Gaskell, A. A.; White, G. F.; Green, J.; Thomson, A. J.; Le Brun, N. E. *Biochem. Soc. Trans.* **2008**, *36*, 1144.
- (48) D'Autreaux, B.; Tucker, N.; Spiro, S.; Dixon, R. *Methods Enzymol.* **2008**, *437*, 235.
- (49) Davidson, A. L.; Dassa, E.; Orelle, C.; Chen, J. *Microbiol. Mol. Biol. Rev.* **2008**, *72*, 317.
- (50) Rees, D. C.; Johnson, E.; Lewinson, O. *Nat. Rev. Mol. Cell Biol.* **2009**, *10*, 218.
- (51) Nevo, Y.; Nelson, N. *Biochim. Biophys. Acta* **2006**, *1763*, 609.
- (52) Courville, P.; Chaloupka, R.; Cellier, M. F. *Biochem. Cell Biol.* **2006**, *84*, 960.
- (53) Papp-Wallace, K. M.; Maguire, M. E. *Annu. Rev. Microbiol.* **2006**, *60*, 187.
- (54) Montanini, B.; Blaudez, D.; Jeandroz, S.; Sanders, D.; Chalot, M. *BMC Genomics* **2007**, *8*, 107.
- (55) Mandal, A. K.; Cheung, W. D.; Arguello, J. M. *J. Biol. Inorg. Chem.* **2002**, *277*, 7201.
- (56) Kuhlbrandt, W. *Nat. Rev. Mol. Cell Biol.* **2004**, *5*, 282.
- (57) Williams, L. E.; Mills, R. F. *Trends Plant Sci.* **2005**, *10*, 491.
- (58) Arguello, J. M.; Eren, E.; Gonzalez-Guerrero, M. *BioMetals* **2007**, *20*, 233.
- (59) Murakami, S. *Curr. Opin. Struct. Biol.* **2008**, *18*, 459.
- (60) Tottey, S.; Rich, P. R.; Rondet, S. A. M.; Robinson, N. J. *J. Biol. Chem.* **2001**, *276*, 19999.
- (61) Zagorski, N.; Wilson, D. B. *Appl. Biochem. Biotechnol.* **2004**, *117*, 33.
- (62) Solioz, M.; Stoyanov, J. V. *FEMS Microbiol. Rev.* **2003**, *27*, 183.
- (63) Guan, L.; Kaback, H. R. *Annu. Rev. Biophys. Biomol. Struct.* **2006**, *35*, 67.
- (64) Law, C. J.; Maloney, P. C.; Wang, D. N. *Annu. Rev. Microbiol.* **2008**, *62*, 289.
- (65) Rodrigue, A.; Effantin, G.; Mandrand-Berthelot, M. A. *J. Bacteriol.* **2005**, *187*, 2912.
- (66) Haydon, M. J.; Cobbett, C. S. *Plant Physiol.* **2007**, *143*, 1705.
- (67) Mithke, M.; Schmidt, S.; Marahiel, M. A. *J. Bacteriol.* **2008**, *190*, 5143.
- (68) Lu, M.; Fu, D. *Science* **2007**, *317*, 1746.
- (69) Toyoshima, C.; Nomura, H. *Nature* **2002**, *418*, 605.
- (70) Toyoshima, C.; Nakasako, M.; Nomura, H.; Ogawa, H. *Nature* **2000**, *405*, 647.
- (71) Wu, C. C.; Rice, W. J.; Stokes, D. L. *Structure* **2008**, *16*, 976.
- (72) Posey, J. E.; Gherardini, F. C. *Science* **2000**, *288*, 1651.
- (73) Archibald, F. *Crit. Rev. Microbiol.* **1986**, *13*, 63.
- (74) Niven, D. F.; Ekins, A.; al-Samurai, A. A. *Can. J. Microbiol.* **1999**, *45*, 1027.
- (75) Touati, D. *Arch. Biochem. Biophys.* **2000**, *373*, 1.
- (76) Laham, N.; Ehrlich, R. *Immunol. Res.* **2004**, *30*, 15.
- (77) Krewulak, K. D.; Vogel, H. J. *Biochim. Biophys. Acta* **2008**, *1778*, 1781.
- (78) Hantke, K. *Curr. Opin. Microbiol.* **2001**, *4*, 172.
- (79) Ferguson, A. D.; Hofmann, E.; Coulton, J. W.; Diederichs, K.; Welte, W. *Science* **1998**, *282*, 2215.
- (80) Ferguson, A. D.; Chakraborty, R.; Smith, B. S.; Esser, L.; van der Helm, D.; Deisenhofer, J. *Science* **2002**, *295*, 1715.
- (81) Braun, V.; Braun, M. *Curr. Opin. Microbiol.* **2002**, *5*, 194.
- (82) Wandersman, C.; Delepelaire, P. *Annu. Rev. Microbiol.* **2004**, *58*, 611.
- (83) Larsen, R. A.; Thomas, M. G.; Postle, K. *Mol. Microbiol.* **1999**, *31*, 1809.
- (84) Ferguson, A. D.; Deisenhofer, J. *Biochim. Biophys. Acta* **2002**, *1565*, 318.
- (85) Kim, M.; Fanucci, G. E.; Cafiso, D. S. *Proc. Natl. Acad. Sci. U.S.A.* **2007**, *104*, 11975.
- (86) Köster, W. *Res. Microbiol.* **2001**, *152*, 291.
- (87) Velayudhan, J.; Hughes, N. J.; McColm, A. A.; Bagshaw, J.; Clayton, C. L.; Andrews, S. C.; Kelly, D. J. *Mol. Microbiol.* **2000**, *37*, 274.
- (88) Ratledge, C.; Dover, L. G. *Annu. Rev. Microbiol.* **2000**, *54*, 881.
- (89) Wandersman, C.; Stojiljkovic, I. *Curr. Opin. Microbiol.* **2000**, *3*, 215.
- (90) Crosa, J. H. *Microbiol. Mol. Biol. Rev.* **1989**, *53*, 517.
- (91) Bruns, C. M.; Nowalk, A. J.; Arvai, A. S.; McTigue, M. A.; Vaughan, K. G.; Mietzner, T. A.; McRee, D. E. *Nat. Struct. Mol. Biol.* **1997**, *4*, 919.
- (92) Yang, A. H.-W.; Macgillivray, R. T. A.; Chen, J.; Luo, Y.; Wang, Y.; Brayer, G. D.; Mason, A. B.; Woodworth, R. C.; Murphy, M. E. P. *Protein Sci.* **2000**, *9*, 49.
- (93) Tom-Yew, S. A. L.; Cui, D. T.; Bekker, E. G.; Murphy, M. E. P. *J. Biol. Chem.* **2005**, *280*, 9283.
- (94) Koropatkin, N.; Randich, A. M.; Bhattacharyya-Pakrasi, M.; Pakrasi, H. B.; Smith, T. J. *J. Biol. Chem.* **2007**, *282*, 27468.
- (95) Shouldice, S. R.; McRee, D. E.; Dougan, D. R.; Tari, L. W.; Schryvers, A. B. *J. Biol. Chem.* **2005**, *280*, 5820.

- (96) Schryvers, A. B.; Stojiljkovic, I. *Mol. Microbiol.* **1999**, *32*, 1117.
- (97) Gray-Owen, S. D.; Schryvers, A. B. *Trends Microbiol.* **1996**, *4*, 185.
- (98) Zhu, W.; Arceneaux, J. E.; Beggs, M. L.; Byers, B. R.; Eisenach, K. D.; Lundrigan, M. D. *Mol. Microbiol.* **1998**, *29*, 629.
- (99) Riccardi, G.; Milano, A.; Pasca, M. R.; Nies, D. H. *FEMS Microbiol. Lett.* **2008**, *287*, 1.
- (100) Giedroc, D. P.; Keating, K. M.; Williams, K. R.; Konigsberg, W. H.; Coleman, J. E. *Proc. Natl. Acad. Sci. U.S.A.* **1986**, *83*, 8452.
- (101) Giedroc, D. P.; Coleman, J. E. *Biochemistry* **1986**, *25*, 4969.
- (102) Natori, Y.; Nanamiya, H.; Akanuma, G.; Kosono, S.; Kudo, T.; Ochi, K.; Kawamura, F. *Mol. Microbiol.* **2007**, *63*, 294.
- (103) Ilbert, M.; Graf, P. C.; Jakob, U. *Antioxid. Redox Signal.* **2006**, *8*, 835.
- (104) Blair, D. E.; Schuttelkopf, A. W.; MacRae, J. I.; van Aalten, D. M. *Proc. Natl. Acad. Sci. U.S.A.* **2005**, *102*, 15429.
- (105) McCarthy, A. A.; Peterson, N. A.; Knijff, R.; Baker, E. N. *J. Mol. Biol.* **2004**, *335*, 1131.
- (106) Hajjaji, H. E.; Dumoulin, M.; Matagne, A.; Colau, D.; Roos, G.; Messens, J.; Collet, J. F. *J. Mol. Biol.* **2009**, *386*, 60.
- (107) Corbin, B. D.; Seeley, E. H.; Raab, A.; Feldmann, J.; Miller, M. R.; Torres, V. J.; Anderson, K. L.; Dattilo, B. M.; Dunman, P. M.; Gerads, R.; Caprioli, R. M.; Nacken, W.; Chazin, W. J.; Skaar, E. P. *Science* **2008**, *319*, 962.
- (108) Frausto da Silva, J.; Williams, R. J. P. *The Biological Chemistry of Elements: The Inorganic Chemistry of Life*, 2nd ed.; Oxford University Press: Oxford, 2001.
- (109) Kehres, D. G.; Maguire, M. E. *FEMS Microbiol. Rev.* **2003**, *27*, 263.
- (110) Morona, J. K.; Morona, R.; Miller, D. C.; Paton, J. C. *J. Bacteriol.* **2002**, *184*, 577.
- (111) Daly, M. J. *Nat. Rev. Microbiol.* **2009**, *7*, 237.
- (112) Anjem, A.; Varghese, S.; Imlay, J. A. *Mol. Microbiol.* **2009**, *72*, 844.
- (113) Haemig, H. A. H.; Brooker, R. J. *J. Membr. Biol.* **2004**, *201*, 97.
- (114) Lawrence, M. C.; Pilling, P. A.; Epa, V. C.; Berry, A. M.; Ogunniyi, A. D.; Paton, J. C. *Structure* **1998**, *6*, 1553.
- (115) Rosenzweig, A. C. *Acc. Chem. Res.* **2001**, *34*, 119.
- (116) Puskarova, A.; Ferianc, P.; Kormanec, J.; Homerova, D.; Farewell, A.; Nystrom, T. *Microbiology* **2002**, *148*, 3801.
- (117) Kershaw, C. J.; Brown, N. L.; Hobman, J. L. *Biochem. Biophys. Res. Commun.* **2007**, *364*, 66.
- (118) David, G.; Blondeau, K.; Schiltz, M.; Penel, S.; Lewit-Bentley, A. *J. Biol. Chem.* **2003**, *278*, 43728.
- (119) Holmes, M. A.; Paulsene, W.; Jide, X.; Ratledge, C.; Strong, R. K. *Structure* **2005**, *13*, 29.
- (120) Loisel, E.; Jacquamet, L.; Serre, L.; Bauvois, C.; Ferrer, J. L.; Vernet, T.; Di Guilmi, A. M.; Durmort, C. *J. Mol. Biol.* **2008**, *381*, 594.
- (121) Banaerjee, S.; Wei, B.; Bhattacharyya-Pakrasi, M.; Pakrasi, H. B.; Smith, T. J. *J. Mol. Biol.* **2003**, *333*, 1061.
- (122) Rukhman, V.; Anati, R.; Melamed-Frank, M.; Adir, N. *J. Mol. Biol.* **2005**, *348*, 961.
- (123) Chandra, B. R.; Yogavel, M.; Sharma, A. *J. Mol. Biol.* **2007**, *367*, 970.
- (124) Lee, Y.-H.; Deka, R. K.; Norgard, M. V.; Radolf, J. D.; Hasemann, C. A. *Nat. Struct. Mol. Biol.* **1999**, *6*, 628.
- (125) Mitrakul, K.; Loo, C. Y.; Gyurko, C.; Hughes, C. V.; Ganeshkumar, N. *Oral Microbiol. Immunol.* **2005**, *20*, 122.
- (126) Ogunniyi, A. D.; Grabowicz, M.; Mahdi, L. K.; Cook, J.; Gordon, D. L.; Sadlon, T. A.; Paton, J. C. *FASEB J.* **2009**, *23*, 731.
- (127) Wei, B.; Randich, A. M.; Bhattacharyya-Pakrasi, M.; Pakrasi, H. B.; Smith, T. J. *Biochemistry* **2007**, *46*, 8734.
- (128) Sabri, M.; Leveille, S.; Dozois, C. M. *Microbiology* **2006**, *152*, 745.
- (129) Loo, C. Y.; Mitrakul, K.; Voss, I. B.; Hughes, C. V.; Ganeshkumar, N. *J. Bacteriol.* **2003**, *185*, 2887.
- (130) Chaloupka, R.; Courville, P.; Veyrier, F.; Knudsen, B.; Tompkins, T. A.; Cellier, M. F. M. *Biochemistry* **2005**, *44*, 726.
- (131) Hao, Z.; Chen, S.; Wilson, D. B. *Appl. Environ. Microbiol.* **1999**, *65*, 4746.
- (132) Grass, G.; Franke, S.; Taudte, N.; Nies, D. H.; Kucharski, L. M.; Maguire, M. E.; Rensing, C. *J. Bacteriol.* **2005**, *187*, 1604.
- (133) Osman, D.; Cavet, J. S.; Allen, I.; Laskin, S. S.; Geoffrey, M. G. In *Advances in Applied Microbiology*; Academic Press: San Diego, 2008; Vol. 65.
- (134) Wernimont, A. K.; Huffman, D. L.; Finney, L. A.; Demeler, B.; O'Halloran, T. V.; Rosenzweig, A. C. *J. Biol. Inorg. Chem.* **2003**, *8*, 185.
- (135) Peariso, K.; Huffman, D. L.; Penner-Hahn, J. E.; O'Halloran, T. V. *J. Am. Chem. Soc.* **2003**, *125*, 342.
- (136) Zhang, L.; Koay, M.; Maher, M. J.; Xiao, Z.; Wedd, A. G. *J. Am. Chem. Soc.* **2006**, *128*, 5834.
- (137) Rensing, C.; Grass, G. *FEMS Microbiol. Rev.* **2003**, *27*, 197.
- (138) Rae, T. D.; Schmidt, P. J.; Pufahl, R. A.; Culotta, V. C.; O'Halloran, T. V. *Science* **1999**, *284*, 805.
- (139) O'Halloran, T. V.; Culotta, V. C. *J. Biol. Chem.* **2000**, *275*, 25057.
- (140) Ma, Z.; Cowart, D. M.; Scott, R. A.; Giedroc, D. P. *Biochemistry* **2009**, *48*, 3325.
- (141) Magnani, D.; Barre, O.; Gerber, S. D.; Solioz, M. *J. Bacteriol.* **2008**, *190*, 536.
- (142) Ward, S. K.; Hoye, E. A.; Talaat, A. M. *J. Bacteriol.* **2008**, *190*, 2939.
- (143) Selvaraj, A.; Balamurugan, K.; Yepiskoposyan, H.; Zhou, H.; Egli, D.; Georgiev, O.; Thiele, D. J.; Schaffner, W. *Genes Dev.* **2005**, *19*, 891.
- (144) Balamurugan, K.; Egli, D.; Hua, H.; Rajaram, R.; Seisenbacher, G.; Georgiev, O.; Schaffner, W. *EMBO J.* **2007**, *26*, 1035.
- (145) Thiele, D. J. *J. Nutr.* **2003**, *133*, 1579S.
- (146) Solioz, M.; Stoyanov, J. V. *FEMS Microbiol. Rev.* **2003**, *27*, 183.
- (147) Arnesan, F.; Banci, L.; Bertini, I.; Mangani, S.; Thompson, A. R. *Proc. Natl. Acad. Sci. U.S.A.* **2003**, *100*, 3814.
- (148) Chillappagari, S.; Miethke, M.; Trip, H.; Kuipers, O. P.; Marahiel, M. A. *J. Bacteriol.* **2009**, *191*, 2362.
- (149) Waldron, K. J.; Tottey, S.; Yanagisawa, S.; Dennison, C.; Robinson, N. J. *J. Biol. Chem.* **2007**, *282*, 3837.
- (150) Ranquet, C.; Ollagnier-de-Choudens, S.; Loiseau, L.; Barras, F.; Fontecave, M. *J. Biol. Chem.* **2007**, *282*, 30442.
- (151) Kim, H. J.; Graham, D. W.; DiSpirito, A. A.; Alterman, M. A.; Galeva, N.; Larive, C. K.; Asunskis, D.; Sherwood, P. M. A. *Science* **2004**, *305*, 1612.
- (152) Mulrooney, S. B.; Hausinger, R. P. *FEMS Microbiol. Rev.* **2003**, *27*, 239.
- (153) Rodionov, D. A.; Hebbeln, P.; Gelfand, M. S.; Eitinger, T. *J. Bacteriol.* **2006**, *188*, 317.
- (154) Schauer, K.; Gouget, B.; Carriere, M.; Labigne, A.; de Reuse, H. M. *Microbiol.* **2007**, *63*, 1054.
- (155) Heddle, J.; Scott, D. J.; Unzai, S.; Park, S.-Y.; Tame, J. R. H. *J. Biol. Chem.* **2003**, *278*, 50322.
- (156) Carrington, P. E.; Al-Mjeni, F.; Zoroddu, M. A.; Costa, M.; Maroney, M. J. *Environ. Health Perspect.* **2002**, *110*, 705.
- (157) Cherrier, M. V.; Martin, L.; Cavazza, C.; Jacquamet, L.; Lemaire, D.; Gaillard, J.; Fontecilla-Camps, J. C. *J. Am. Chem. Soc.* **2005**, *127*, 10075.
- (158) Cherrier, M. V.; Cavazza, C.; Bochot, C.; Lemaire, D.; Fontecilla-Camps, J. C. *Biochemistry* **2008**, *47*, 9937.
- (159) Borths, E. L.; Locher, K. P.; Lee, A. T.; Rees, D. C. *Proc. Natl. Acad. Sci. U.S.A.* **2002**, *99*, 16642.
- (160) Borths, E. L.; Poolman, B.; Hvorup, R. N.; Locher, K. P.; Rees, D. C. *Biochemistry* **2005**, *44*, 16301.
- (161) Locher, K. P.; Lee, A. T.; Rees, D. C. *Science* **2002**, *296*, 1091.
- (162) Eitinger, T.; Suhr, J.; Moore, L.; Smith, J. A. C. *Biomaterials* **2005**, *18*, 399.
- (163) Fulkerson, J. F., Jr.; Mobley, H. L. *J. Bacteriol.* **2000**, *182*, 1722.
- (164) Dosanjh, N. S.; Michel, S. L. *Curr. Opin. Chem. Biol.* **2006**, *10*, 123.
- (165) Degen, O.; Eitinger, T. *J. Bacteriol.* **2002**, *184*, 3569.
- (166) Niegowski, D.; Eshaghi, S. *Cell. Mol. Life Sci.* **2007**, *64*, 2564.
- (167) Eshaghi, S.; Niegowski, D.; Kohl, A.; Molina, D. M.; Lesley, S. A.; Nordlund, P. *Science* **2006**, *313*, 354.
- (168) Mendel, R. R. *Dalton Trans.* **2005**, *21*, 3404.
- (169) Mendel, R. R.; Bittner, F. *Biochim. Biophys. Acta* **2006**, *1763*, 621.
- (170) Kletzin, A.; Adams, M. W. W. *FEMS Microbiol. Rev.* **1996**, *18*, 5.
- (171) Hu, Y.; Rech, S.; Gunsalus, R. P.; Rees, D. C. *Nat. Struct. Mol. Biol.* **1997**, *4*, 703.
- (172) Gerber, S.; Comellas-Bigler, M.; Goetz, B. A.; Locher, K. P. *Science* **2008**, *321*, 246.
- (173) Anderson, L. A.; McNairn, E.; Leubke, T.; Pau, R. N.; Boxer, D. H. *J. Bacteriol.* **2000**, *182*, 7035.
- (174) Wu, X.; Sinani, D.; Kim, H.; Lee, J. *J. Biol. Chem.* **2009**, *284*, 4112.
- (175) Grass, G.; Otto, M.; Fricke, B.; Haney, C. J.; Rensing, C.; Nies, D. H.; Munkelt, D. *Arch. Microbiol.* **2005**, *183*, 9.
- (176) Wei, Y.; Fu, D. *J. Biol. Chem.* **2005**, *280*, 33716.
- (177) Grant, R. A.; Filman, D. J.; Finkel, S. E.; Kolter, R.; Hogle, J. M. *Nat. Struct. Mol. Biol.* **1998**, *5*, 294.
- (178) Papinutto, E.; Dundon, W. G.; Pitulis, N.; Battistutta, R.; Montecucco, C.; Zanotti, G. *J. Biol. Chem.* **2002**, *277*, 15093.
- (179) Shcolnick, S.; Shaked, Y.; Keren, N. *Biochim. Biophys. Acta* **2006**, *1767*, 814.
- (180) Kloosterman, T. G.; van der Kooi-Pol, M. M.; Bijlsma, J. J.; Kuipers, O. P. *Mol. Microbiol.* **2007**, *65*, 1049.
- (181) Palmiter, R. D.; Cole, T. B.; Quaife, C. J.; Findley, S. D. *Proc. Natl. Acad. Sci. U.S.A.* **1996**, *93*, 14934.
- (182) Palmiter, R. D.; Cole, T. B.; Findley, S. D. *EMBO J.* **1996**, *15*, 1784.
- (183) Palmiter, R. D.; Findley, S. D. *EMBO J.* **1995**, *14*, 639.
- (184) Wei, Y.; Fu, D. *J. Biol. Chem.* **2006**, *281*, 23492.
- (185) Grass, G.; Fan, B.; Rosen, B. P.; Franke, S.; Nies, D. H.; Rensing, C. *J. Bacteriol.* **2001**, *183*, 4664.
- (186) Nies, D. H. *Plasmid* **1992**, *27*, 17.



- (187) Guffanti, A. A.; Wei, Y.; Rood, S. V.; Krulwich, T. A. *Mol. Microbiol.* **2002**, *45*, 145.
- (188) Moore, C. M.; Gaballa, A.; Hui, M.; Ye, R. W.; Helmann, J. D. *Mol. Microbiol.* **2005**, *57*, 27.
- (189) Kuroda, M.; Hayashi, H.; Ohta, T. *Microbiol. Immunol.* **1999**, *43*, 115.
- (190) Cherezov, V.; Hofer, N.; Szebenyi, D. M.; Kolaj, O.; Wall, J. G.; Gillilan, R.; Srinivasan, V.; Jaroniec, C. P.; Caffrey, M. *Structure* **2008**, *16*, 1378.
- (191) Wei, Y.; Li, H.; Fu, D. *J. Biol. Chem.* **2004**, *279*, 39251.
- (192) Rahman, M.; Patching, S.; Ismat, F.; Henderson, P.; Herbert, R.; Baldwin, S.; McPherson, M. *Mol. Membr. Biol.* **2008**, *25*, 683.
- (193) Anton, A.; Weltrowski, A.; Haney, C. J.; Franke, S.; Grass, G.; Rensing, C.; Nies, D. H. *J. Bacteriol.* **2004**, *186*, 7499.
- (194) Chao, Y.; Fu, D. *J. Biol. Chem.* **2004**, *279*, 17173.
- (195) Blindauer, C. A. *Chem. Biodivers.* **2008**, *5*, 1990.
- (196) Sazinsky, M. H.; Agarwal, S.; Arguello, J. M.; Rosenzweig, A. C. *Biochemistry* **2006**, *45*, 9949.
- (197) Sazinsky, M. H.; Mandal, A. K.; Arguello, J. M.; Rosenzweig, A. C. *J. Biol. Chem.* **2006**, *281*, 11161.
- (198) Dmitriev, O.; Tsivkovskii, R.; Abildgaard, F.; Morgan, C. T.; Markley, J. L.; Lutsenko, S. *Proc. Natl. Acad. Sci. U.S.A.* **2006**, *103*, 5302.
- (199) Gonzalez-Guerrero, M.; Arguello, J. M. *Proc. Natl. Acad. Sci. U.S.A.* **2008**, *105*, 5992.
- (200) Argüello, J. M. *J. Membr. Biol.* **2003**, *195*, 93.
- (201) Dutta, S. J.; Liu, J.; Hou, Z.; Mitra, B. *Biochemistry* **2006**, *45*, 5923.
- (202) Okkeri, J.; Haltia, T. *Biochim. Biophys. Acta* **2006**, *1757*, 1485.
- (203) Mandal, A. K.; Arguello, J. M. *Biochemistry* **2003**, *42*, 11040.
- (204) Walker, J. M.; Huster, D.; Ralle, M.; Morgan, C. T.; Blackburn, N. J.; Lutsenko, S. *J. Biol. Chem.* **2004**, *279*, 15376.
- (205) Achila, D.; Banci, L.; Bertini, I.; Bunce, J.; Ciofi-Baffoni, S.; Huffman, D. L. *Proc. Natl. Acad. Sci. U.S.A.* **2006**, *103*, 5729.
- (206) Banci, L.; Bertini, I.; Cantini, F.; Felli, I. C.; Gonnelli, L.; Hadjiladis, N.; Pierattelli, R.; Rosato, A.; Voulgaris, P. *Nat. Chem. Biol.* **2006**, *2*, 367.
- (207) Banci, L.; Bertini, I.; Ciofi-Baffoni, S.; Kandias, N. G.; Robinson, N. J.; Spyroulias, G. A.; Su, X. C.; Tottey, S.; Vanarotti, M. *Proc. Natl. Acad. Sci. U.S.A.* **2006**, *103*, 8320.
- (208) Pufahl, R. A.; Singer, C. P.; Peariso, K. L.; Lin, S. J.; Schmidt, P. J.; Fahmi, C. J.; Culotta, V. C.; Penner-Hahn, J. E.; O'Halloran, T. V. *Science* **1997**, *278*, 853.
- (209) Liu, T.; Reyes-Caballero, H.; Li, C.; Scott, R. A.; Giedroc, D. P. *Biochemistry* **2007**, *46*, 11057.
- (210) Arnesano, F.; Banci, L.; Bertini, I.; Cantini, F.; Ciofi-Baffoni, S.; Huffman, D. L.; O'Halloran, T. V. *J. Biol. Chem.* **2001**, *276*, 41365.
- (211) Banci, L.; Bertini, I.; Ciofi-Baffoni, S.; D'Onofrio, M.; Gonnelli, L.; Marhuenda-Egea, F. C.; Ruiz-Duenas, F. J. *J. Mol. Biol.* **2002**, *317*, 415.
- (212) Borrelly, G. P.; Blindauer, C. A.; Schmid, R.; Butler, C. S.; Cooper, C. E.; Harvey, I.; Sadler, P. J.; Robinson, N. J. *Biochem. J.* **2004**, *378*, 293.
- (213) Banci, L.; Bertini, I.; Ciofi-Baffoni, S.; Finney, L. A.; Outten, C. E.; O'Halloran, T. V. *J. Mol. Biol.* **2002**, *323*, 883.
- (214) Banci, L.; Bertini, I.; Ciofi-Baffoni, S.; Su, X. C.; Miras, R.; Bal, N.; Mintz, E.; Catty, P.; Shokes, J. E.; Scott, R. A. *J. Mol. Biol.* **2006**, *356*, 638.
- (215) Mitra, B.; Sharma, R. *Biochemistry* **2001**, *40*, 7694.
- (216) Liu, J.; Dutta, S. J.; Stemmler, A. J.; Mitra, B. *Biochemistry* **2006**, *45*, 763.
- (217) Arguello, J. M.; Gonzalez-Guerrero, M. *Structure* **2008**, *16*, 833.
- (218) Toyoshima, C.; Inesi, G. *Annu. Rev. Biochem.* **2004**, *73*, 269.
- (219) Huster, D.; Lutsenko, S. *J. Biol. Chem.* **2003**, *278*, 32212.
- (220) Rosenzweig, A. C.; Huffman, D. L.; Hou, M. Y.; Wernimont, A. K.; Pufahl, R. A.; O'Halloran, T. V. *Structure* **1999**, *7*, 605.
- (221) Banci, L.; Bertini, I.; Ciofi-Baffoni, S.; Su, X. C.; Borrelly, G. P.; Robinson, N. J. *J. Biol. Chem.* **2004**, *279*, 27502.
- (222) Nies, D. H. *FEMS Microbiol. Rev.* **2003**, *27*, 313.
- (223) Zhou, T.; Radaev, S.; Rosen, B. P.; Gatti, D. L. *J. Biol. Chem.* **2001**, *276*, 30414.
- (224) Silver, S. *Gene* **1996**, *179*, 9.
- (225) von Rozycki, T.; Nies, D. H. Antonie Leeuwenhoek 2008, *Online Contents*.
- (226) Goldberg, M.; Pribyl, T.; Juhnke, S.; Nies, D. H. *J. Biol. Chem.* **1999**, *274*, 26065.
- (227) Pos, K. M. *Biochim. Biophys. Acta* **2009**, *1794*, 782.
- (228) Schmidt, T.; Schlegel, H. G. *J. Bacteriol.* **1994**, *176*, 7045.
- (229) Silver, S. *FEMS Microbiol. Rev.* **2003**, *27*, 341.
- (230) Loftin, I. R.; Franke, S.; Blackburn, N. J.; McEvoy, M. M. *Protein Sci.* **2007**, *16*, 2287.
- (231) Xue, Y.; Davis, A. V.; Balakrishnan, G.; Stasser, J. P.; Staehlin, B. M.; Focia, P.; Spiro, T. G.; Penner-Hahn, J. E.; O'Halloran, T. V. *Nat. Chem. Biol.* **2008**, *4*, 107.
- (232) Seeger, M. A.; von Ballmoos, C.; Eicher, T.; Brandstatter, L.; Verrey, F.; Diederichs, K.; Pos, K. M. *Nat. Struct. Mol. Biol.* **2008**, *15*, 199.
- (233) Seeger, M. A.; Schiefner, A.; Eicher, T.; Verrey, F.; Diederichs, K.; Pos, K. M. *Science* **2006**, *313*, 1295.
- (234) Murakami, S.; Nakashima, R.; Yamashita, E.; Matsumoto, T.; Yamaguchi, A. *Nature* **2006**, *443*, 173.
- (235) Koronakis, V.; Sharff, A.; Koronakis, E.; Luisi, B.; Hughes, C. *Nature* **2000**, *405*, 914.
- (236) Mikolosko, J.; Bobyk, K.; Zgurskaya, H. I.; Ghosh, P. *Structure* **2006**, *14*, 577.
- (237) Hirakata, Y.; Srikumar, R.; Poole, K.; Gotoh, N.; Suematsu, T.; Kohno, S.; Kamihira, S.; Hancock, R. E.; Speert, D. P. *J. Exp. Med.* **2002**, *196*, 109.
- (238) Chen, H.; Hu, J.; Chen, P. R.; Lan, L.; Li, Z.; Hicks, L. M.; Dinner, A. R.; He, C. *Proc. Natl. Acad. Sci. U.S.A.* **2008**, *105*, 13586.
- (239) Lim, D.; Poole, K.; Strynadka, N. C. *J. Biol. Chem.* **2002**, *277*, 29253.
- (240) Blindauer, C. A.; Harrison, M. D.; Parkinson, J. A.; Robinson, A. K.; Cavet, J. S.; Robinson, N. J.; Sadler, P. J. *Proc. Natl. Acad. Sci. U.S.A.* **2001**, *98*, 9593.
- (241) Barkay, T.; Miller, S. M.; Summers, A. O. *FEMS Microbiol. Rev.* **2003**, *27*, 355.
- (242) Qin, J.; Rosen, B. P.; Zhang, Y.; Wang, G.; Franke, S.; Rensing, C. *Proc. Natl. Acad. Sci. U.S.A.* **2006**, *103*, 2075.
- (243) Wang, Y.; Hemmingsen, L.; Giedroc, D. P. *Biochemistry* **2005**, *44*, 8976.
- (244) Liu, T.; Ramesh, A.; Ma, Z.; Ward, S. K.; Zhang, L.; George, G. N.; Talaat, A. M.; Sacchettini, J. C.; Giedroc, D. P. *Nat. Chem. Biol.* **2007**, *3*, 60.
- (245) Stoyanov, J. V.; Hobman, J. L.; Brown, N. L. *Mol. Microbiol.* **2001**, *39*, 502.
- (246) Strausak, D.; Solioz, M. *J. Biol. Chem.* **1997**, *272*, 8932.
- (247) De Pina, K.; Desjardin, V.; Mandrand-Berthelot, M. A.; Giordano, G.; Wu, L. F. *J. Bacteriol.* **1999**, *181*, 670.
- (248) Patzer, S. I.; Hantke, K. *Mol. Microbiol.* **1998**, *28*, 1199.
- (249) Wu, J.; Rosen, B. P. *J. Biol. Chem.* **1993**, *268*, 52.
- (250) Morby, A. P.; Turner, J. S.; Huckle, J. W.; Robinson, N. J. *Nucleic Acids Res.* **1993**, *21*, 921.
- (251) Cavet, J. S.; Graham, A. I.; Meng, W.; Robinson, N. J. *J. Biol. Chem.* **2003**, *278*, 44560.
- (252) Harvie, D. R.; Andreini, C.; Cavallaro, G.; Meng, W.; Connolly, B. A.; Yoshida, K.; Fujita, Y.; Harwood, C. R.; Radford, D. S.; Tottey, S.; Cavet, J. S.; Robinson, N. J. *Mol. Microbiol.* **2006**, *59*, 1341.
- (253) Qin, J.; Fu, H. L.; Ye, J.; Benze, K. Z.; Stemmler, T. L.; Rawlings, D. E.; Rosen, B. P. *J. Biol. Chem.* **2007**, *282*, 34346.
- (254) Eicken, C.; Pennella, M. A.; Chen, X.; Koshlap, K. M.; VanZile, M. L.; Sacchettini, J. C.; Giedroc, D. P. *J. Mol. Biol.* **2003**, *333*, 683.
- (255) Ye, J.; Kandegedara, A.; Martin, P.; Rosen, B. P. *J. Bacteriol.* **2005**, *187*, 4214.
- (256) Banci, L.; Bertini, I.; Cantini, F.; Ciofi-Baffoni, S.; Cavet, J. S.; Dennison, C.; Graham, A. I.; Harvie, D. R.; Robinson, N. J. *J. Biol. Chem.* **2007**, *282*, 30181.
- (257) Arunkumar, A. I.; Pennella, M. A.; Kong, X.; Giedroc, D. P. *Biomol. NMR Assign.* **2007**, *1*, 99.
- (258) Arunkumar, A. I.; Campanello, G. C.; Giedroc, D. P. *Proc. Natl. Acad. Sci. U.S.A.* **2009**, *106*, in press (doi: 10.1073/pnas.0905558106).
- (259) Liu, T.; Golden, J. W.; Giedroc, D. P. *Biochemistry* **2005**, *44*, 8673.
- (260) Thelwell, C.; Robinson, N. J.; Turner-Cavet, J. S. *Proc. Natl. Acad. Sci. U.S.A.* **1998**, *95*, 10728.
- (261) Busenlehner, L. S.; Weng, T. C.; Penner-Hahn, J. E.; Giedroc, D. P. *J. Mol. Biol.* **2002**, *319*, 685.
- (262) Busenlehner, L. S.; Giedroc, D. P. *J. Inorg. Biochem.* **2006**, *100*.
- (263) Apuy, J. L.; Busenlehner, L. S.; Russell, D. H.; Giedroc, D. P. *Biochemistry* **2004**, *43*, 3824.
- (264) Shi, W.; Dong, J.; Scott, R. A.; Ksenzenko, M. Y.; Rosen, B. P. *J. Biol. Chem.* **1996**, *271*, 9291.
- (265) Busenlehner, L. S.; Apuy, J. L.; Giedroc, D. P. *J. Biol. Inorg. Chem.* **2002**, *7*, 551.
- (266) Sun, Y.; Wong, M. D.; Rosen, B. P. *J. Biol. Chem.* **2001**, *276*, 14955.
- (267) Ordoñez, E.; Thiyagarajan, S.; Cook, J. D.; Stemmler, T. L.; Gil, J. A.; Mateos, L. M.; Rosen, B. P. *J. Biol. Chem.* **2008**, *283*, 25706.
- (268) Liu, T.; Nakashima, S.; Hirose, K.; Shibusaka, M.; Katsuhara, M.; Ezaki, B.; Giedroc, D. P.; Kasamo, K. *J. Biol. Chem.* **2004**, *279*, 17810.
- (269) Hirose, K.; Ezaki, B.; Liu, T.; Nakashima, S. *Toxicol. Lett.* **2006**, *163*, 250.
- (270) Kandegedara, A.; Thiyagarajan, S.; Kondapalli, K. C.; Stemmler, T. L.; Rosen, B. P. *J. Biol. Chem.* **2009**, *284*, 14958.
- (271) VanZile, M. L.; Chen, X.; Giedroc, D. P. *Biochemistry* **2002**, *41*, 9765.
- (272) Cavet, J. S.; Meng, W.; Pennella, M. A.; Appelhoff, R. J.; Giedroc, D. P.; Robinson, N. J. *J. Biol. Chem.* **2002**, *277*, 38441.

- (273) Lipsitz, R. S.; Tjandra, N. *Annu. Rev. Biophys. Biomol. Struct.* **2004**, *33*, 387.
- (274) Saha, R. P.; Chakrabarti, P. *BMC Struct. Biol.* **2006**, *6*, 24.
- (275) Mandal, S.; Chatterjee, S.; Dam, B.; Roy, P.; Das Gupta, S. K. *Microbiology* **2007**, *153*, 80.
- (276) Barbosa, R. L.; Benedetti, C. E. *J. Bacteriol.* **2007**, *189*, 6185.
- (277) Gueune, H.; Durand, M.-J.; Thouand, G.; DuBow, M. S. *Appl. Environ. Microbiol.* **2008**, *74*, 1954.
- (278) Lund, P. A.; Ford, S. J.; Brown, N. L. *J. Gen. Microbiol.* **1986**, *132* (Pt 2), 465.
- (279) O'Halloran, T.; Walsh, C. *Science* **1987**, *235*, 211.
- (280) Lund, P. A.; Brown, N. L. *J. Mol. Biol.* **1989**, *205*, 343.
- (281) O'Halloran, T. V.; Frantz, B.; Shin, M. K.; Ralston, D. M.; Wright, J. G. *Cell* **1989**, *56*, 119.
- (282) Permina, E. A.; Kazakov, A. E.; Kalinina, O. V.; Gelfand, M. S. *BMC Microbiol.* **2006**, *6*, 49.
- (283) Outten, C. E.; Outten, F. W.; O'Halloran, T. V. *J. Biol. Chem.* **1999**, *274*, 37517.
- (284) Frantz, B.; O'Halloran, T. V. *Biochemistry* **1990**, *29*, 4747.
- (285) Checa, S. K.; Espariz, M.; Audero, M. E.; Botta, P. E.; Spinelli, S. V.; Soncini, F. C. *Mol. Microbiol.* **2007**, *63*, 1307.
- (286) Lee, S. W.; Glickmann, E.; Cooksey, D. A. *Appl. Environ. Microbiol.* **2001**, *67*, 1437.
- (287) Borremans, B.; Hobman, J. L.; Provoost, A.; Brown, N. L.; van Der Lelie, D. *J. Bacteriol.* **2001**, *183*, 5651.
- (288) Heldwein, E. E.; Brennan, R. G. *Nature* **2001**, *409*, 378.
- (289) Godsey, M. H.; Baranova, N. N.; Neyfakh, A. A.; Brennan, R. G. *J. Biol. Chem.* **2001**, *276*, 47178.
- (290) Utschig, L. M.; Bryson, J. W.; O'Halloran, T. V. *Science* **1995**, *268*, 380.
- (291) Shewchuk, L. M.; Verdine, G. L.; Nash, H.; Walsh, C. T. *Biochemistry* **1989**, *28*, 6140.
- (292) Chen, K.; Yuldasheva, S.; Penner-Hahn, J. E.; O'Halloran, T. V. *J. Am. Chem. Soc.* **2003**, *125*, 12088.
- (293) Stoyanov, J. V.; Brown, N. L. *J. Biol. Chem.* **2003**, *278*, 1407.
- (294) Brown, N. L.; Stoyanov, J. V.; Kidd, S. P.; Hobman, J. L. *FEMS Microbiol. Rev.* **2003**, *27*, 145.
- (295) Ralston, D. M.; O'Halloran, T. V. *Proc. Natl. Acad. Sci. U.S.A.* **1990**, *87*, 3846.
- (296) Watanabe, S.; Kita, A.; Kobayashi, K.; Miki, K. *Proc. Natl. Acad. Sci. U.S.A.* **2008**, *105*, 4121.
- (297) Pomposiello, P. J.; Bennik, M. H. J.; Demple, B. J. *Bacteriol.* **2001**, *183*, 3890.
- (298) Ding, H.; Demple, B. *Proc. Natl. Acad. Sci. U.S.A.* **2000**, *97*, 5146.
- (299) Lo, F. C.; Chen, C. L.; Lee, C. M.; Tsai, M. C.; Lu, T. T.; Liaw, W. F.; Yu, S. S. *J. Biol. Inorg. Chem.* **2008**, *13*, 961.
- (300) Strocher, U. H.; Kidd, S. P.; Stafford, S. L.; Jennings, M. P.; Paton, J. C.; McEwan, A. G. *J. Infect. Dis.* **2007**, *196*, 1820.
- (301) Kidd, S. P.; Potter, A. J.; Apicella, M. A.; Jennings, M. P.; McEwan, A. G. *Mol. Microbiol.* **2005**, *57*, 1676.
- (302) Kim, S. O.; Merchant, K.; Nudelman, R.; Beyer, W. F., Jr.; Keng, T.; DeAngelo, J.; Hausladen, A.; Stamler, J. S. *Cell* **2002**, *109*, 383.
- (303) Newberry, K. J.; Huffman, J. L.; Miller, M. C.; Vazquez-Laslop, N.; Neyfakh, A. A.; Brennan, R. G. *J. Biol. Chem.* **2008**, *283*, 26795.
- (304) Storz, G.; Imlay, J. A. *Curr. Opin. Microbiol.* **1999**, *2*, 188.
- (305) Demple, B. *Nat. Chem. Biol.* **2008**, *4*, 653.
- (306) Dietrich, L. E.; Teal, T. K.; Price-Whelan, A.; Newman, D. K. *Science* **2008**, *321*, 1203.
- (307) Dietrich, L. E.; Price-Whelan, A.; Petersen, A.; Whiteley, M.; Newman, D. K. *Mol. Microbiol.* **2006**, *61*, 1308.
- (308) Gorodetsky, A. A.; Dietrich, L. E.; Lee, P. E.; Demple, B.; Newman, D. K.; Barton, J. K. *Proc. Natl. Acad. Sci. U.S.A.* **2008**, *105*, 3684.
- (309) Iwig, J. S.; Leitch, S.; Herbst, R. W.; Maroney, M. J.; Chivers, P. T. *J. Am. Chem. Soc.* **2008**, *130*, 7592.
- (310) Iwig, J. S.; Rowe, J. L.; Chivers, P. T. *Mol. Microbiol.* **2006**, *62*, 252.
- (311) Smaldone, G. T.; Helmann, J. D. *Microbiology* **2007**, *153*, 4123.
- (312) Rosenzweig, A. C.; O'Halloran, T. V. *Curr. Opin. Chem. Biol.* **2000**, *4*, 140.
- (313) Herring, C. D.; Blattner, F. R. *J. Bacteriol.* **2004**, *186*, 6714.
- (314) Farmer, E. E.; Davoine, C. *Curr. Opin. Plant Biol.* **2007**, *10*, 380.
- (315) Booth, I. R.; Ferguson, G. P.; Miller, S.; Li, C.; Gunasekera, B.; Kinghorn, S. *Biochem. Soc. Trans.* **2003**, *31*, 1406.
- (316) Nguyen, T. T.; Eiamphungporn, W.; Mader, U.; Liebeke, M.; Lalk, M.; Hecker, M.; Helmann, J. D.; Antelmann, H. *Mol. Microbiol.* **2009**, *71*, 876.
- (317) Portmann, R.; Poulsen, K. R.; Wimmer, R.; Solioz, M. *Biomaterials* **2006**, *19*, 61.
- (318) Cobine, P. A.; George, G. N.; Jones, C. E.; Wickramasinghe, W. A.; Solioz, M.; Dameron, C. T. *Biochemistry* **2002**, *41*, 5822.
- (319) Cantini, F.; Banci, L.; Solioz, M. *Biochem. J.* **2009**, *417*, 493.
- (320) Safo, M. K.; Zhao, Q.; Ko, T. P.; Musayev, F. N.; Robinson, H.; Scarsdale, N.; Wang, A. H.; Archer, G. L. *J. Bacteriol.* **2005**, *187*, 1833.
- (321) Johnston, A. W.; Todd, J. D.; Curson, A. R.; Lei, S.; Nikolaidou-Katsaridou, N.; Gelfand, M. S.; Rodionov, D. A. *Biomaterials* **2007**, *20*, 501.
- (322) Lucarelli, D.; Russo, S.; Garman, E.; Milano, A.; Meyer-Klaucke, W.; Pohl, E. *J. Biol. Chem.* **2007**, *282*, 9914.
- (323) Maciag, A.; Dainese, E.; Rodriguez, G. M.; Milano, A.; Provvedi, R.; Pasca, M. R.; Smith, I.; Palu, G.; Riccardi, G.; Manganello, R. *J. Bacteriol.* **2007**, *189*, 730.
- (324) Diaz-Mireles, E.; Wexler, M.; Sawers, G.; Bellini, D.; Todd, J. D.; Johnston, A. W. *Microbiology* **2004**, *150*, 1447.
- (325) Ahn, B. E.; Cha, J.; Lee, E. J.; Han, A. R.; Thompson, C. J.; Roe, J. H. *Mol. Microbiol.* **2006**, *59*, 1848.
- (326) Lee, J. W.; Helmann, J. D. *Nature* **2006**, *440*, 363.
- (327) Carpenter, B. M.; Gancz, H.; Gonzalez-Nieves, R. P.; West, A. L.; Whitmire, J. M.; Michel, S. L. J.; Merrell, D. S. *PLoS ONE* **2009**, *4*, e5369.
- (328) Masse, E.; Gottesman, S. *Proc. Natl. Acad. Sci. U.S.A.* **2002**, *99*, 4620.
- (329) Lee, J. W.; Helmann, J. D. *Biomaterials* **2007**, *20*, 485.
- (330) Pohl, E.; Haller, J. C.; Mijovilovich, A.; Meyer-Klaucke, W.; Garman, E.; Vasil, M. L. *Mol. Microbiol.* **2003**, *47*, 903.
- (331) Traore, D. A.; El Ghazouani, A.; Ilango, S.; Dupuy, J.; Jacquamet, L.; Ferrer, J. L.; Caux-Thang, C.; Duarte, V.; Latour, J. M. *Mol. Microbiol.* **2006**, *61*, 1211.
- (332) Traore, D. A. K.; Ghazouani, A. E.; Jacquamet, L.; Borel, F.; Ferrer, J.-L.; Lascoux, D.; Ravanat, J.-L.; Jaquinod, M.; Blondin, G.; Caux-Thang, C.; Duarte, V.; Latour, J.-M. *Nat. Chem. Biol.* **2009**, *5*, 53.
- (333) An, Y. J.; Ahn, B. E.; Han, A. R.; Kim, H. M.; Chung, K. M.; Shin, J. H.; Cho, Y. B.; Roe, J. H.; Cha, S. S. *Nucleic Acids Res.* **2009**, *37*, 3442.
- (334) Jacquamet, L.; Traoré, D.; Ferrer, J.; Proux, O.; Testemale, D.; Hazemann, J.; Nazrenko, E.; El Ghazouani, A.; Caux-Thang, C.; Duarte, V.; Latour, J. M. *Mol. Microbiol.* **2009**, *73*, 20.
- (335) Pequeur, L.; D'Autreaux, B.; Dupuy, J.; Nicolet, Y.; Jacquamet, L.; Brutscher, B.; Michaud-Soret, I.; Bersch, B. *J. Biol. Chem.* **2006**, *281*, 21286.
- (336) Outten, C. E.; Tobin, D. A.; Penner-Hahn, J. E.; O'Halloran, T. V. *Biochemistry* **2001**, *40*, 10417.
- (337) Giedroc, D. P. *Mol. Microbiol.* **2009**, *73*, 1.
- (338) Todd, J. D.; Wexler, M.; Sawers, G.; Yeoman, K. H.; Poole, P. S.; Johnston, A. W. *Microbiology* **2002**, *148*, 4059.
- (339) Bodenmiller, D. M.; Spiro, S. J. *Bacteriol.* **2006**, *188*, 874.
- (340) Wu, Y.; Outten, F. W. *J. Bacteriol.* **2009**, *191*, 1248.
- (341) Tucker, N. P.; Hicks, M. G.; Clarke, T. A.; Crack, J. C.; Chandra, G.; Le Brun, N. E.; Dixon, R.; Hutchings, M. I. *PLoS One* **2008**, *3*, e3623.
- (342) Sangwan, I.; Small, S. K.; O'Brian, M. R. *J. Bacteriol.* **2008**, *190*, 5172.
- (343) Small, S. K.; Puri, S.; O'Brian, M. R. *Biomaterials* **2009**, *22*, 89.
- (344) Que, Q.; Helmann, J. D. *Mol. Microbiol.* **2000**, *35*, 1454.
- (345) Spiering, M. M.; Ringe, D.; Murphy, J. R.; Marletta, M. A. *Proc. Natl. Acad. Sci. U.S.A.* **2003**, *100*, 3808.
- (346) White, A.; Ding, X.; vanderSpek, J. C.; Murphy, J. R.; Ringe, D. *Nature* **1998**, *394*, 502.
- (347) Wylie, G. P.; Rangachari, V.; Bienkiewicz, E. A.; Marin, V.; Bhattacharya, N.; Love, J. F.; Murphy, J. R.; Logan, T. M. *Biochemistry* **2005**, *44*, 40.
- (348) Liu, C.; Mao, K.; Zhang, M.; Sun, Z.; Hong, W.; Li, C.; Peng, B.; Chang, Z. *J. Biol. Chem.* **2008**, *283*, 2439.
- (349) D'Aquino, J. A.; Tetenbaum-Novatt, J.; White, A.; Berkovitch, F.; Ringe, D. *Proc. Natl. Acad. Sci. U.S.A.* **2005**, *102*, 18408.
- (350) D'Aquino, J. A.; Lattimer, J. R.; Denninger, A.; D'Aquino, K. E.; Ringe, D. *Biochemistry* **2007**, *46*, 11761.
- (351) Schmitt, M. P. *J. Bacteriol.* **2002**, *184*, 6882.
- (352) Kliegman, J. I.; Griner, S. L.; Helmann, J. D.; Brennan, R. G.; Glasfeld, A. *Biochemistry* **2006**, *45*, 3493.
- (353) Glasfeld, A.; Guedon, E.; Helmann, J. D.; Brennan, R. G. *Nat. Struct. Biol.* **2003**, *10*, 652.
- (354) Sen, K. I.; Sienkiewicz, A.; Love, J. F.; vanderSpek, J. C.; Fajer, P. G.; Logan, T. M. *Biochemistry* **2006**, *45*, 4295.
- (355) DeWitt, M. A.; Kliegman, J. I.; Helmann, J. D.; Brennan, R. G.; Farrens, D. L.; Glasfeld, A. *J. Mol. Biol.* **2007**, *365*, 1257.
- (356) Golyanskiy, M.; Li, S.; Woods, V. L., Jr.; Cohen, S. M. *J. Biol. Inorg. Chem.* **2007**, *12*, 699.
- (357) Sen, K. I.; Logan, T. M.; Fajer, P. G. *Biochemistry* **2007**, *46*, 11639.
- (358) Chivers, P. T.; Sauer, R. T. *Protein Sci.* **1999**, *8*, 2494.
- (359) Schreier, E. R.; Sintchak, M. D.; Guo, Y.; Chivers, P. T.; Sauer, R. T.; Drennan, C. L. *Nat. Struct. Biol.* **2003**, *10*, 794.
- (360) Raumann, B. E.; Rould, M. A.; Pabo, C. O.; Sauer, R. T. *Nature* **1994**, *367*, 754.



- (361) Somers, W. S.; Phillips, S. E. *Nature* **1992**, *359*, 387.
- (362) Schreiter, E. R.; Wang, S. C.; Zamble, D. B.; Drennan, C. L. *Proc. Natl. Acad. Sci. U.S.A.* **2006**, *103*, 13676.
- (363) Bloom, S. L.; Zamble, D. B. *Biochemistry* **2004**, *43*, 10029.
- (364) Wang, S. C.; Dias, A. V.; Bloom, S. L.; Zamble, D. B. *Biochemistry* **2004**, *43*, 10018.
- (365) Carrington, P. E.; Chivers, P. T.; Al-Mjeni, F.; Sauer, R. T.; Maroney, M. J. *Nat. Struct. Biol.* **2003**, *10*, 126.
- (366) Chivers, P. T.; Sauer, R. T. *Chem. Biol.* **2002**, *9*, 1141.
- (367) Diederix, R. E. M.; Fauquant, C.; Rodrigue, A.; Mandrand-Berthelot, M.-A.; Michaud-Soret, I. *Chem. Commun.* **2008**, *15*, 1813.
- (368) Contreras, M.; Thiberge, J. M.; Mandrand-Berthelot, M. A.; Labigne, A. *Mol. Microbiol.* **2003**, *49*, 947.
- (369) Dian, C.; Schauer, K.; Kapp, U.; McSweeney, S. M.; Labigne, A.; Terradot, L. *J. Mol. Biol.* **2006**, *361*, 715.
- (370) Chivers, P. T.; Tahirov, T. H. *J. Mol. Biol.* **2005**, *348*, 597.
- (371) Bradley, M. J.; Chivers, P. T.; Baker, N. A. *J. Mol. Biol.* **2008**, *378*, 1155.
- (372) Leitch, S.; Bradley, M. J.; Rowe, J. L.; Chivers, P. T.; Maroney, M. J. *J. Am. Chem. Soc.* **2007**, *129*, 5085.
- (373) Phillips, C. M.; Schreiter, E. R.; Guo, Y.; Wang, S. C.; Zamble, D. B.; Drennan, C. L. *Biochemistry* **2008**, *47*, 1938.
- (374) Maddocks, S. E.; Oyston, P. C. *Microbiology* **2008**, *154*, 3609.
- (375) Tropol, D.; van der Meer, J. R. *Microbiol. Mol. Biol. Rev.* **2004**, *68*, 474.
- (376) Aslund, F.; Zheng, M.; Beckwith, J.; Storz, G. *Proc. Natl. Acad. Sci. U.S.A.* **1999**, *96*, 6161.
- (377) Zheng, M.; Aslund, F.; Storz, G. *Science* **1998**, *279*, 1718.
- (378) Choi, H.; Kim, S.; Mukhopadhyay, P.; Cho, S.; Woo, J.; Storz, G.; Ryu, S. *Cell* **2001**, *105*, 103.
- (379) Hausladen, A.; Privalle, C. T.; Keng, T.; DeAngelo, J.; Stamler, J. S. *Cell* **1996**, *86*, 719.
- (380) Hess, D. T.; Matsumoto, A.; Kim, S. O.; Marshall, H. E.; Stamler, J. S. *Nat. Rev. Mol. Cell Biol.* **2005**, *6*, 150.
- (381) Haridas, V.; Kim, S. O.; Nishimura, G.; Hausladen, A.; Stamler, J. S.; Gutterman, J. U. *Proc. Natl. Acad. Sci. U.S.A.* **2005**, *102*, 10088.
- (382) Chen, H.; Xu, G.; Zhao, Y.; Tian, B.; Lu, H.; Yu, X.; Xu, Z.; Ying, N.; Hu, S.; Hua, Y. *PLoS ONE* **2008**, *3*, e1602.
- (383) Paget, M. S.; Buttner, M. J. *Annu. Rev. Genet.* **2003**, *37*, 91.
- (384) Lee, J. W.; Soonsanga, S.; Helmann, J. D. *Proc. Natl. Acad. Sci. U.S.A.* **2007**, *104*, 8743.
- (385) Chen, P. R.; Nishida, S.; Poor, C. B.; Cheng, A.; Bae, T.; Kuechenmeister, L.; Dunman, P. M.; Missiakas, D.; He, C. *Mol. Microbiol.* **2009**, *71*, 198.
- (386) Mukhopadhyay, P.; Zheng, M.; Bedzyk, L. A.; LaRossa, R. A.; Storz, G. *Proc. Natl. Acad. Sci. U.S.A.* **2004**, *101*, 745.
- (387) Schüttelkopf, A. W.; Boxer, D. H.; Hunter, W. N. *J. Mol. Biol.* **2003**, *326*, 761.
- (388) Alekshun, M. N.; Levy, S. B.; Mealy, T. R.; Seaton, B. A.; Head, J. F. *Nat. Struct. Biol.* **2001**, *8*, 710.
- (389) Wilkinson, S. P.; Grove, A. *Curr. Issues Mol. Biol.* **2006**, *8*, 51.
- (390) Hong, M.; Fungthong, M.; Helmann, J. D.; Brennan, R. G. *Mol. Cell* **2005**, *20*, 131.
- (391) Chen, P. R.; Bae, T.; Williams, W. A.; Duguid, E. M.; Rice, P. A.; Schneewind, O.; He, C. *Nat. Chem.* **2006**, *2*, 591.
- (392) Cheung, A. L.; Nishina, K. A.; Trotonda, M. P.; Tamber, S. *Int. J. Biochem. Cell Biol.* **2008**, *40*, 355.
- (393) Riboldi-Tunncliffe, A.; Isaacs, N. W.; Mitchell, T. J. *FEBS Lett.* **2005**, *579*, 5353.
- (394) Adamou, J. E.; Heinrichs, J. H.; Erwin, A. L.; Walsh, W.; Gayle, T.; Dormitzer, M.; Dagan, R.; Brewah, Y. A.; Barren, P.; Lathigra, R.; Langermann, S.; Koenig, S.; Johnson, S. *Infect. Immun.* **2001**, *69*, 949.
- (395) Lluall, D.; Poquet, I. *Appl. Environ. Microbiol.* **2004**, *70*, 5398.
- (396) Aranda, J.; Garrido, M. E.; Cortes, P.; Llagostera, M.; Barbe, J. *Infect. Immun.* **2008**, *76*, 1590.
- (397) Ramos, J. L.; Martinez-Bueno, M.; Molina-Henares, A. J.; Teran, W.; Watanabe, K.; Zhang, X.; Gallegos, M. T.; Brennan, R.; Tobes, R. *Microbiol. Mol. Biol. Rev.* **2005**, *69*, 326.
- (398) Orth, P.; Schnappinger, D.; Hillen, W.; Saenger, W.; Hinrichs, W. *Nat. Struct. Biol.* **2000**, *7*, 215.
- (399) Orth, P.; Saenger, W.; Hinrichs, W. *Biochemistry* **1999**, *38*, 191.
- (400) Palm, G. J.; Lederer, T.; Orth, P.; Saenger, W.; Takahashi, M.; Hillen, W.; Hinrichs, W. *J. Biol. Inorg. Chem.* **2008**, *13*, 1097.
- (401) Brenot, A.; Weston, B. F.; Caparon, M. G. *Mol. Microbiol.* **2007**, *63*, 1185.
- (402) Kuriyan, J.; Eisenberg, D. *Nature* **2007**, *450*, 983.
- (403) Shi, W.; Chance, M. R. *Cell. Mol. Life Sci.* **2008**, *65*, 3040.
- (404) Mounicou, S.; Szpunar, J.; Lobinski, R. *Chem. Soc. Rev.* **2009**, *38*, 1119.
- (405) Skaar, E. P.; Humayun, M.; Bae, T.; DeBord, K. L.; Schneewind, O. *Science* **2004**, *305*, 1626.
- (406) Shouldice, S. R.; Skene, R. J.; Dougan, D. R.; Snell, G.; McRee, D. E.; Schryvers, A. B.; Tari, L. W. *J. Bacteriol.* **2004**, *186*, 3903.
- (407) Banci, L.; Bertini, I.; Ciofi-Baffoni, S.; Del Conte, R.; Gonnelli, L. *Biochemistry* **2003**, *42*, 1939.
- (408) Hollenstein, K.; Frei, D. C.; Locher, K. P. *Nature* **2007**, *446*, 213.
- (409) Eswaran, J.; Koronakis, E.; Higgins, M. K.; Hughes, C.; Koronakis, V. *Curr. Opin. Struct. Biol.* **2004**, *14*, 741.
- (410) Li, H.; Jogl, G. *J. Mol. Biol.* **2007**, *368*, 1358.
- (411) Wimmer, R.; Herrmann, T.; Solioz, M.; Wuthrich, K. *J. Biol. Chem.* **1999**, *274*, 22597.
- (412) Banci, L.; Bertini, I.; Del Conte, R. *Biochemistry* **2003**, *42*, 13422.

CR900077W